INFORMATION TO USERS

The most advanced technology has been used to photograph and reproduce this manuscript from the microfilm master. UMI films the original text directly from the copy submitted. Thus, some dissertation copies are in typewriter face, while others may be from a computer printer.

In the unlikely event that the author did not send UMI a complete manuscript and there are missing pages, these will be noted. Also, if unauthorized copyrighted material had to be removed, a note will indicate the deletion.

Oversize materials (e.g., maps, drawings, charts) are reproduced by sectioning the original, beginning at the upper left-hand corner and continuing from left to right in equal sections with small overlaps. Each oversize page is available as one exposure on a standard 35 mm slide or as a 17″ × 23″ black and white photographic print for an additional charge.

Photographs included in the original manuscript have been reproduced xerographically in this copy. 35 mm slides or 6″ × 9″ black and white photographic prints are available for any photographs or illustrations appearing in this copy for an additional charge. Contact UMI directly to order.

Accessing the World's Information since 1938

300 North Zeeb Road, Ann Arbor, MI 48106-1346 USA

Order Number 8820916

Influence functions of structures bonded to a saturated elastic half-space

Xu, Jimin, Ph.D.

City University of New York, 1988

U·M·I
300 N. Zeeb Rd.
Ann Arbor, MI 48106

PLEASE NOTE:

In all cases this material has been filmed in the best possible way from the available copy. Problems encountered with this document have been identified here with a check mark ✓.

1. Glossy photographs or pages _____
2. Colored illustrations, paper or print _____
3. Photographs with dark background _____
4. Illustrations are poor copy _____
5. Pages with black marks, not original copy ✓
6. Print shows through as there is text on both sides of page _____
7. Indistinct, broken or small print on several pages _____
8. Print exceeds margin requirements _____
9. Tightly bound copy with print lost in spine _____
10. Computer printout pages with indistinct print _____
11. Page(s) _____ lacking when material received, and not available from school or author.
12. Page(s) _____ seem to be missing in numbering only as text follows.
13. Two pages numbered _____. Text follows.
14. Curling and wrinkled pages _____
15. Dissertation contains pages with print at a slant, filmed as received _____
16. Other _____

_____

_____

INFLUENCE FUNCTIONS OF STRUCTURES

BONDED TO A SATURATED ELASTIC HALF-SPACE

by

JIMIN XU

A dissertation submitted to the Graduate Faculty in Engineering in partial fulfillment of the requirements for the degree of Doctor of Philosophy , The City University of New York .

1988

This manuscript has been read and accepted for the Graduate Faculty in Engineering in satisfaction of the dissertation requirement for the degree of Doctor of Philosophy .

Jan. 19, 1988 — date

Mumtaz K. Kassir — Chairman of Examining Committee

Jan. 20, 1988 — date

Jacques E. Benveniste — Executive Officer

Professor J. E. Benveniste

Professor C. J. Costantino

Professor C. M. Miller

Professor M. K. Kassir

Chairman and Mentor

The City University of New York

ABSTRACT

INFLUENCE FUNCTIONS OF STRUCTURES
BONDED TO SATURATED ELASTIC HALF-SPACE

by

Jimin Xu

Advisor : Professor Mumtaz K. Kassir

This dissertation is concerned with the propagation of harmonic waves generated by a moveable rigid strip footing in contact with a saturated porous elastic half-space . A comprehensive analytical solution is developed to generate the influence functions when the footing undergoes the basic modes of motion . The problem is formulated within the framework of Biot's classical theory of two-phase media in which the solid portion obeys the laws of linear elasticity and the fluid is governed by Darcy's law . Linear hysteretic damping characteristics of the medium are included in the constitutive relations . Integral Transform techniques are used to reduce the mixed boundary-value

problem of a welded (and smooth) surface footing to a set of coupled Fredholm integral equations of the first kind and a numerical solution is provided . Frequency-dependent interaction functions (stiffnesses and radiation damping coefficients) of two typical soil samples consisting of saturated dense sand and saturated medium soft clay are computed and exhibited graphically to reveal the influence of pore water , permeability effects and hysteretic damping characteristics of the medium . It is concluded that the impact of pore fluid on the influence functions is quite substantial . Because of the soil permeability , the pore fluid becomes essentially trapped in the soil and tends to move with the solid skeleton . This is especially true for the vertical and rocking modes of response in which the motion of the surface footing is resisted by the half-space medium through the coupling effect at the interface of the solid portion and the trapped fluid . In that vicinity , the shear holding the fluid portion causes both the soil skeleton and the trapped fluid to move together . Substantial inscreases are also observed in the magnitude of the coupling coefficients compared to the dry case . For the horizontal mode , the influence functions are marginally affected by the soil permeability .

Soil hysteretic damping ratios ranging from 0% to 10% are assumed to study the impact of non-linearity of actual soil media on the influence functions . The results obtained indicate considerable increases in the radiation damping coefficients for all three modes of

response , especially for the sandy material . Moderate changes in the stiffnesses are observed due to the hysteretic damping effect .

A parametric study to reveal the impact of soil permeability on the type of contact condition assumed between the surface footing and the underneath-half-space is also carried out . Appreciable differences between the welded and smooth contacts for all three modes of response are indicated when the half-space is fully saturated , while almost identical results are obtained between the two types of contact conditions when the medium is assumed dry .

The differences between the responses of the sand and clay are mainly reflected in the type of the contact conditions between the footing and the underneath-half-space . The results indicate that the clay material is more sensitive to the type of contact than the sandy material .

Finally , it is worth mentioning that the results presented here are useful in determining the response of surface structures to dynamic loading , in particular , seismic excitations and machine vibrations .

ACKNOWLEDGEMENTS

I wish to express my sincere gratitude to my advisor , Professor Mumtaz k. Kassir , for his expert guidance and constant support during the course of this research .

I would also like to thank the members of my Doctoral Committee and the department of civil engineering for their encouragement and many invaluable advises . I am especially grateful to Professor Charles A. Miller for his inspiration and continuous academic and financial supports which make this research possible .

TO MY PARENTS

TABLE OF CONTENTS

LIST OF FIGURES

LIST OF PLOTS

LIST OF TABLES

NOMENCLATURE

A	Abbreviation
$A_n^{(j)}$	Coefficients in the contact shear stress expansion .
a	Half width of the footing.
$a_j, j=1,2,3,$	Abbreviations
B	Abbreviation
$B_n^{(j)}$	Coefficients in the contact normal stress expansion .
b_1	$1/(\beta_2\omega_1^2 - \beta_1\omega_2^2 - 2\gamma\omega_c^2)/2$
C	Abbreviation.
c	$c = E_c c_2/(\rho V_c^2)$
c_1	$c_1 = \nu/(1-\nu)$
c_2	$c_2 = (1-2\nu)/[2(1-\nu)]$
d	Velocity of an incident wave.
d^*	Average diameter of the solid skeleton pores.
E_c	Confined modulus.
e	$e = \partial u_x/\partial x + \partial u_y/\partial y + \partial u_z/\partial z$
$\underline{e}_j, j=x,y,$	unit base vectors in x and y directions.
$F(s,\omega)$	Rayleigh function for the saturated medium.
$F_1(s,\omega)$	$F_1(s,\omega) = 2(s^2 - \gamma\omega^2/V_c^2) + 2n_3(\beta_1 n_2 - \beta_2 n_1)$.
$F_2(s,\omega)$	$F_2(s,\omega) = 2\gamma\omega^2/V_c^2 - \omega^2/V_3^2 + F_1(s,\omega)$.

$F^{(j)}, j=1,,7,$ Resulting vertical force acting on the footing by the halfspace.

f Porosity of solid skeleton .

f_t $f_t = \pi v^*/4d^*$

H Horizontal surface line load.

$H^{(j)}, j=1,,7,$ Resulting horizontal force acting on the footing by the halfspace.

h $2h$ = Height of the footing.

i $i = (-1)^{1/2}$.

K $K = \alpha' / (E_c + \alpha^2 \alpha')$

k The coefficient of permeability.

k_I $k_I = \omega/d$

l Integer subscript.

$M^{(j)}, j=1,,7,$ Resulting rocking moment acting on the footing by the halfspace.

N $N = \rho'/\rho$

$n_j(s), j=1,2,3,$ $n_j(s) = (s^2 - \omega^2/v_j^2)^{1/2}$

P Vertical surface line load.

p Fluid pore pressure.

$Q_j, j=x,y,$ Complex-valued functions specifying the amplitude and phase of an incident wave.

s Wave number .

$\bar{s}$ $\bar{s} = as$

t Time variable.

U Horizontal displacement of the center of the footing.

$U_j, j=x,y,z,$ Components of the fluid displacements.

$u_j, j=x,y,z,$ Components of displacements of the solid skeleton.

$u_j^k(x-\xi), j=x,y, k=H,P,$ Green functions.

V Veritical displacement of the center of the footing.

V_c Compressional velocity .

$V_j, j=1,2,$ Velocities of the compresional body waves.

V_3 Velocity of the shear body wave.

V_s Shear Velocity.

$W_j, j=x,y,z,$ $W_j = f(U_j-u_j)$.

$x,y,z,$ Coordinates.

α Compressibility of solid fraction.

α' Compressibility of fluid fraction.

$\beta_j, j=1,2,$ $\beta_j=\lambda_j(a_j+\alpha)/[\lambda_2(a_2+\alpha) - \lambda_1(a_1+\alpha)]$

γ Abbreviation.

γ' Unit weight of the fluid.

Δ Abbreviation.

Δ_c Abbreviation.

ε Fluid volumetric strain.

θ Angular rotation about the mass center of the footing.

λ_c Hysteretic damping ratio for hydrostatic compression .

λ_s Hysteretic damping ratio for deviatoric strain.

μ Shear modulus.

ν Poison's ratio.

ν^* Kinematic viscosity of fluid.

ξ Integration variable.

$\bar{\xi}$ $\bar{\xi}=a\xi$.

π $\pi=3.1415926$

ρ Total mass density of bulk material.

ρ' Mass density of fluid.

$\tau_j, j=x,y,xy$, Total stresses of the solid skeleton.

$\phi_j, j=1,2,3$, Arbitraty constants.

$\phi_j, j=f,s$, Potential functions.

$\Psi_j, j=f,s$, Potential functions.

Ω $\Omega = \partial u_x/\partial y - \partial u_y/\partial x$

ω circular frequency.

$\bar{\omega}$ $\bar{\omega} = a\omega/V_s$

CHAPTER 1. INTRODUCTION

The effect of flexibility of a soil on the dynamic response of embedded foundations and the attached structures, particularly when subjected to seismic excitation , has been a subject of considerable interest and research for many years . This effect , usually characterized by the dynamic force-displacement relationships , plays an important role in assessing and evaluating the structural responses to seismic events , especially when dealing with very stiff and massive structures (such as nuclear power plants) and relatively soft soils . Moreover , when the soil which supports the structure is saturated by ground water , it is expected that the structural responses and soil-structure interaction are significantly modified due to the influence of the soil-water system on the embeded structures .

Performing the seismic response analyses of a nuclear power plant facility and other important structures, generally speaking , requires a multidisciplinary effort . One of the major factors which play a key role in the prediction of the structural response during soil-structure interaction process is an adequate knowledge of the force-displacement characteristics of the soil foundation . This relationship may be identified in the form of an impedance (stiffness) function or , a compliance (flexibility) function, and the combination of such functions corresponding to motions of a foundation of different

modes will form a set of the influence functions or interaction coefficients which characterize the interactive dynamic relation of the soil half-space to the atop foundation . Because of its special use in determining the ground structure responses to seismic motions , the evaluation of the influence functions for typical soil foundations becomes essential in developing a better understanding of the soil-structure interaction phenomenon .

For a single-phase elastic half-space , considerable amount of work has been done on the topic begining with the work of Lamb (1904) . Several analytical techniques , such as integral transforms , Green's functions , etc. , as well as finite element have been developed to treat various aspects of the topic . Confining attention to the analytical work and citing the available references , Reissner (1936) and Miller and Pursey (1954) treated the problem of a uniform oscillating pressure acting on a circular region on an elastic half space . The problem of most physical interest occurs when displacements corresponding to indentation by a rigid body are prescribed over a given region and the surface exterior to this region are stress free . Quinlan (1953) , Sung (1953) and Bycroft (1956) approached these two-and-three-dimensional problems by assuming the dynamic stress distribution to be proportional to the static stress distribution . Reissner and Sagoci (1944) , Ufliand (1961) , Collins (1962) and Gladwell (1968) discussed problems of

torsional oscillations of a rigid disk attached to semi-infinite elastic solids . Awjobi and Grootenhius (1965) , Zakorko and Rostovtsev (1965) and Robertson (1966) investigated the vertical and/or rocking oscillations of a smooth disk in contact with a half-space . Luco and Westmann (1971) and Luco and Mita (1987) presented the dynamic compliances of the circular footing for a wide range of values of the input frequency which can be used in soil-structure interaction studies . Karasadhi , Keer and Lee (1968) determined the force-displacement relationships due to harmonic oscillations of a smooth rectangular footing at the surface of an isotropic elastic half-space . The corresponding problem of a welded footing was investigated by Luco and Westmann (1972) and some limited numerical results were obtained . Utilizing a formulation suggested by Thau (1967) and approximating the contact stresses , Dien (1972) obtained a solution for welded (and smooth) rectangular oscillator undergoing basic modes of motion . The solution , which gives accurate results for smooth footing , is also valid over the frequency range of interest in seismic response analysis . Extending the work by Karasadhi ,Keer and Lee (1968) , Freedman and Keer (1971) obtained the solution for an orthotropic half-space . Althougth the above-mentioned solutions of the interaction coefficients are mostly two-dimentional and linear, they have been proven to be adequate and acceptable for most practical consideration in analyzing soil-structure interaction problems .

When the medium consists of an elastic soil saturated by ground water , usually refered to as two-phase medium , there is a conspicous lack of analytical solutions needed to provide meaningful insight into the impact of the soil-water system on the seismic response of surface footings . The basic equations governing the propagation of waves in such a medium were developed by Biot (1956,1962) . Biot's theory takes into account the effects of fluid viscosity and compressibilty and gives rise to coupling between the solid and fluid states of stress . In this theory , three types of waves are found to exist in the infinite medium , two dilatational and one shear wave . The first of the dilatational waves propagates like the compression wave in an elastic solid with little dispersion , while the second dilatational wave is highly attenuated and travels at much slower rate . Because the trapped mass of the fluid in the pores of the solid skeleton changes with time , the shear wave velocity is influenced by the permeability of the fluid and the elastic characteristics of the solid material . The presence of Rayleigh-type surface waves in Biot's field equations were investigated by Jones (1961) and Deresiewicz (1962) who also studied the Love waves and layering effects . Waves in saturated layered media were studied by Philippacopoulos(1987) . To the best knowledge of the author , there are no half-space analytical solutions to Biot's general field equations . Paul (1976a,b) solved some transient , two-dimensional surface loading problems where the dissipation effect of the fluid , represented by the viscosity term in Biot'equations , is neglected . Such solutions are of

limited use in determining the seismic response of a saturated soil to surface footings . Finite element methods have been applied by Lung (1980) and Costantino (1986) to solve half-plane wave propagation problems for the two-phase medium . Although damping characteristics of the medium were included in the formulation , the interaction coefficients were generated for a medium without structural damping . These authors conclude that the dissipation of the pore water significantly affects the interaction coefficients over the frequency range of interest . It should be mentioned that the unrealistic oscillations in their results are due to the numerical nature of satisfying the radiation conditions in finite element methods . In finite element methods , finite domains are considered to model a half-space and this requires the adoption of special boundary conditions (transmitting boundaries) to assure outward radiation of the waves . See also the work by Dasgopta (1980) . This implies that the reliability of the finite element code needs be checked with known analytical works to assure its accuracy and validity . The development of such analytical capability motivates the present research .

A detailed analytical investigation of the impact of the water content and its interaction with the surrounding soil skeletons on the interaction coefficients is performed in the course of this work . When the porous soil is saturated by ground water , the system is

characterized as two-phase medium in which the soil and the trapped water are coupled together through the soil permeability . It is known that the interaction between the soil skeleton and the trapped water greatly influence the dynamic strain of the soil and have significant effect on the soil-structure interaction process .

The basic problem of the soil-structure interaction is illustrated in Fig.1 . It involves the determination of the response of a structure situated at or near the surface of a water saturated half space , when subjected to seismic excitation . Formulation of a plain strain model is presented in this research . It is considered to be appropriate for long structures subjected to in-plane motions , namely the motions perpendicular to the long axis . Such a plane-strain model is shown in Fig.2 , in which a rigid footing (foundation) sits on the surface of a saturated half space , and is subjected to the basic modes of oscillatory motions , namely , the horizontal , vertical and rocking as well as their combinations . The model is then supplied with appropriate boundary conditions and special mathematical techniques are used to formulate the problem and to provide solutions to generate frequency-dependent interaction coefficients for the basic modes of motion .

The major objective of this research is to generate the interaction coefficients (both stiffnesses and radiation damping coefficients) for a two-phase elastic medium . The solid skeleton is assumed linearly elastic with hysteretic damping characteristics while the fluid is viscous and compressible . Biot's generalized field equations govern the motions in the solid and fluid parts of the medium . The plan of dissertation is arranged as follows : Chapter two contains the basic equations governing the wave propagation . Linear hysteretic damping properties of the system have been included in the constitutive equations to account for non-linearities in the modeling of the medium as is customarily done in soil-structure interaction problems . Also , the compressive and shear waves are separated using suitable potential function representation of the displacements in the solid and fluid parts . For this purpose it is found convenient to assume identical hysteretic damping ratios for the normal and shearing strains . Integral transform solutions , appropriate to the medium under consideration , are then developed .

In Chapter three , the responses to vibratory harmonic surface line loads are investigated . Solutions of the displacement fields due to both the horizontal and vertical vibratory surface line loads are obtained . These solutions are used in latter chapters to generate the appropriate Green ' s functions for formulating the problems under consideration .

The formulation of the problem of diffraction of harmonic waves by a moveable rigid footing in contact with the saturated half-plane is carried out in Chapter four . Here , the procedure employed follows the one suggested by Thau (1967) and Oien (1971) . It is assumed that the diffraction of harmonic waves by a movable rigid strip footing be divided into two problems , namely ,the diffraction of waves by a fixed strip footing , and the radiation caused by the forced motion of an inertialess footing . The solution of the first problem yields the loading on the footing due to the incident waves which tend to force the footing to move . The solution to the second problem yields the loads acting on the footing due to the resistance of the half space to a forced motion . The loads given by these two problems constitute a set of interaction coefficients which completely characterize the interacton of the rigid footing with the fully saturated surrounding medium and can be determined without regard to the inertia porperties of the footing . Utilizing the Green's functions mentioned earlier and approximating the contact stresses beneath the strip in a manner which reflects and preserves the essential behavior of the solution (namely , by square root singularity characteristics) , the problem of determining the influence functions for welded (and smooth) footing is reduced in chapter four to coupled Fredholm integral equations of the first kind . To facilitate the numerical work , the integral equations are then transformed into algebraic equations . The expressions for the representative influence

functions are given which contain coefficients to be determined numerically . Once these interaction coefficients have been determined , various methods of seismic response analyses , such as lumped parameter method using frequency-dependent interaction coefficients , can be employed to perform a complete soil-structure interaction analysis .

Chapter five contains the numerical results of the interaction coefficients of two typical media consisting of saturated dense sand and saturated medium soft clay and a discussion of the results , in particular , the modifications due to pore water and damping characteristics of the system are pointed out . It is concluded that the impact of pore fluid on the influence functions is quite substantial . Because of the soil permeability , the pore fluid becomes essentially trapped in the soil and tends to move with the solid skeleton . This is especially true for the vertical and rocking modes of response in which the motion of the surface footing is resisted by the half-space medium through the coupling effect at the interface of the solid portion and the trapped fluid due to the shear holding the fluid portion to move together with the solid skeleton of the soil . Substantial inscreases are also observed for the coupling coefficients . For the horizontal mode , the influence functions are affected to some small degree by the soil permeability .

Soil hysteretic damping ratios ranging from 0% to 10% are assumed to study the impact of non-linearity of actual soil media on the influence functions . The results obtained indicate considerable increases in the radiation damping coefficients for all three modes of response , especially for the sandy material . Moderate changes in the stiffnesses are observed due to the hysteretic damping effect .

The impact of the soil permeability is also found to be significant depending on the type of contact condition assumed between the surface footing and the underneath half-space . Appreciable differences between the welded and smooth contact conditions for all three modes of response are indicated when the half-space is fully saturated , while almost identical results are obtained between the two types of contact conditions when the half- space medium is assumed dry .

The differences between the responses of the sand and clay are mainly reflected in the type of the contact conditions assumed between the footing and the underneath half space . The results indicate that the saturated clay material is more sensitive to the type of contact conditions than the sandy material .

Finally , Chapter six includes conclusions and some suggestions for future research activities on this topics . This reseach has shown

that by taking the water content into consideration in the formulation , some significant impacts on the interaction coefficients occur which will in turn affect performing the dynamic responses of the structures . It is hoped that this research could assist in developing better appreciation of the nature of such interaction effects in dealing with structures built in partially or fully saturated soils .

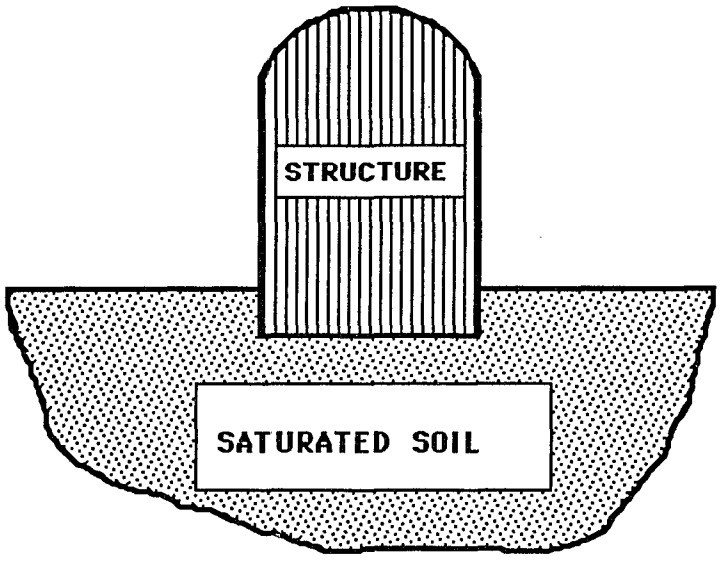

FIGURE 1. SOIL-STRUCTURE INTERACTION PROBLEM.

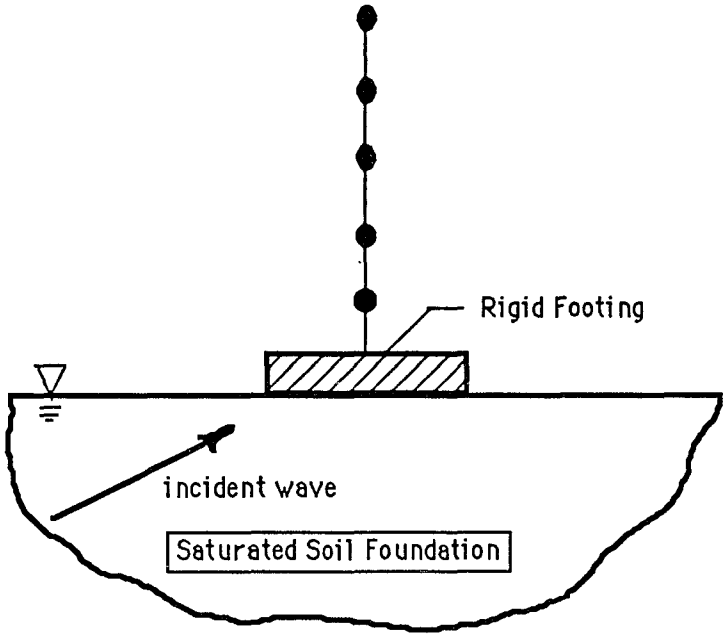

Two dimensional Plane-Strain Model

FIGUTRE 2. TWO DIMENSIONAL PLANE-STRAIN MODEL.

CHAPTER-2. WAVE PROPAGATION IN POROUS SATURATED MEDIA

In this chapter , the basic equations governing wave propagation in a dissipative saturated soil-water medium are developed using the well-known Biot's classical theory which includes the coupling between the solid and fluid stress states through the soil permeability effect . The significance of this interaction effect on the characteristics of body waves which differ from those developed in an ideal elastic solid is also examined . General expressions for the stress and displacement fields , appropriate to a plane strain medium , are developed in terms of wave potentials .

2.1 BASIC EQUATIONS:

Consider an element of the two-phased elastic material consisting of solid matrix and pore fluid . With reference to Cartesian coordinates , denote the components of the solid displacement field by u_j and those of the average fluid portion by U_j (j=x,y,z) . The latter components are defined such that the volume of fluid displaced through unit areas normal to the reference axes are fU_j where f designates the porosity of the medium . It is worth mentioning here that in Biot's theory , the medium is composed of a statistically isotropic porous material in such a way that for all cross sections , the same ratio of

the fluid area to the solid area is maintained and thus the porosity , f , is identical throughout the medium . The displacement components of the fluid relative to the solid and measured in terms of the volume per unit area of the bulk material are $W_j = f(U_j - u_j)$. Because of its occurrence in a variety of applications , the problem is viewed as one in plane strain , namely , a saturated half-space bounded by the plane y = 0 and occupying the region $y \geq 0$, $|x| < \infty$, $|z| < \infty$.

Based upon Biot's classical formulation (1962) and assuming isotropic elastic properties , the pore fluid pressure (p) in the medium is governd by Darcy ' s law and given by the relation

$$p = \alpha' (-\alpha e + \varepsilon) \quad , \qquad (2.1)$$

in which α , α' represent the compressibilities of the solid and fluid particles , respectively , and e , ε are the corresponding solid dilatation and fluid volumetric strains defined as

$$e = \partial u_x/\partial x + \partial u_y/\partial y \quad , \qquad (2.2a)$$

$$\varepsilon = - (\partial w_x/\partial x + \partial w_y/\partial y) \quad , \qquad (2.2b)$$

In as much as this research is motivated by determining the response of a soil-structure system to dynamic loading , the structural damping properties of the soil , which are independent of the frequency , are included in the stress - strain relations . It follows that the components of the total bulk stress tensor are related to the displacements and velocites through the relations

$$\tau_{xx} = E_c (\partial u_x/\partial x + c_1 \partial u_y/\partial y) - \alpha p + \lambda_c E_c (\partial \dot{u}_x/\partial x + c_1 \partial \dot{u}_y/\partial y) \quad ,(2.3a)$$

$$\tau_{yy} = E_c (c_1 \partial u_x/\partial x + \partial u_y/\partial y) - \alpha p + \lambda_c E_c (c_1 \partial \dot{u}_x/\partial x + \partial \dot{u}_y/\partial y) \quad ,(2.3b)$$

$$\tau_{xy} = c_2 E_c [\partial u_x/\partial y + \partial u_y/\partial x + \lambda_s (\partial \dot{u}_x/\partial y + \partial \dot{u}_y/\partial x)] \quad ,(2.3c)$$

where the term λ_c represents the hysteretic damping ratio associated with hydrostatic compression while λ_s represents the hysteretic damping ratio associated with deviatoric (or shear) strains . The constants c_1 , c_2 and E_c (confined modulus) depict the elastic characteristics of the solid portion of the material and are defined as follows :

$$c_1 = \nu /(1 - \nu) \quad , \quad (2.4a)$$

$$2c_2 = 1 - c_1 \quad , \quad (2.4b)$$

$$E_c = (1 - \nu) E / (1 + \nu) (1 - 2\nu) \quad , \quad (2.4c)$$

$$E_c c_2 = \mu \quad , \quad (2.4d)$$

Here , E , μ and ν designate the modulus of elasticity , shearing modulus and Poisson's ratio of the solid skeleton , repectively . In equations (2.3) , a dot over a symbol represents differentiation with respect to the time variable (t) .

Applying Lagrange's equations , the governing equations of small motion at a point in the two-phased medium can be expressed in the form of

$$\frac{\partial \tau_{xx}}{\partial x} + \frac{\partial \tau_{xy}}{\partial y} = \rho \ddot{u}_x + \rho' \ddot{w}_x \quad , \quad (2.5a)$$

$$\frac{\partial \tau_{xy}}{\partial x} + \frac{\partial \tau_{yy}}{\partial y} = \rho \ddot{u}_y + \rho' \ddot{w}_y \quad , \quad (2.5b)$$

for the total bulk stresses , and

$$-\frac{\partial p}{\partial x} = \rho' \ddot{u}_x + \frac{1}{f}\rho' \dot{w}_x + \frac{\gamma'}{k}\dot{w}_x \quad , \quad (2.6a)$$

$$-\frac{\partial p}{\partial y} = \rho' \ddot{u}_y + \frac{1}{f}\rho' \dot{w}_y + \frac{\gamma'}{k}\dot{w}_y \quad , \quad (2.6b)$$

for the pore pressure . In equations (2.5) and (2.6) , ρ designates the mass density of the composite solid - fluid medium , ρ' is the mass density of the fluid and γ' , k are , respectively , the unit weight and the coefficient of permeability . In Biot' work (1962) , the term γ'/k is replaced by η/k where η and k represent Biot' s definition of the fluid viscosity and soil permeability , respectively . The notation adopted here is more commonly used in current soil mechanics terminology . Upon neglecting the inertia terms in equations (2.6) whose effect can be obtained by simple superposition of a static solution to the dynamic stress state , one obtains the well known Darcy ' s law governing the seepage effects through soils . It should also be pointed out that the afore-mentioned formulation is valid for relatively low frequency motions where the assumptions of laminar or Poiseuile flow hold . The cutoff frequency , f_t , as determined by Biot , is given by the relation

$$f_t = \pi \nu^* / 4d^{*2} \quad , \quad (2.7)$$

where ν^* and d^* represent the kinematic viscosity of the fluid and the average diameter of the pores , respectively . For a typical sandy medium with an average pore diameters of 0.01 cm or less , and saturated with water at 15° c , the cutoff frequency is about 100 cycles/second , well beyond any frequency range of practical interest in Soil-Structure Interaction problems . Further details can be found in Biot 's original work (1956) .

Inserting relations (2.1) through (2.4) into equations (2.5) and (2.6) render

$$V_c^2 \frac{\partial}{\partial x}(e - \alpha k \varepsilon) + V_s^2 \frac{\partial \Omega}{\partial y} = \ddot{u}_x + N \ddot{w}_x$$

$$-\frac{E_c}{\rho}\left[\lambda_c \frac{\partial^2 \dot{u}_x}{\partial x^2} + c_2 \lambda_s \frac{\partial^2 \dot{u}_x}{\partial y^2} + (c_1 \lambda_c + c_2 \lambda_s) \frac{\partial^2 \dot{u}_y}{\partial x \partial y}\right] , \quad (2.8a)$$

$$V_c^2 \frac{\partial}{\partial y}(e - \alpha k \varepsilon) - V_s^2 \frac{\partial \Omega}{\partial x} = \ddot{u}_y + N \ddot{w}_y$$

$$-\frac{E_c}{\rho}\left[c_2 \lambda_s \frac{\partial^2 \dot{u}_y}{\partial x^2} + \lambda_c \frac{\partial^2 \dot{u}_y}{\partial y^2} + (c_1 \lambda_c + c_2 \lambda_s) \frac{\partial^2 \dot{u}_x}{\partial x \partial y}\right] , \quad (2.8b)$$

and

$$KV_c^2 \frac{\partial}{\partial x}(\alpha e - \varepsilon) = N\ddot{u}_x + \frac{N}{f}\dot{w}_x + \frac{\gamma'}{k\rho}\dot{w}_x \quad , \quad (2.8c)$$

$$KV_c^2 \frac{\partial}{\partial y}(\alpha e - \varepsilon) = N\ddot{u}_y + \frac{N}{f}\dot{w}_y + \frac{\gamma'}{k\rho}\dot{w}_y \quad , \quad (2.8d)$$

in which , $\Omega = \partial u_x/\partial y - \partial u_y/\partial x$, designates the rotation of an element of the solid skeleton , $N = \rho'/\rho$, V_c and V_s represent compressional and shear velocities of the bulk material , respectively , and K is a dimensionless modulus , defined as :

$$V_c^2 = (E_c + \alpha^2\alpha') / \rho \quad , \quad (2.9a)$$

$$V_s^2 = \mu / \rho \quad , \quad (2.9b)$$

$$K = \alpha' / (E_c + \alpha^2\alpha') \quad , \quad (2.9c)$$

Equations (2.8) represent the displacement equations of motion

governing the propagation of elastic waves in a saturated porous material possessing linear hysteretic damping . In an unbounded domain , these equations give rise to two distinct dilatational waves and one distortional wave . One wave of dilatation is transmitted through the fluid portion while the other is transmitted through the solid skeleton . These two waves are coupled with each other through the stiffnesses of the solid and fluid components of the system as well as through the coupling effect produced by motions of the solid and pore fluid . Furthermore , the dilatational and the distortional waves are also coupled through the hysteretic damping ratios . For the mere purpose of possible implementation of conventional approaches to wave propagation problems , the body waves must be decomposed into separate dilatational and distortional ones . This will facilitate the mathematical solution as well as simplify the physical interpretations of the results . Although generally the hysteretic damping ratios of the hydrostatic and shearing strains are not equal in an actual material , it is necessary to assume them equal in order to facilitate the aforementioned decomposition of the waves . Fortunately they do not vary significantly from each other in typical soil materials , and the previous assumption is usually justified in analyzing soil-structure interaction problems . Upon incorporating the assumption $\lambda_S = \lambda_C$, the separation of the dilatational waves from the distortional wave in the governing equations is readily achieved utilizing the potential functions as described in the next section .

2.2 COMPRESSIVE AND SHEAR WAVES:

In order to determine the equations of propagation governing the compressive and shear waves , the following substitutions are introduced into equations (2.8)

$$u_x = \partial\phi_s/\partial x - \partial\psi_s/\partial y \quad , \quad (2.10a)$$

$$u_y = \partial\phi_s/\partial y + \partial\psi_s/\partial x \quad , \quad (2.10b)$$

$$w_x = \partial\phi_f/\partial x - \partial\psi_f/\partial y \quad , \quad (2.10c)$$

$$w_y = \partial\phi_f/\partial y + \partial\psi_f/\partial x \quad , \quad (2.10d)$$

where ϕ_s , ϕ_f , ψ_s , ψ_f represent the potential functions to be determined . It is found that the compressive waves are governed by

$$V_c^2 \nabla^2 (\phi_s + \alpha k \phi_f + \frac{k}{\alpha'} E_c \lambda_c \dot{\phi}_s) = \ddot{\phi}_s + N \ddot{\phi}_f \quad , \quad (2.11a)$$

$$K V_c^2 \nabla^2 (\alpha \phi_s + \phi_f) = N \ddot{\phi}_s + \frac{N}{f} \ddot{\phi}_f + \frac{\gamma'}{k\rho} \dot{\phi}_f \quad , \quad (2.11b)$$

while the shear wave is determined from the set :

$$v_s^2 \nabla^2 (\psi_s + \lambda_c \dot{\psi}_s) = \ddot{\psi}_s + N \dot{\psi}_s \quad , (2.12a)$$

$$-\left(\frac{\gamma'}{k\rho} \right) \dot{\psi}_f = N \ddot{\psi}_s + \frac{N}{f} \dot{\psi}_f \quad , (2.12b)$$

For vibratory loading introduced at the boundary of the half-space with harmonic time dependence $e^{i\omega t}$, ω being the applied frequency , equations (2.11) and (2.12) admit exponential solutions , appropriate to propagation of waves in the medium , of the form

$$(\phi_s , \phi_f , \psi_s , \psi_f) \sim e^{-ny+i(\omega t - sx)} \quad , (2.13)$$

where n is as yet unknown complex parameter and s and ω are real . s represents the wave number and $2\pi/s$ is the wave length . In order to insure bounded displacements and stresses at remote distance and also an outward traveling of a train of waves from the source (radiation condition) , both the real and imaginary parts of n must satisfy the requirements:

$$\mathrm{Re}\, n \geq 0 \quad \text{and} \quad \mathrm{Im}\, n \geq 0 \quad , (2.14)$$

Upon substituting expressions (2.13) into (2.11) and carrying out the necessary algebraic manipulation , it is found that (omitting the term $e^{i\omega t}$ for brevity) :

$$\begin{Bmatrix} \phi_s \\ \phi_f \end{Bmatrix} = e^{-isx} \sum_{j=1}^{2} \begin{Bmatrix} 1 \\ a_j \end{Bmatrix} \phi_j(s)\, e^{-n_j y} \qquad , \quad (2.15)$$

where $\phi_j(s)$, j=1,2 , are arbitrary coefficients and the exponents , n_j , are defined as :

$$\left.\begin{aligned} n_j &= \sqrt{s^2 - \omega^2 / V_j^2} \\ \mathrm{Re}\, n_j &\geq 0 \ , \ j = 1 , 2 \\ \mathrm{Im}\, n_j &\geq 0 \ , \ j = 1 , 2 \end{aligned}\right\} \qquad , \quad (2.16)$$

The "Wave velocities" , V_j , and the coefficients , a_j , j= 1 , 2 , in equations (2.15) and (2.16) are complex-valued functions of the material

parameters and the applied frequency , and are given in appendix A . In a similar manner , examining wave equations (2.12) , the shear wave is found to be governed by the potential functions :

$$\begin{Bmatrix} \Psi_s \\ \Psi_f \end{Bmatrix} = \phi_3(s)\, e^{-n_3 y - isx} \begin{Bmatrix} 1 \\ a_3 \end{Bmatrix} \quad , \quad (2.17)$$

Here , the exponent , n_3 , stands for

$$\left.\begin{aligned} n_3 &= \sqrt{s^2 - \omega^2 / V_3^2} \\ \mathrm{Re}\, n_3 &\geq 0 \text{ and } \mathrm{Im}\, n_3 \geq 0 \end{aligned}\right\} \quad , \quad (2.18)$$

and the quantities V_3 and a_3 are complex-valued functions of the material properties and the applied frequency , and decribed in appendix A .

Equations (2.15) and (2.17) represent the basic solutions to the potential functions for both compression and shear waves in terms of arbitrary constants ϕ_j , $j = 1 , 2 , 3$. Examination of the equations (2.15) and (2.17) readily reveal the influence of structural coupling in the compression waves while the three waves are interrelated through the hysteretic damping ratios . By assuming ϕ_j to be functions of the parameter s , more general solutions of the type given in equations (2.15) and (2.17) can be built up . For any particular application , the transform parameters $\phi_j(s)$, $j = 1,2,3$, are uniquely determined from the imposed boundary conditions of the problem in hand .

2.3 TOTAL BULK STRESSES AND DISPLACEMENT COMPONENTS:

Utilizing equations (2.10) in conjunction with (2.15) and (2.17), it is readily shown that the expressions for the displacements in a saturated half-space are :

$$u_x = (-is\phi_1 e^{-n_1 y} - is\phi_2 e^{-n_2 y} + n_3\phi_3 e^{-n_3 y}) e^{-isx} \quad , (2.19a)$$

$$u_y = (-n_1\phi_1 e^{-n_1 y} - n_2\phi_2 e^{-n_2 y} + is\phi_3 e^{-n_3 y}) e^{-isx} \quad , (2.19b)$$

$$w_x = (-ia_1 s\phi_1 e^{-n_1 y} - ia_2 s\phi_2 e^{-n_2 y} + a_3 n_3\phi_3 e^{-n_3 y}) e^{-isx} \quad , (2.19c)$$

$$w_y = (-n_1 a_1\phi_1 e^{-n_1 y} - n_2 a_2\phi_2 e^{-n_2 y} - isa_3\phi_3 e^{-n_3 y}) e^{-isx} \quad , (2.19d)$$

and those for the pore pressure and bulk stresses immediately follow from equations (2.1) and (2.3). They are :

$$\tau_{xy} = \mu(1 + i\omega\lambda_c)[2is(n_1\phi_1 e^{-n_1 y} + n_2\phi_2 e^{-n_2 y}) - (s^2 + n_3^2)\phi_3 e^{-n_3 y}] e^{-isx} \quad , (2.20a)$$

$$\tau_{yy} = \mu (1 + i\omega\lambda_c) [\sum_{j=1}^{2} \{ 2s^2 - (\frac{1}{c_2} + \frac{\alpha\alpha'(\alpha+a_j)}{\mu(1+i\omega\lambda_c)}) \frac{\omega^2}{V_j^2} \} \phi_j \, e^{-n_j y}$$

$$- 2isn_3 \phi_3 \, e^{-n_3 y} \;] \, e^{-isx} \qquad , (2.20b)$$

$$\tau_{xx} = - \mu (1 + i\omega\lambda_c) [\sum_{j=1}^{2} \{ 2s^2 + (\frac{c_1}{c_2} + \frac{\alpha\alpha'(\alpha+a_j)}{\mu(1+i\omega\lambda_c)}) \frac{\omega^2}{V_j^2} \} \phi_j \, e^{-n_j y}$$

$$+ 2isn_3 \phi_3 \, e^{-n_3 y} \;] \, e^{-isx} \qquad , (2.20c)$$

$$p = \alpha'\omega^2 \, e^{-isx} \sum_{j=1}^{2} (\frac{\alpha + a_j}{V_j^2}) \phi_j(s) \, e^{-n_j y} \qquad , (2.20d)$$

The unknown coefficients ϕ_j , j = 1 , 2 , 3 , are determined from the boundary conditions of a particular application . Also , it is pointed out that in equations (2.19) and (2.20) , as in the sequel , the term $e^{i\omega t}$ is omitted .

CHAPTER 3. VIBRATORY HARMONIC SURFACE LOADS

In this chapter , the general solutions developed previously is utilized to determine response of the saturated half-space to vibratory harmonic surface line loads . Figure 3 shows the surface loads to be imposed on the half space . These solutions will be used in later sections as Green 's functions for formulating the mixed boundary value problem . The corresponding solutions for the single - phase half space medium were developed by Lamb (1904) .

3.1 RESPONSE TO HORIZONTAL SURFACE LINE LOAD:

When the surface of the half-space is subjected to a finite distribution of tangential periodic loading described by the relations:

$$p(x,0) = \tau_{yy}(x,0) = 0 \quad , \quad (3.1a)$$

$$\tau_{xy}(x,0) = \tau_0 e^{-isx} \quad , \quad \tau_0 = \text{constant.} \quad , \quad (3.1b)$$

The unknown quantities ϕ_j , j = 1,2,3 , can be determined by inserting (3.1) into equations (2.20) and working out the necessary algebra . It is found that

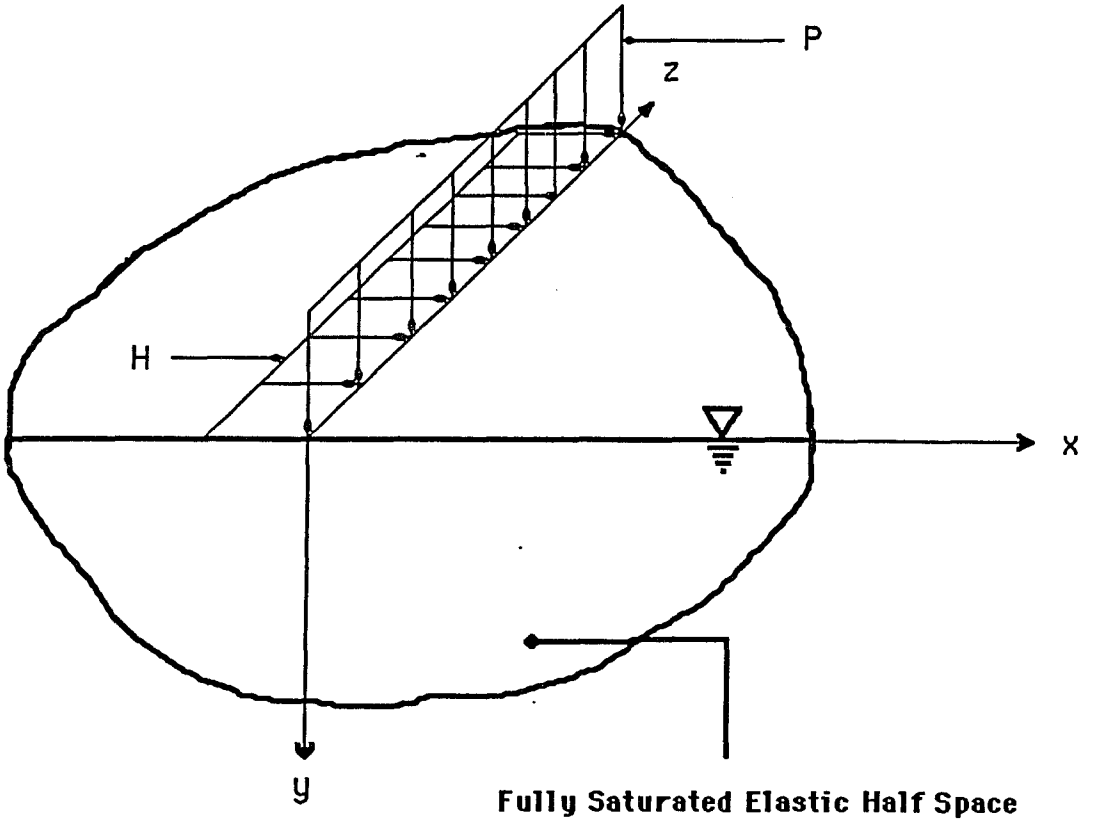

FIGURE(3)- CONCENTRATEDSURFACE LINE LOADS .

$$\phi_1 = 2i\beta_2 s n_3 \tau_0 / [\mu F(s,\omega)] \quad , \quad (3.2a)$$

$$\phi_2 = -\beta_1 \phi_1 / \beta_2 \quad , \quad (3.2b)$$

$$\phi_3 = -2(s^2 - \gamma\omega^2/V_c^2)\, \tau_0 / [\mu F(s,\omega)] \quad , \quad (3.2c)$$

in which $F(s,\omega)$ designates the Rayleigh function

$$F(s,\omega) = 2(1+i\omega\lambda_c)[(s^2 + n_3^2)(s^2 - \gamma\omega^2/V_c^2) + 2 n_3 s^2 (\beta_1 n_2 - \beta_2 n_1)] \quad , \quad (3.3)$$

and β_j , $j = 1$, 2 and γ are frequency dependent abbreviations introduced for algebriac convenience and are available in appendix A . The expressions of the displacement components can easily be computed from equations (2.19) and (3.2) . They are

$$u_x = \frac{2\gamma n_3 \omega^2 / V_c^2}{\mu F(s,\omega)} \tau_0 \, e^{-isx} \quad , \quad (3.4a)$$

$$u_y = \frac{i s F_1(s,\omega)}{\mu F(s,\omega)} \tau_0 \, e^{-isx} \quad , \quad (3.4b)$$

where $F_1(s,\omega) = 2(s^2 - \gamma\,\omega^2/V_c^2) + 2n_3(\beta_1 n_2 - \beta_2 n_1)$, (3.5)

The response to a concentrated line load of magnitude H per unit length of strip , acting parallel to the x-axis at x = y = 0 , is obtained by superimposing the stress distribution (3.1) such that the resultant forms a concentrated tangential line load . For this purpose , set $\tau_0 = Hds/(2\pi)$ in equations (3.1b) and integrate the resulting expressions with respect to s over the interval $(-\infty,\infty)$, leading to

$$\tau_{xy}(x,0) = g(x) = \frac{H}{2\pi}\int_{-\infty}^{\infty} e^{-isx}\, ds \qquad , (3.6)$$

Upon introducing the notation

$$\int_{-\infty}^{\infty} g(\xi)\, e^{is\xi}\, d\xi = H \qquad , (3.7)$$

and noting the definition of the Fourier integral and its inversion formula

$$g(x) = \frac{1}{2\pi}\int_{-\infty}^{\infty} e^{-isx}\, ds \int_{-\infty}^{\infty} g(\xi)\, e^{is\xi}\, d\xi \qquad , (3.8)$$

a representation of the tangential surface stresses can be achieved .

Now assume that

$$g(x) = \begin{cases} \infty & x = 0 \\ 0 & x \neq 0 \end{cases} \quad , \quad (3.9)$$

and also impose on g(x) the condition

$$\int_{-\infty}^{\infty} g(\xi)\, d\xi = H \quad , \text{ H is finite .} \quad , \quad (3.10)$$

then equation (3.9) reduces to (3.6) and H is the apparent concentrated tangential line load. Therefore , it is concluded that (3.4) become

$$u_x(x,0) = \frac{H}{\pi\mu} \int_{-\infty}^{\infty} \frac{\gamma n_3 \omega^2 / V_c^2}{F(s,\omega)} e^{-isx}\, ds \quad , (3.11a)$$

$$u_y(x,0) = \frac{iH}{2\pi\mu} \int_{-\infty}^{\infty} \frac{s F_1(s,\omega)}{F(s,\omega)} e^{-isx}\, ds \quad , (3.11b)$$

which give the surface displacements due to the horizontal loading .

3.2 RESPONSE TO VERTICAL SURFACE LOAD

For a vibratory vertical surface loading , the boundary conditions can be stated as

$$p(x,0) = \tau_{xy}(x,0) = 0 \quad , \quad (3.12a)$$

$$\tau_{yy}(x,0) = \sigma_0 e^{-isx} \quad , \quad \sigma_0 = \text{constant} . \quad , \quad (3.12b)$$

It can be immediatelly seen from equations (2.20) and (3.12) that

$$\phi_1 = \beta_2 \sigma_0 (s^2 + n_3^2) / [\mu F(s,\omega)] \quad , \quad (3.13a)$$

$$\phi_2 = - \beta_1 \phi_1 / \beta_2 \quad , \quad (3.13b)$$

$$\phi_3 = - 2 i s \sigma_0 (\beta_1 n_2 - \beta_2 n_1) / [\mu F(s,\omega)] \quad , \quad (3.13c)$$

Following the procedure employed previously , the response to a concentrated normal line load of magnitude P per unit length of strip , acting at $x = y = 0$, is obtained by setting $\sigma_0 = P /(2\pi)$ in equations (3.13) and integrating over interval $(-\infty , \infty)$. It follows that the surface values of the displacements are given by

$$u_x(x,0) = -\frac{iP}{2\pi\mu}\int_{-\infty}^{\infty}\frac{s\,F_2(s,\omega)}{F(s,\omega)}\,e^{-isx}\,ds \qquad , (3.14a)$$

$$u_y(x,0) = \frac{P}{2\pi\mu}\int_{-\infty}^{\infty}\frac{(\beta_2 n_1 - \beta_1 n_2)\,\omega^2/V_3^2}{F(s,\omega)}\,e^{-isx}\,ds \quad , (3.14b)$$

where $F_2(s,\omega) = 2\gamma\,\omega^2/V_c^2 - \omega^2/V_3^2 + F_1(s,\omega)$, (3.15)

In the sequel , equations (3.11) and (3.14) are used to develop the Green's functions suitable for the process of generating the influence functions , and the requirements Re $n_j \geq 0$ and Im $n_j \geq 0$, 1 , 2 , 3 , in these expressions must always be maintained to ensure outgoing waves and bounded stresses and displacements at the remote distance . In the complex s-plane , a proper interpretation of the integrals in equations (3.11) and(3.14) would require branch cuts be taken along the arcs Re $n_j = 0$ through the complex branch points ω/V_j , $j = 1 , 2 , 3$. Also , the complex poles of the Rayleigh function , $F(s,\omega)$, must be determined and contour integrations performed . However , in this case , the function $F(s,\omega)$ does not possess any real root due to the presence of the soil

permeability and the hysteretic damping and the integrals are well defined throughout their range of validity , namely , the real s-axis . Numerical treatment of these integrals can be carried out without any difficulties . The expressions for the stress components can be readily developed utilizing expressions (3.11) and (3.14) .

CHAPTER 4. DIFFRACTION OF HARMONIC WAVES BY A MOVEABLE RIGID FOOTING.

The problem of the diffraction of waves by a moveable rigid footing bonded to the surface of the water-saturated two-phase half-space is treated in this chapter . Figure (4) shows the geometry of the problem under consideration . The method of approach adopted is based on the principle of superposition commomly used to tackle complicated linear systems . Any linear system of problems can be resolved into several numbers of more fundamental , simpler basic problems whose solutions can be easily obtained in a conventional manner . The combination of these basic problems gives rise to the solution to the original system without much loss of accuracy . This philosophy is commonly adopted by many authors and employed here to formulate the diffraction problems in the first part of the chapter . The Green's function approach , which has been widely applied in mathematical physics and has been shown to be very powerful in the evalution of mixed boundary value problems , is utilized to generate the solutions to the influence functions which are essential in the soil-structure interaction process and constitute the primary objective of this work .

4.1. A RIGID STRIP IN CONTACT WITH A HALF-SPACE.

This section contains a description of the formulation required

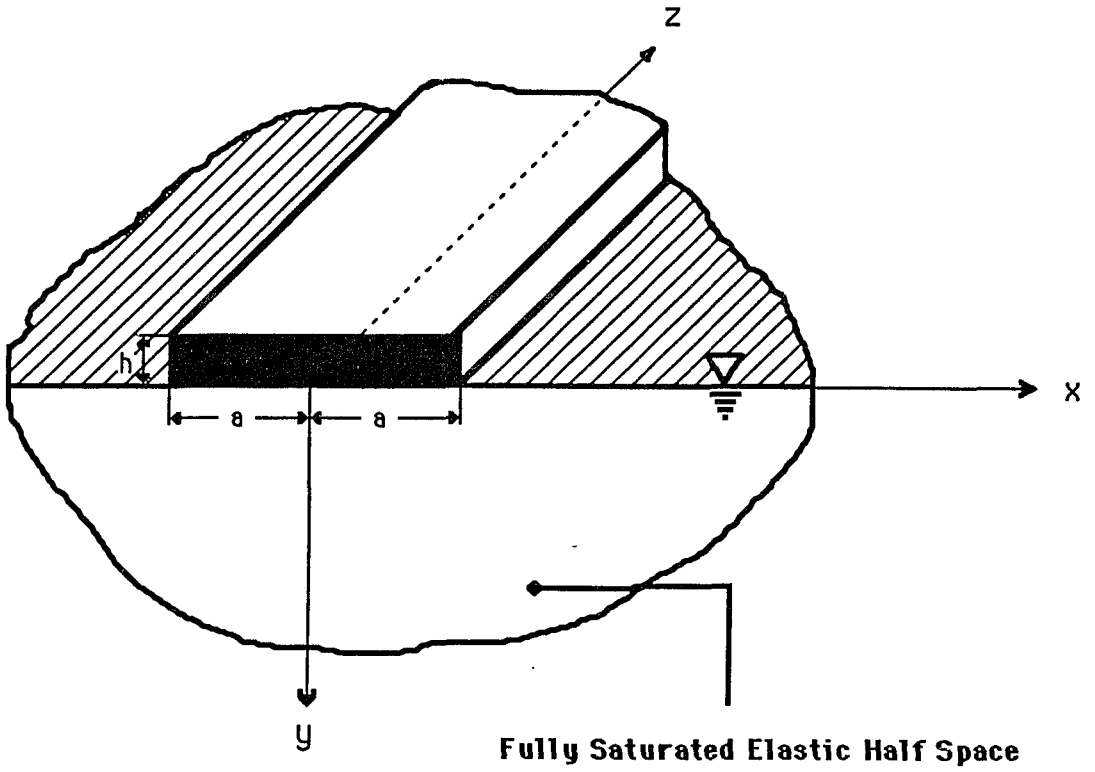

FIGURE(4) - RIGID STRIP IN CONTACT WITH A SATURATED ELASTIC HALF-SPACE.

to determine the influence functions which characterize the dynamic interaction of a mobile structure in contact with the surface of a saturated half-space . Once the influence functions are known , the response to harmonic excitation in the half-space is simply reduced to solving a set of algebraic equations obtained from the Newtonian equations of motion of the structure's model .

Consider a rigid rectangular strip of infinite length and half-width = a in contact with the free surface of the half-space and subjected to a plane incident wave excitation as shown in Figure (4) . Two types of contact conditions are investigated . One type depicts perfect bond (or welded contact) in which there is complete continuity between displacements and stresses of the strip and the underlying soil in the area of the contact while the second contact condition is concerned with partial bond (or smooth contact) in which the continuity in some of stress components is relaxed at the contact area . The formulation suggested by Thau (1967) and Dien (1971) which treats the diffraction of waves as consisting of two more seperate problems is adopted here . Similar techniques have previously been used by Junger (1953) and Smith (1962) in analyzing the effect of acoustic waves on structures immersed in fluids . Briefly , the desired solution is sought in two steps : The first step involves the radiation of waves into the

half-space by the strip vibrating as an inertialess rigid body , and the second determines the diffraction of the incident waves by a fixed strip . Since the influence functions needed to determine the dynamic interaction between structure and the surrounding medium are obtained from the radiation solution , attention is focused on this part of the formulation . Additional details are available in the cited references .

For an incident displacement in the solid skeleton , $\underline{u}^I(x,y)$, it is required to construct a scattered field , $\underline{u}^S(x,y)$, such that beneath the strip the following condition holds

$$\underline{u}^I(x,0) + \underline{u}^S(x,0) = U\,\underline{e}_x + (V + x\,\theta)\,\underline{e}_y \qquad , (4.1)$$

The right side of equation (4.1) defines the rigid body motion of the base of the strip , i.e. , U , V and θ are , respectively , the horizontal displacement of the center of the strip , vertical displacement of the center of the strip and angular rotation about the mass center of the strip ; and $\underline{e}_x$ and $\underline{e}_y$ are the unit base vectors . The factor $e^{i\omega t}$ in equation (4.1) is , of course , implied but omitted for brevity . In the region $|x| > a$ of the boundary , the surface tractions associated with the scattered field are required to vanish . This describes the boundary conditions for perfect contact between the strip and half-space . For

partial or smooth contact , additional stresses must vanish beneath the strip , namely , shearing stress for vertical and rocking motions and normal stress for horizontal motion . Upon specifying the incident field , equation (4.1) becomes :

$$\underline{u}^S(x,0) = (U - Q_x e^{-\omega x/d}) \underline{e}_x + (V + x\,\theta - Q_y e^{-\omega x/d}) \underline{e}_y \quad , (4.2)$$

where Q_x and Q_y are complex-valued functions specifying the amplitude and phase of the incident motion , and d is the apparent velocity of the incident wave observed on the free surface and thus the wave number can be readily defined as $k_I = \omega/d$.

As mentioned previously the scattered field is determined in two parts , $\underline{u}^S{}_1(x,y)$ and $\underline{u}^S{}_2(x,y)$, and each part can be decomposed into symmetric and antisymmetric components about the $x = 0$ plane . Thus , in the region $y = 0$, $|x| \le a$,

$$\underline{u}^S{}_1(x,0) = Q_x [\underline{u}^{(1)} + \underline{u}^{(2)}] + Q_y [\underline{u}^{(3)} + \underline{u}^{(4)}] \quad , (4.3a)$$

$$\underline{u}^S{}_2(x,0) = U \underline{u}^{(5)} + V \underline{u}^{(6)} + x\theta \underline{u}^{(7)} \quad , (4.3b)$$

such that on the interval $|x| \le a$ the displacements $\underline{u}^{(j)}$, $j = 1,2,,,7$, satisfy the boundary conditions

$$\underline{u}^{(1)} = -\cos(k_I x)\,\underline{e}_x \,, \qquad \underline{u}^{(2)} = -\sin(k_I x)\,\underline{e}_x \,; \qquad , \quad (4.4a)$$

$$\underline{u}^{(3)} = \sin(k_I x)\,\underline{e}_y \,, \qquad \underline{u}^{(4)} = -\cos(k_I x)\,\underline{e}_y \,; \qquad , \quad (4.4b)$$

$$\underline{u}^{(5)} = \underline{e}_x \,, \qquad \underline{u}^{(6)} = \underline{e}_y \,, \qquad \underline{u}^{(7)} = x\,\underline{e}_y \,; \qquad , \quad (4.4c)$$

Associated with the scattered displacements $\underline{u}^{(j)}$ in equations (4.3) , there are unknown surface tractions $\tau_{yy}^{(j)}(x,0) = \sigma^{(j)}(x)$ and $\tau_{xy}^{(j)}(x,0) = \tau^{(j)}(x)$ beneath the strip to be determined while outside the strip the surface tractions must vanish , namely , for $|x| > a$

$$\tau_{yy}^{(j)}(x,0) = \tau_{xy}^{(j)}(x,0) = 0 \,. \qquad , \quad (4.5)$$

Equations (4.4) and (4.5) constitute the mixed boundary conditions for the problem of interest by which the displacements $\underline{u}^{(j)}$ can be determined without regard to the actual rigid-body motion of the strip .

The surface tractions $\tau_{yy}^{(j)}$ and $\tau_{xy}^{(j)}$ in the interval $|x| \leq a$ give rise to resultant forces and overturning moment which are determined by consideration of equilibrium of the weightless rigid strip such that

$$F^{(j)} = \int_{-a}^{a} \sigma^{(j)}(x)\, dx \quad , \quad (4.6a)$$

$$H^{(j)} = \int_{-a}^{a} \tau^{(j)}(x)\, dx \quad , \quad (4.6b)$$

$$M^{(j)} = \int_{-a}^{a} x\, \sigma^{(j)}(x)\, dx \quad , \quad (4.6c)$$

Here , $F^{(j)}$, $H^{(j)}$ and $M^{(j)}$ represent , respectively , the amplitude per unit length of the vertical force , horizontal force and moment acting on the strip . By virtue of the existing symmetry implied in the problem , it is readily concluded from eqations (4.6) that $F^{(j)} = 0$ for $j = 1 , 3 , 5 , 7$ while for j = even , $H^{(j)} = M^{(j)} = 0$. The remaining eleven forces and

momonts , namely , $F^{(j)}$ for j = 2 , 4 , 6 and $H^{(j)}$ and $M^{(j)}$ for j = 1 , 3 , 5 , 7 constitute the complete set of influence functions . These functions give rise to the following forces and moments :

$$F^s = Q_x F^{(2)} + Q_y F^{(4)} + V F^{(6)} \quad , (4.7a)$$

$$H^s = Q_x H^{(1)} + Q_y H^{(3)} + U H^{(5)} + \theta H^{(7)} \quad , (4.7b)$$

$$M^s = Q_x M^{(1)} + Q_y M^{(3)} + U M^{(5)} + \theta M^{(7)} \quad , (4.7c)$$

In equations (4.7) , the influence functions obtained from the immobile strip (terms with j = 1 , 2, 3 , 4) provide the loads which force the motion of the mobile strip . The remaining terms (j = 5 , 6 , 7) represent the resistance of the half-space to the motion of the strip , and these are the desired interaction coefficients in soil-structure interaction problems . Numerical values of these functions are determined in the sequel , and can be used as the foundation's interaction spring-dashpot coefficients in carrying out the analysis of a structure and its surroundings . The motions of small amplitude of the rigid strip can be determined from the dynamic equations of motion

$$- m\omega^2 (U + h\,\theta) = H^S \quad , \quad (4.8a)$$

$$- m\omega^2 V = F^S \quad , \quad (4.8b)$$

$$- I\omega^2 \theta = M^S - h H^S \quad , \quad (4.8c)$$

Here , m , I represent the mass per unit length of the rigid strip and mass moment of inertia about the centroid located at x = 0 , y = - h , respectively , and 2h gives the height of the strip . Upon substituting the expressions (4.7) into the equations (4.8) and solving for the amplitudes of the motion of the strip , the response of the strip to an incident excitation can be described by the relations :

$$U = [\,(I\omega^2 + m\omega^2 h^2 + M^{(7)})(Q_x H^{(1)} + Q_y H^{(3)})$$

$$- (m\omega^2 h + H^{(7)})(Q_x M^{(1)} + Q_y M^{(3)})\,]/\Delta \quad , (4.9a)$$

$$V = - (Q_x P^{(2)} + Q_y P^{(4)}) / (m\omega^2 + F^{(6)}) \quad , (4.9b)$$

$$\theta = [(m\omega^2 + H^{(5)})(Q_x M^{(1)} + Q_y M^{(3)})$$

$$- (m\omega^2 h + M^{(7)})(Q_x H^{(1)} + Q_y H^{(3)})]/\Delta \quad , (4.9c)$$

in which the following abbreviation has been adopted .

$$\Delta = (m\omega^2 h + H^{(7)})(m\omega^2 h + M^{(5)})$$

$$- (m\omega^2 + H^{(5)})(I\omega^2 + m\omega^2 h^2 + M^{(7)}) \quad , (4.9d)$$

For a foundation attached to a system of oscillators modeling the vibrational modes of a flexible structure , instead of using equations (4.9) , the influence functions are used to form the equivalent interaction spring-dashpot coefficients representing the interaction effects between the foundation and the underneath half-space in carrying out the dynamic analysis of the structure .

4.2. CONSTRUCTION OF GREEN'S FUNCTIONS

Upon replacing x by x - ξ in equations (3.11) and (3.14) and setting the line loads H = 1 and P = 1 in these equations , the Green 's functions can be constructed as follows

$$u_x^H(x-\xi) = \frac{1}{\pi\mu}\int_{-\infty}^{\infty} \frac{\gamma n_3 \omega^2/V_c^2}{F(s,\omega)} e^{-is(x-\xi)}\, ds \quad , \quad (4.10a)$$

$$u_y^H(x-\xi) = \frac{i}{2\pi\mu}\int_{-\infty}^{\infty} \frac{s F_1(s,\omega)}{F(s,\omega)} e^{-is(x-\xi)}\, ds \quad , \quad (4.10b)$$

$$u_x^P(x-\xi) = -\frac{i}{2\pi\mu}\int_{-\infty}^{\infty} \frac{s F_2(s,\omega)}{F(s,\omega)} e^{-is(x-\xi)}\, ds \quad , \quad (4.10c)$$

$$u_y^P(x-\xi) = \frac{1}{2\pi\mu}\int_{-\infty}^{\infty} \frac{(\beta_2 n_1 - \beta_1 n_2)\,\omega^2/V_3^2}{F(s,\omega)} e^{-is(x-\xi)} ds \quad , \quad (4.10d)$$

The physical interpretation of the Green's functions is that $u_j^k(x-\xi,)$, j = x , y and k = H , P , represent the j component of the response of the saturated half-space at the location (x,o) due to the application of a concentrated line load of unit magnitude at location (ξ,0) in the direction indicated by k . The Green's functions are used in the sequel to formulate the equations governing the influence functions .

4.3. INFLUENCE FUNCTIONS

Utilizing the Green ' s functions developed in section 4.2 for the saturated half-space and using the principle of superposition , the problem of determining the unknown suface tractions , $\sigma^{(j)}(x)$ and $\tau^{(j)}$, appearing in equations (4.4) and (4.5) , is reduced to the solution of the following two coupled integral equations valid for $|x| \leq a$

$$\int_{-a}^{a} \tau^{(j)}(\xi)\, u_x^H(x-\xi)\, d\xi + \int_{-a}^{a} \sigma^{(j)}(\xi)\, u_x^P(x-\xi)\, d\xi = u_x^{(j)}(x) \quad , \quad (4.11a)$$

$$\int_{-a}^{a} \tau^{(j)}(\xi)\, u_y^H(x-\xi)\, d\xi + \int_{-a}^{a} \sigma^{(j)}(\xi)\, u_y^P(x-\xi)\, d\xi = u_y^{(j)}(x) \quad , \quad (4.11b)$$

In equations (4.11) , $u^H{}_x$, $u^H{}_y$, $u^P{}_x$ and $u^P{}_y$ are Green ' s functions expressions given in equations (4.10) . The first integral in equation (4.11a) represents the horizontal component $u_x{}^{\tau}$ of the displacement at the surface location (x,0) due to the contact shear stress $\tau^{(j)}$ beneath the footing while the second integral gives the contribution to the surface horizontal displacement $u_x{}^{\sigma}$ at (x,0) from the contact normal

stress $\sigma^{(j)}$ and the total horizontal displacement must match the horizontal movement of the footing at the same contact point to satisfy the continuity requirement . The continuity of the vertical direction is guaranteed by equation (4.11b) . Equations (4.11) can also be interpreted as an alternative description of the boundary conditions (4.4) which also provide explicit relationships between the contact stresses and contact displacements . Outside the footing , the surface tractions $\sigma^{(j)}(x)$ and $\tau^{(j)}$ for $|x| \geq a$ must vanish , as required by the boundary conditions (4.5) . A glance at equations (4.10) and (4.11) would indicate that a closed form solution for the contact stresses is not feasible and the integral equations (4.11) must be treated either by perturbation or numerical means . As a preliminary to the numerical evaluation , equations (4.11) are placed in non-dimensional form by scaling the independent variables against the length (a) , i.e.

$$x=a\bar{x} \ , \ \xi=a\bar{\xi} \ , \ \bar{s} = a\, s \ ,$$

$$\bar{\sigma}^{(j)}(\bar{\xi}) = \sigma^{(j)}(a\bar{\xi}) \ , \ \bar{\tau}^{(j)}(\bar{\xi}) = \tau^{(j)}(a\bar{\xi}) \qquad , \ (4.12)$$

It follows that

$$\int_{-1}^{1} \bar{\tau}^{(j)}(\bar{\xi})\, u_x^H(\bar{x}-\bar{\xi})\, d\bar{\xi} + \int_{-1}^{1} \bar{\sigma}^{(j)}(\bar{\xi})\, u_x^P(\bar{x}-\bar{\xi})\, d\bar{\xi} = \frac{1}{a} u_x^{(j)}(a\bar{x}), \quad (4.13a)$$

$$\int_{-1}^{1} \bar{\tau}^{(j)}(\bar{\xi})\, u_y^H(\bar{x}-\bar{\xi})\, d\bar{\xi} + \int_{-1}^{1} \bar{\sigma}^{(j)}(\bar{\xi})\, u_y^P(\bar{x}-\bar{\xi})\, d\bar{\xi} = \frac{1}{a} u_y^{(j)}(a\bar{x}), \quad (4.13b)$$

Equations (4.13) constitute a pair of coupled inhomogeneous Fredholm integral equations of the first kind for the unknown contact stresses in the region $|\bar{x}| \leq 1$. It can be shown that a unique solution exists due to the good behavior of the Green'functions . A numerical solution to these equations can be achieved by postulating a proper series expansion for the contact stresses , which would reflect and preserve the essential characteristics of the solution , and would yield a set of indepedent algebraic equations for the unknown coefficients in the contact stress expansions .

From the mathematical viewpoint , it is reasonable to expect the contact stresses , in case of welded footing , to possess an oscillatory singularity of the type $r^{-1/2}\sin(\varepsilon_0 \ln r)$ where r is the small distance from the edge of the footing and ε_0 is a constant which depends

on poisson's ratio of the solid material of the medium . This follows from the classical work of Muskhelishvili (1957) and Williams (1959) and also from the work of Luco and Westmann (1972) for the dry half-space . For a smooth contact beneath the strip , the oscillatory part of the singularity disappears and only the square root part ($r^{-1/2}$) remains. Practically speaking , most of the relevant information needed for interaction analysis can be obtained by assuming a dominant square root singularity in the contact stresses for all types of contacts . In view of these observations , and guided by the work of Dien(1971) , the following representation of the unknown contact stresses are assumed ($|\bar{x}| \leq 1$):

$$\bar{\tau}^{(j)}(\bar{x}) = \sum_{n=0}^{\infty} A_n^{(j)} (1-\bar{x}^2)^{-1/2} T_n(\bar{x}) \quad , \quad (4.14a)$$

$$\bar{\sigma}^{(j)}(\bar{x}) = \sum_{n=0}^{\infty} B_n^{(j)} (1-\bar{x}^2)^{-1/2} T_n(\bar{x}) \quad , \quad (4.14b)$$

where $T_n(\bar{x})$ are the Chebyshev polynomials . With this representation , a square root singularity in the contact streses is implied , and a standard numerical scheme can be adopted to reduce equations (4.13) into algebraic equations for the unknown coefficients $A_n^{(j)}$ and $B_n^{(j)}$.

Inserting the series expansions (4.14) into equations (4.13), making use of the Green's functions in equations (4.10) and utilizing the well known relations (Erdyli 1954):

$$\int_{-1}^{1} (1-\bar{x}^2)^{-1/2} T_n(\bar{x})\, e^{\mp i\bar{s}\bar{x}}\, d\bar{x} = (-i)^n \pi J_n(\mp\bar{s}) \quad , \quad (4.15)$$

where J_n are the usual Bessel functions of the first kind of order n, it follows that

$$\sum_{n=0}^{\infty} A_n^{(j)} \frac{i^n}{2} \int_{-\infty}^{\infty} \frac{2\gamma\, \omega_c^2\, \bar{n}_3(\bar{s})}{F(\bar{s})} J_n(\bar{s})\, e^{-i\bar{s}\bar{x}}\, d\bar{s}$$

$$- \sum_{m=0}^{\infty} B_m^{(j)} \frac{i^{m+1}}{2} \int_{-\infty}^{\infty} \frac{\bar{s}\, F_2(\bar{s})}{F(\bar{s})} J_m(\bar{s})\, e^{-i\bar{s}\bar{x}}\, d\bar{s} = \frac{\mu}{a} u_x^{(j)}(a\bar{x}) \quad , \quad (4.16a)$$

$$\sum_{m=0}^{\infty} A_n^{(j)} \frac{i^{n+1}}{2} \int_{-\infty}^{\infty} \frac{\bar{s}\, F_1(\bar{s})}{F(\bar{s})} J_n(\bar{s})\, e^{-i\bar{s}\bar{x}}\, d\bar{s}$$

$$+ \sum_{m=0}^{\infty} B_m^{(j)} \frac{i^m}{2} \int_{-\infty}^{\infty} \frac{[\beta_2 \bar{n}_1(\bar{s}) - \beta_1 \bar{n}_2(\bar{s})]\, \omega_3^2}{F(\bar{s})} J_m(\bar{s})\, e^{-i\bar{s}\bar{x}}\, d\bar{s} = \frac{\mu}{a} u_y^{(j)}(a\bar{x}) , \quad (4.16b)$$

in which the previously defined parameters have been non-dimensionalized by the length a , i.e. , $\omega_c = a\omega/V_c$, $\omega_j = a\omega/V_j$ and $\bar{n}_j(\bar{s}) = (\bar{s}^2 - \omega_j^2)^{1/2}$, j = 1 , 2 , 3 . The frequency dependent functions $F(\bar{s})$, $\bar{F}_1(\bar{s})$ and $F_2(\bar{s})$ are the non-dimensionalized functions as given in section 3.1 .

With a view toward reducing equations (4.16) into algebraic equations, they are multiplied by the normalizing function $(1-\bar{x}^2)^{-1/2} T_l(\bar{x})$, l=integers , and an integation is performed over the interval $|\bar{x}| \leq 1$. After a permissible interchange in the order of integration and use is made of relation (4.15) , the following set of independent algebraic equations is obtained :

$$\sum_n \alpha_{nl} A_n^{(j)} - \sum_m c_{ml} B_m^{(j)} = \frac{2\mu}{a\pi} \int_{-1}^{1} \frac{u_x^{(j)}(a\theta)}{\sqrt{1-\theta^2}} T_l(\theta)\, d\theta \quad , (4.17a)$$

$$\sum_n c'_{nl} A_n^{(j)} + \sum_m \beta_{ml} B_m^{(j)} = \frac{2\mu}{a\pi} \int_{-1}^{1} \frac{u_y^{(j)}(a\theta)}{\sqrt{1-\theta^2}} T_l(\theta)\, d\theta \quad , (4.17b)$$

In equations (4.17) , the coefficients α_{nl} ,,,,, β_{ml} denote integrals defined over the interval $(-\infty,\infty)$. The integrands of these integrals are either odd or even with reference to the parameter of integration and hence the range of integration can be reduced . α_{nl} and β_{nl} are even functions for even values (n+1) and become odd functions for odd values of (n+1) . It follows that α_{nl} and β_{nl} vanish for odd values of (n+1) , and for even values are given by

$$\alpha_{nl} = (-1)^l i^{n+l} \int_0^\infty \frac{4\gamma\omega_c^2 \bar{n}_3(\bar{s})}{F(\bar{s})} J_n(\bar{s}) J_l(\bar{s}) d\bar{s} \qquad , (4.18a)$$

$$\beta_{nl} = (-1)^l i^{n+l} \int_0^\infty \frac{2\omega_3^2 [\beta_2 \bar{n}_1(\bar{s}) - \beta_1 \bar{n}_2(\bar{s})]}{F(\bar{s})} J_n(\bar{s}) J_l(\bar{s}) d\bar{s} \qquad , (4.18b)$$

similarly , C_{nl} and C'_{nl} become odd functions for even values of (n+l) and therefore vanish for even values of (n+l) while for (n+l)=odd , they become even functions and can evaluated from

$$C_{nl} = (-1)^l i^{n+l+1} \int_0^\infty \frac{2\bar{s} F_2(\bar{s})}{F(\bar{s})} J_n(\bar{s}) J_l(\bar{s}) d\bar{s} \qquad , (4.19a)$$

$$C'_{nl} = (-1)^l i^{n+l+1} \int_0^\infty \frac{2\bar{s} F_1(\bar{s})}{F(\bar{s})} J_n(\bar{s}) J_l(\bar{s}) d\bar{s} \qquad , (4.19b)$$

For a strip in smooth contact with the half-space , the coefficients $C_{n1}=C'_{n1}= 0$ and equations (4.17) uncouple and immediately yield the coefficients $A_n^{(j)}$ and $B_n^{(j)}$.

The next step in the analysis is to confirm that integrals (4.18) and (4.19) are amenable to numerical treatment . For this purpose , expanding the integrands asymptotically for small and large values of $\bar{s}$, it can be readily shown that the integrands are well behaved at both limits of integration . The relevant detailed discussion is given in Appendix B . In the absence of hysteretic damping of the medium , the roots of the Rayleigh function , $F(\bar{s})$, are in general complex (Jones 1961) . For the material parameters and hysteretic damping ratios used in this work , the roots of $F(\bar{s})$ are all complex and lie outside the $\bar{s}$-axis . Hence , numerical evaluation of integrals (4.18) and (4.19) can be carried out in a routine manner . In order to assure rapid convergence at the upper limit of integration , the integrands are expanded for large values of $\bar{s}$ and some integrals containing the lowest order terms are evaluated in closed form using results listed in Erdelyi(1954) . The remaining integrals are found to converge very rapidly and smoothly . Note that the integrals (4.18) and (4.19) need be computed only once at each specifed frequency .

The integrals appearing in the forcing terms of equations (4.17) depend upon the mode of motion of the footing and can be easily evaluated using the orthogonality relations of the Chebyshev polynomials

$$\int_{-1}^{1} (1-\bar{x}^2)^{-1/2}\, T_m(\bar{x})\, T_n(\bar{x})\, d\bar{x} = \begin{cases} \pi & m=n=0 \\ \frac{\pi}{2} & m=n>0 \\ 0 & m\neq n \end{cases} \quad ,(4.20)$$

The orthogonality relations (4.20) can also be used to show that the influence functions are related to the expansion coefficients of the series representation of the contact stress distributions by substituting the contact stress expansions (4.14) into the contact force-stress relations (4.6) , leading to

$$H^{(j)} = \pi a\, A_0^{(j)}/\mu$$

$$F^{(j)} = \pi a\, B_0^{(j)}/\mu \qquad , (4.21)$$

$$M^{(j)} = \pi\, B_1^{(j)}/2\mu$$

Here the forces , $H^{(j)}$, $F^{(j)}$ are normalized by the shear modulus μ and the moment , $M^{(j)}$ is normalized by (μa^2) . The real part of $H^{(j)}$ gives the

stiffness corresponding to horizontal mode of motion of the strip while the imaginery part , Im $H^{(j)}$, gives the corresponding damping coefficients of the medium . Similar interpretations can be given to the remaining influence functions .

It should be pointed out that the integral equations (4.11) involve an implicit assumption that the pore pressure p is equal to zero on the surface of the half-space , including the region beneath the footing . It follows that the vibrations of the footing against the half-space are solely supported along the surface by the solid skeleton . This assumption requires a porous foundation . However , it will be shown in the next chapter (see section 5.2.4) that the average displacement of the fluid portion relative to the solid portion along the contact region is negligible . Thus it is reasonable to assume that the solution developed corresponds to the motion of a rigid foundation .

This is as far as the solution can be analytically developed . An approximate(numerical) solutions for $A_n^{(j)}$ and $B_n^{(j)}$ in equations (4.17) can be obtained by truncating the series expansions for the contact stresses at the same number of terms and solving the resulting algebraic equations . This will be done in the sequel .

CHAPTER 5. NUMERICAL EVALUATION OF THE INFLUENCE FUNCTIONS AND DISCUSSION OF THE RESULTS

Since a knowledge of the force-displacement relationship for a foundation in contact with a soil is essential in the soil-structure interaction process , the accuracy of the evaluation of the influence functions representing such relationship is imperative to the accuracy of assessing and determining the response of structures to dynamic loading . This chapter contains the numerical procedure and the results for representive influence functions . Discussion is also made , on a quantitative basis , of the impacts of ground water and variations of other related parameters on the behavior of influence functions as compared with the corresponding dry cases . As indicated in equations (4.21) the influence functions are determined from a knowledge of the constants $A_0^{(j)}$, $B_0^{(j)}$ and $B_1^{(j)}$ and these in turn are determined from the set of algebraic equations (4.17) . The constants $A_0^{(j)}$,,,, $B_1^{(j)}$ appear in the contact stress expressions (4.14) . The first step in obtaining the influence functions is to investigate their behavior for small values of $\bar{\omega} = a\omega/V_s$.

5.1 BEHAVIOR OF INFLUENCE FUNCTIONS FOR LOW FREQUENCY $\bar{\omega}$

For a single-phase material , the behavior of the foundation compliances at the low frequency factor $\bar{\omega}$ has been studied by

Luco(1972) . He found out that the compliances for the vertical and horizontal modes of motion become infinite as $\bar{\omega} \rightarrow 0$, namely , the influence functions (the inverse of the compliance) for the vertical and horizontal modes vanish at the zero frequency . For the rocking mode of motion , it was found that the compliance become finite as $\bar{\omega}$ approaches zero . Such behavior of the influence functions at zero frequency can be interpreted as corresponding to the possibility of a rigid body motion of the half-space in the static case , which is characteristic of the two-dimensional problem under consideration . In order to investigate the nature of the influence functions at $\bar{\omega} \rightarrow 0$ for the saturated material , examine the limiting behavior of the coefficients α_{n1} , β_{n1} , etc. in equations (4.17) at the low frequency .

For the coefficient α_{n1} , for example , expanding the integrand of α_{n1} given in equation (4.18a) for low frequency factor $\bar{\omega}$, giving rise to the following limiting expression for α_{n1}

$$\alpha_{n1} \sim \int_0^{\infty} \lim_{\bar{\omega} \rightarrow 0} \left[\frac{\gamma}{\beta_2 \lambda_1 - \beta_1 \lambda_2 - 2\gamma} \right] \frac{1}{\bar{s}} J_n(\bar{s}) J_1(\bar{s}) d\bar{s} \quad , (5.1)$$

The first term in equation (5.1) becomes constant as $\bar{\omega}$ approaches zero , while the remaining terms are independent of the freqency factor $\bar{\omega}$. Thus , equation (5.1) can be written as

$$\mathfrak{A}_{nl} \sim \int_0^\infty \frac{1}{\bar{s}} J_n(\bar{s}) J_l(\bar{s}) d\bar{s} \qquad , n \text{ and } l = \text{integers} \quad , (5.2)$$

It follows that for $\bar{\omega} \to 0$

$$\mathfrak{A}_{nl} \sim \int_0^\infty \frac{1}{\bar{s}} J_n(\bar{s}) J_l(\bar{s}) d\bar{s} = \begin{cases} \infty & n = l = 0 \\ \\ \text{finite} & n \text{ or } l \neq 0 \end{cases} \quad , (5.3)$$

Same can also be developed for $\mathfrak{B}_{nl}$, $\mathfrak{C}_{nl}$ etc. . Making use of the expressions (4.21) and the relation (5.3) in conjunction with the equations (4.17) , it can be immediately concluded that at the zero

frequency , the coefficients $\mathfrak{A}_{00}$, $\mathfrak{B}_{00}$ approach infinity , resulting the constants A_0 and B_0 to be zero since the products $\mathfrak{A}_{00} A_0$ and $\mathfrak{B}_{00}B_0$ from equations (4.17) must be finite , and therefore from the relations (4.21) , $H^{(j)}$ and $P^{(j)}$, namely the influence functions (stiffnesses only since the imaginary part disappears in the limit) for the horizontal and vertical modes , respectively , vanish at the zero frequency . Similarly , since $\mathfrak{B}_{11}$ is finite , B_1 becomes finite , therefore resulting in finite influence functions for the rocking mode at the zero frequency .

5.2 NUMERICAL EVALUATION OF THE INFLUENCE FUNCTIONS

The analytical formulation of the previous chapter resulted in a set of algebraic equations (4.17) for the influence functions of a surface footing attached to a saturated elastic half-space . The solution to these equations was carried out numerically on a digital computer and the results are presented in this section . Calculations were performed to compute the stiffnesses and radiation damping coefficients , which are the real and imaginary parts , respectively , of the influence functions , for dimensionless input frequencies in the range up to 5 . The dimensionless frequency is defined as $\bar{\omega} = a\omega/V_s$. Four hysteretic damping ratios of the medium (λ_c) were considered , namely , 0% , 1% , 5% and 10% . Two types of material parameters , appropriate to saturated dense sand and saturated medium soft clay whose properties are given in the Table 1 and Table 2 , respectively , have been used to illustrate the use of the present formulation . The coefficients of permeability in both English and S.I. unit are given in Table 3 . In all cases considered , the applied horizontal and vertical loads have been normalized by the shear modulus μ and the moment by (μa^2) . For the case of saturated dense sand , two values of the permeability coefficients (k) , namely , 0.1 and 0.001 cm/sec. , were used in order to explore the influence of permeability on the influence functions .

Table 1. Material Parameters for Saturated Dense Sand

ν =0.25	
α = 1	(saturated porous material)
α'= 293.9 × 10^3	psi
f = 0.35	
ρ = 0.11937 × 10^{-3}	lb-sec^2/in^4
ρ' = 0.0327 × 10^{-3}	lb-sec^2/in^4
E_c = 14 × 10^3	psi
V_c = 39,869	in/sec.
V_s = 4,908	in/sec.

Table 2. Material Parameters for Saturated Soft Clay

ν =0.25	
α = 1	(saturated porous material)
α'= 293.9 × 10^3	psi
f = 0.4	
ρ = 0.18597× 10^{-3}	lb-sec^2/in^4
ρ' = 0.0374 × 10^{-3}	lb-sec^2/in^4
E_c = 21 × 10^2	psi
V_c = 39,895	in/sec.
V_s = 1,940	in/sec.

Table 3. Coefficients of Permeability

Material	English (in/sec.)	S.I. unit (cm/sec)
sand	3.937×10^{-2} - 3.937×10^{-4}	0.1 - 0.001
clay	3.937×10^{-6}	0.00001

In carrying out the numerical work , let n = m = l in equations (4.17) . It follows that equations (4.17) can be recast in the following matrix form

$$\begin{pmatrix} \mathfrak{A}_{00} & \mathfrak{A}_{01} & \cdots & \mathfrak{A}_{0n} & \mathfrak{C}_{00} & \mathfrak{C}_{01} & \cdots & \mathfrak{C}_{0n} \\ \mathfrak{A}_{10} & \mathfrak{A}_{11} & & & \mathfrak{C}_{10} & \mathfrak{C}_{11} & & \\ \vdots & & \ddots & & \vdots & & \ddots & \\ \mathfrak{A}_{n0} & & \cdots & \mathfrak{A}_{nn} & \mathfrak{C}_{n0} & & \cdots & \mathfrak{C}_{nn} \\ \mathfrak{C}'_{00} & \mathfrak{C}'_{01} & \cdots & \mathfrak{C}'_{0n} & \mathfrak{B}_{00} & \mathfrak{B}_{01} & \cdots & \mathfrak{B}_{0n} \\ \mathfrak{C}'_{10} & \mathfrak{C}'_{11} & & & \mathfrak{B}_{10} & \mathfrak{B}_{11} & & \\ \vdots & & \ddots & & \vdots & & \ddots & \\ \mathfrak{C}'_{n0} & & \cdots & \mathfrak{C}'_{nn} & \mathfrak{B}_{n0} & & \cdots & \mathfrak{B}_{nn} \end{pmatrix} \begin{pmatrix} A_0^{(j)} \\ A_1^{(j)} \\ \vdots \\ A_n^{(j)} \\ B_0^{(j)} \\ B_1^{(j)} \\ \vdots \\ B_n^{(j)} \end{pmatrix} = \begin{pmatrix} D_0^{(j)} \\ D_1^{(j)} \\ \vdots \\ D_n^{(j)} \\ E_0^{(j)} \\ E_1^{(j)} \\ \vdots \\ E_n^{(j)} \end{pmatrix} \quad ,(5.4)$$

Now , equation (5.4) is a set of algebraic equations for the unknowns $A_i^{(j)}$ and $B_i^{(j)}$ which are related to influence functions by equations (4.21) . The superscript j designates the mode of motion , $\mathcal{C}_{ik}$, $\mathcal{B}_{ik}$, $\mathcal{C}_{ik}$ and $\mathcal{C}'_{ik}$ are the integrals given in the equations (4.18) and (4.19) and $D_i^{(j)}$ and $E_i^{(j)}$ represent the following integrals :

$$D_i^{(j)} = \frac{2\mu}{a\pi} \int_{-1}^{1} \frac{u_x^{(j)}(a\theta)}{\sqrt{1-\theta^2}} T_i(\theta)\, d\theta \qquad , (5.5a)$$

$$E_i^{(j)} = \frac{2\mu}{a\pi} \int_{-1}^{1} \frac{u_y^{(j)}(a\theta)}{\sqrt{1-\theta^2}} T_i(\theta)\, d\theta \qquad , (5.5b)$$

In equations (5.5) , $u_x^{(j)}$ and $u_y^{(j)}$ are the components of the surface displacement at the contact between the footing and the half space and are determined through the boundary conditions given by equations (4.4) . For the horizontal mode of motion , given by the first equation in equations (4.4c) , the superscript j = 5 and $u_x^{(5)} = 1$ and $u_y^{(5)} = 0$ are substituted into equations (5.5) with the aid of the relation (4.20) ,

resulting in

$$D_i^{(5)} = \begin{cases} 0 & i \neq 0 \\ \dfrac{2\mu}{a} & i = 0 \end{cases} \quad , \text{(5.6a)}$$

$$E_i^{(5)} = 0 \quad , \text{(5.6b)}$$

For other modes , same approach is used to determine $D_i^{(j)}$ and $E_i^{(j)}$ and therefore will not be repeated here .

We now take a look at the coefficient matrix in equations (5.4) and observe that this matrix is independent of the mode specifier j and therefore its contents can be evaluated independent of the modes of motion and the corresponding boundary conditions as well . To solve the equations (5.4) , Cholesky method is utilized . This approach first factorizes the coefficient matrix into the product of a lower triangular matrix and an unit upper triangular matrix and then saves

the factorized matrices in a storage . With each supply of a right hand load vector for different motion mode , forward and back substitutions can be proceeded for the solution to the unknown constant vector without distortion of the factorized matrices .

Several terms of the series expansions (4.14) for the contact stresses were tried out and in each case the convergence was tested . It was concluded that by retaining four terms , adequate accuracy , within less than 1% is attainable in most cases . The numerical convergence of the integrals appearing in equations (4.18) and (4.19) at the upper limit was improved by the sheme outlined in Appendix B . For a smooth contact between the strip and the half-space , the coefficients C_{ik} and C'_{ik} vanish and extremely good convergence was observed in solving equations (4.17) , and somewhat slower convergence was encountered in the welded case because of the presence of the coefficients C_{ik} and C'_{ik} which stand for slow converging integrals .

In the limiting case of a dry half-space ($\lambda_c \neq 0$) , the following parameters are used to remove the influence of the pore fluid : $p = p' = \alpha' = \gamma' = a_j (j=1,2,3) = 0$. One of the compression waves

is eliminated (the one associated with n_2 in equations 2.19 and 2.20), and V_c , V_s reduce , respectively , to the usual longitudinal and shear velocities in an elastic medium . More details about the reduction is given in Appendix C . For $\lambda_c = 0$, the integrals $\mathcal{G}_{ik}$, $\mathcal{B}_{ik}$, etc. in equations (5.4) can not be evaluated by direct integration because of occurance of the singularity of the integrand on the real axis on which the integration is taken . These singularities are due to the decay of velocities of body waves and Rayleigh surface waves from complex to real quantities and contribute the branch cuts and real roots to the Rayleigh function $F(\bar{s})$ which appears as a denominator in the integrals $\mathcal{G}_{ik}$, $\mathcal{B}_{ik}$, etc. . To tackle this problem , Lamb (1904) and later Quinlan (1953) , Karasudhi , Keer and Lee (1968) and Dien (1971) discussed the use of contour integration technique to evaluate the integrals properly .

To perform the contour integration , the integral must be first defined in the complex plane over a suitable contour and with proper branch cuts . The contour path discussed by Lamb (1904) and Karasudhi , Keer and Lee (1968) and shown in Figure 5 is employed . The small semi-circles in this contour surround the

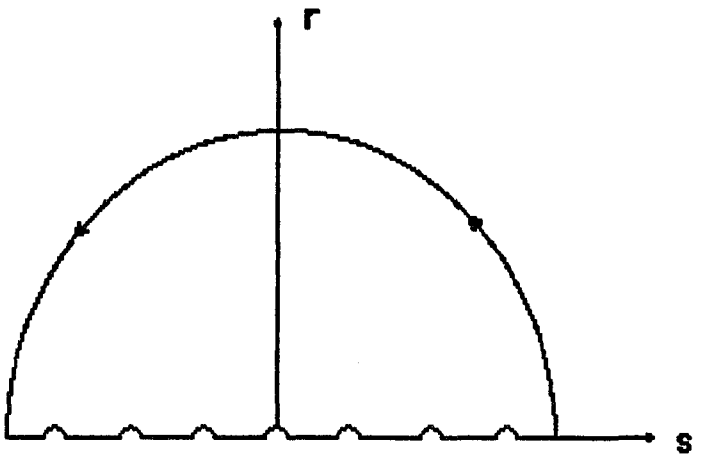

FIGURE 5. TYPICAL CONTOUR FOR INFINITE INTEGRATIONS

roots of the Rayleigh function $F(\bar{s})$ and the branch cuts which are introduced to make the integrand single-valued and are designed to avoid interfering with the deformation of the contour . Therefore , the integration of the infinite integral having singularities along the real axis can now be performed , using standard contour integration methods , utilizing the closed deformed smooth contour , inside which the integrand is analytical . Karasudhi , Keer and Lee (1968) solved the footing problems for smooth contact by this contour . Oien (1971) utilized a similar contour and solved the footing problems for both smooth and welded contacts .

Finally , the numerical results obtained are displayed graphically .

Plots (1) -(29) represent the influence functions for the dense sand material while Plots (30) - (51) correspond to the influence functions for the medium soft clay material . A discussion of these results follows in the sequel .

5.2.1 Impacts of The Pore Fluid and Its Permeability

Plots (1) - (3) display the influence functions for the horizontal , vertical and rocking modes of motion of a smooth strip against the surface of the saturated sandy half-space . In these plots , the hysteretic damping ratio of the medium is assumed zero (λ_c=0) and permeability k=0.01 cm/sec. . The top part of Plot (1) represents the horizontal stiffness (K_{HH} = Re $H^{(5)}$) , which is the horizontal force per unit length of the strip required to cause a unit horizontal displacement . The lower figure represents the horizontal damping coefficient (C_{HH} = Im $H^{(5)}$) . Plots (1) - (3) also contain the influence functions pertaining to a dry elastic medium over a frequency range of 0 - 3 . These are shown dotted in the figures and were obtained from Dien (1971) . The impact of pore fluid on the reponse of the medium is illustrated by comparing the dotted and solid curves .

In Plot (1) , the effective stiffness of the two - phased medium is about (50-100)% higher than the corresponding value of the dry medium while there is no appreciable change in the damping coefficients between the two cases . Plots (2) and (3) reveal higher increase in the damping coefficient for the saturated medium ,

especially at the higher end of the frequency range . The increase is about 150% . Also , the stiffness changes sign at the higher frequencies for both the vertical and rocking modes of motion . These results are in qualitative agreement with those obtained by Lung (1980) and Costantino(1986) . Quantitatively , good agreements are found at the low frequency . At the high frequency end , the horizontal and vertical stiffnesses found by the analytical method are about 30% less than the corresponding finite element results . For vertical damping coefficient and both rocking damping coefficient and stiffness the results by Lung (1980) and Costantino(1986) are higher by more than 50% . Since in Plots (2) - (4) no hysteretic damping of the material was included , the variation in the interaction coefficients is entirely due to the presence of the pore fluid and its permeability effects .

Plots (30)-(32) and Plots(41)-(43) reveal the influence functions for the smooth contact of the clay soil with 1% hysteretic damping for fully saturated and dry condition , respectively . Rather similar characteristics are found in the results regarding to the impact of permeability effects .

5.2.2 Type of Contact and Hysteretic Damping Effects

In order to explore the effects of both hysteretic damping and complete and partial contacts between the strip and half-space , the interaction coefficients were computed for both models with k=0.01 cm/sec. and λ_c = 1% , 5% , 10% and the results for the sandy material are shown in Plots (4) - (22) and the results for the clay are illustrated in Plots (30) - (51) .

It is interesting to observe that the interaction coefficients in both models of contacts are practically identical over low range of the frequency $\bar{\omega}$. For higher range of values of $\bar{\omega}$, there is appreciable deviation in the values of the influence functions between the two contact models , especially in the vertical and rocking modes of the motion . However this tendency decreases as the ratio of the hysteretic damping increases . It is also found that the clay material is much more sensitive to the contact condition than the dense sand .

Plots (4) - (14) and (30) - (40) also reveal the impact of including the hysteretc damping of the medium on the interaction coefficients . There is an appreciable increase in the magnitude of the effective stiffness in each of the three modes of motion . For the horizontal motion , the character of the effective stiffness changes in sign as the

damping ratio increases . Also , in this case , the magnitude of the stiffness exhibits tremendous increase near the higher end of the frequency . It is also observed , in this case , that the sandy material gives about 60% higher value of the stiffness than the clay .

For the vertical and rocking motions , the effective stiffnesses increase significantly with the presence of the hysteretic damping , especially for the clay material , the increase is about 100 - 200% .

For all cases , the radiation damping coefficients can increase by a factor of more than two to three and also the sandy material exhibits higher value of the coefficient than the clay .

The variation of the influence function $H^{(7)}$ (which is equivalent to $M^{(5)}$) with the wave number $\bar{\omega}$ is shown in Plots (10) , (14) for the sand and Plots (36) , (40) for the clay . This function reveals the coupling effect between the horizontal translational and rocking motions of a perfectly bonded strip to the medium . Based on the classical reciprocity theorem in elastodynamic , one would expect identical numerical values of the functions $H^{(7)}$ and $M^{(5)}$ in the present formulation . Indeed , the actual numerical computation of both these coefficients gave reasonable accuracy . The effect of increasing the

hysteretic damping ratio of the medium (λ_c) on the variation of the coupled stiffness and coupled damping coefficient with $\bar{\omega}$ could be observed . In obtaining the results of these plots , λ_c is assumed to be 5% , 10% . As expected , both the effective stiffnesses and the effective damping coefficients increase rapidly as the damping ratio becomes higher .

Plots (15) - (22) for the sand material and (41) - (51) for the clay show the impact of including hysteretic damping of the dry medium (k=0 , λ_c= 1% , 5% , 10%) on the interaction coefficients . First , the smooth and welded contact gave almost identical results . Second , an appreciable reduction , about (50 - 150)% , in the effective stiffnesses and damping coefficients is observed for the clay for both types of contact compared to the corresponding cases where k=0.01 cm/sec. in the vertical and rocking modes of motion except for the rocking motions with λ_c= 5% , 10% in which appreciable increases are observed in both the effective stiffnesses and radiation damping coefficients . The increases in the effective influence functions in the fully saturated case are totally attributable to permeability effects and pore fluid stiffnesses . Comparisons of the results for the dry materials with those for the fully saturated materials clearly indicate that the pore fluid has a major influence on the response near the higher values of the wave number $\bar{\omega}$ considered in this study .

5.2.3 Influences of Variation of Permeability

Finally , the effects of varying the coefficient of permeability (k) on the interaction functions are exhibited for the sand material in Plots (23) through (25) for the smooth contact and Plots (26) through (29) for the welded contact for the basic modes of motion of the strip . The computations were carried out for a strip atop a saturated medium with λ_c= 5% and two values of k , namely , k = 0.1 cm/sec. and 0.001cm/sec. were examined . These two values correspond to seepage in soils consisting of typical medium and fine sands , respectively . The dotted curves correspond to k=0.1 cm/sec. .

It is clearly indicated from Plots (23) and (26) that influence functions for horizontal response are almost identical for both smooth and welded contacts . It is also observed from Plots (28) and (29) that only in the rocking motion and the coupling function there is appreciable difference between the influence functions for both the smooth and welded contacts throughout the range of the frequency considered . The difference is about (10 - 20)% in the rocking stiffness K_{RR} and tends to increase with increasing values of $\bar{\omega}$. In the vertical motion , almost identical influence functions were obltained for the low frequency . Appreciable deference is felt about less than 20% for

values of $\bar{\omega}$ above 3 . As to be expected , the coupled stiffness , K_{RH} , and the coupled damping coefficients , C_{RH} given in Plot (29) , are strongly influenced by the speed of seapage of the pore fluid . The deferences of up to 20% are observed in the coupled stiffness and coupled damping coefficient .

5.2.4 Computation of $W_y(x,0)$

Significant distortion of the continuity at the interface of the contact between the footing and the underneath-half-space could severely affect the evaluations of the influence functions . The vertical component of such displacement w_y is quantitatively studied for the vibration of the vertical mode since its effect seems more important . The w_y at center of the contact are evaluated for the sandy material with the permeability k = 0.01cm/sec. and λ_c =0 , 5 % , respectively , and the results are plotted against dimensionless frequency factor $\bar{\omega}$.

Figure 6 , 7 show the variations of w_y with the frequency factor $\bar{\omega}$ when the footing is subject to the vertical oscillation of unit amplitude . It can be readily seen from these figures that the relative fluid displacement w_y at the contact which should become zero from the physical point of view exhibits negligible amount of deviation from zero . Such invisible discontinuity that takes place along the contact area may not significantly affect the solution for the influence functions . This is because the relative displacement w is mainly controlled by the solid perneability which characterizes shearing effects at the interface between the solid skeleton and the trapped pore fluid . Thus the assumption of zero contact pressure proves to be reasonable .

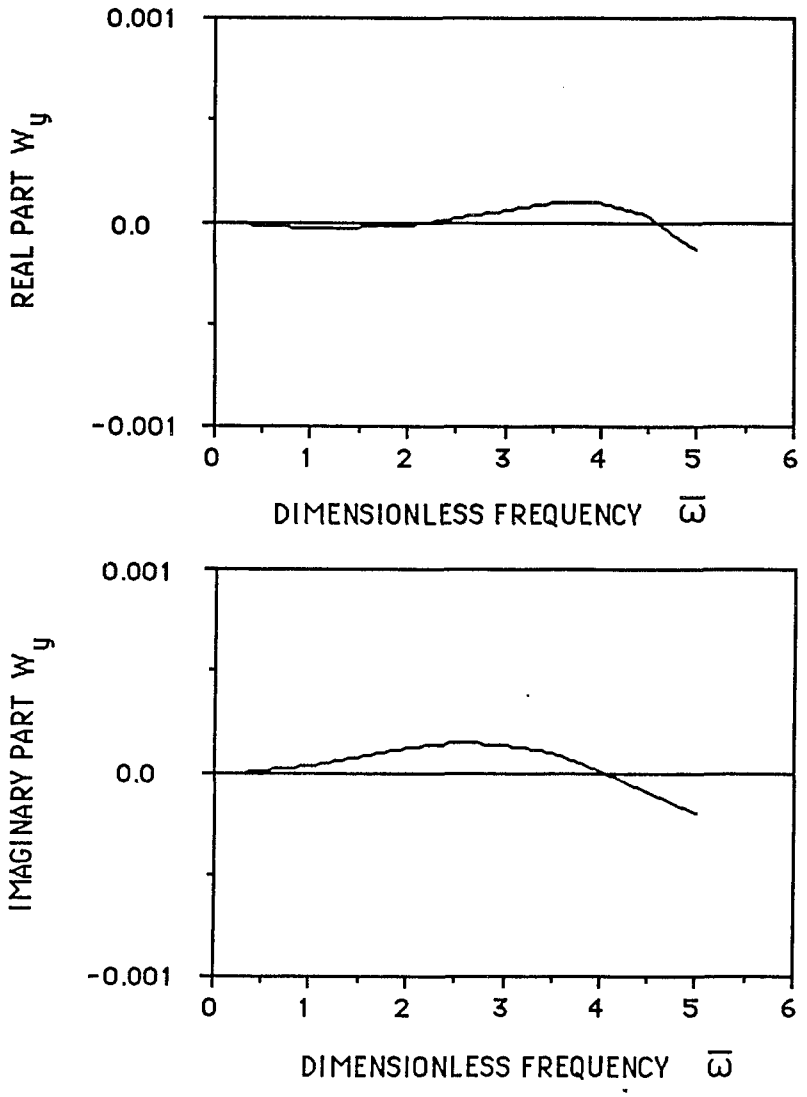

FIGURE(6) RELATIVE DISPLACEMENT W_y OF THE FLUID PORTION AT THE CENTER OF THE CONTACT BETWEEN FOOTING AND HALF-SPACE FOR VERTICAL MODE, k = 0.01cm/sec AND $\lambda_c = 0\ \%$.

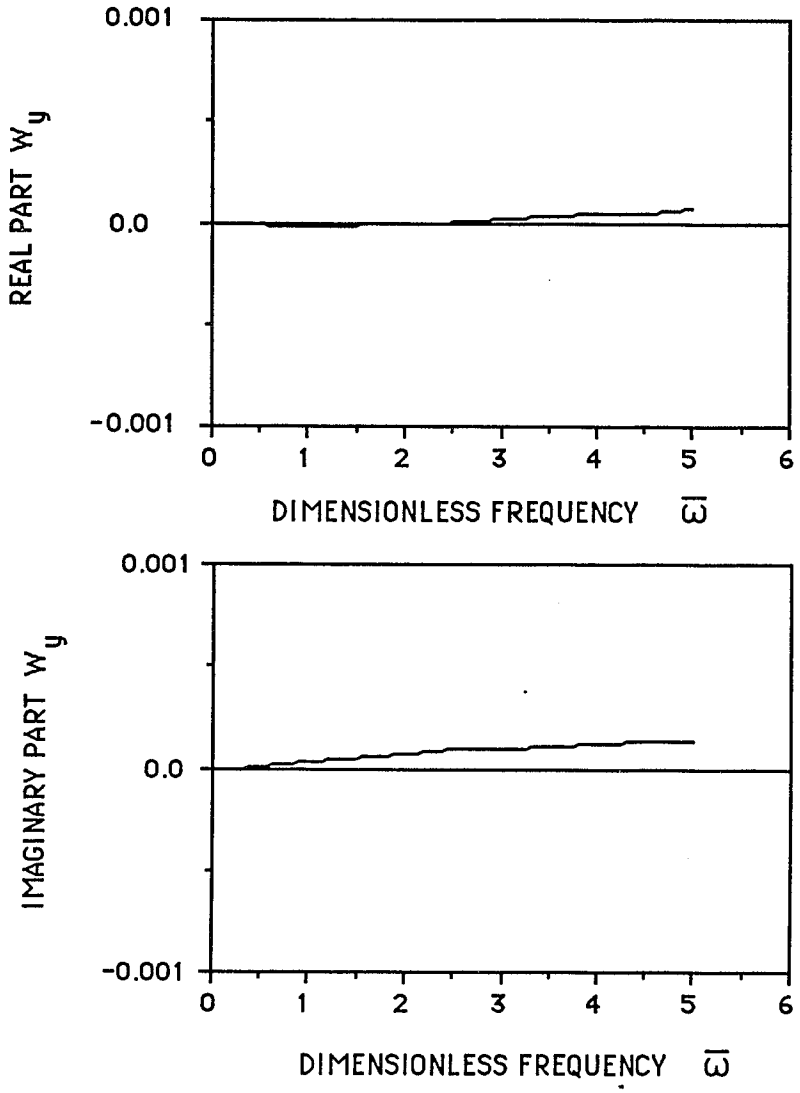

FIGURE(7) RELATIVE DISPLACEMENT W_y OF THE FLUID PORTION AT THE CENTER OF THE CONTACT BETWEEN FOOTING AND HALF-SPACE FOR VERTICAL MODE, k = 0.01cm/sec AND $\lambda_c = 5\%$.

CHAPTER 6. CONCLUSIONS AND SUGGESTIONS FOR FUTURE RESEARCH

Based upon the Biot's classical theory an analytical formulation has been developed to determine the dynamic force-displacement relationships for harmonic transverse motion of a rigid surface foundation in contact with a fully fluid-saturated , elastic half-space medium . Linear hysteretic damping characteristics of the solid have been included in the stress - strain relations . Complete calculations of the influence functions for two different soil samples , namely , a dense sand and a medium soft clay , have been performed . The results are compared with the corresponding values obtained for the dry soils .

For the fully saturated medium , it can be concluded that the impact of pore fluid on the influence functions is quite substantial . Because of the soil permeability , the pore fluid becomes essentially trapped in the soil and tends to move with the solid skeleton . This is especially true for the vertical and rocking modes of response in which the motion of the surface footing is resisted by the half-space medium through the coupling effect at the interface of the solid portion and the trapped fluid due to the shear holding the fluid portion to move together with the solid skeleton of the soil . Inscrease is also observed for the coupling coefficients . For the horizontal mode , the influence functions

are affected to some small degree by the soil permeability .

Soil hysteretic damping ratios ranging from 0% to 10% are assumed to study the impact of non-linearity of actual soil media on the influence functions . Results obtained indicate considerable increases in the radiation damping coefficients for all three modes of response , especially for the sandy material . Moderate changes in the stiffnesses are observed due to the hysteretic damping effect .

The impact of the soil permeability is also found to be significant depending on the type of contact condition assumed between the surface footing and the underneath half-space . Appreciable differences between the welded and smooth contact conditions for all three modes of response are indicated when the half-space is fully saturated , while almost identical results are obtained between the two types of contact conditions when the half- space medium is dry medium .

The differences between sand and clay are mainly reflected on the type of the contact conditions between the footing and the underneath half space . The observation of the results indicates that the clay material is more sensitive to the type of the contact conditions than the sandy material .

As an extension to this research work , it is recommended that the future activities on this subject concentrate on the following areas . The first area is to extend the objectives accomplished in this thesis into more general case including the feature of the partial saturation to provide a quantitative assessment for the level of the saturation above which the impact of the fluid content become effective .

The second area for future study is to generate the influence functions for diferent shapes of footings (circular for example) vibrating against the surface of a saturated elastic half-space .

The third area is to consider the case where $\lambda_c \neq \lambda_s$. A potential representation suitable for decoupling the body waves in the equation of motion may be feasible . Other research areas such as effect of embedded footing , solution to account for the flexibility of the footing , as well as interaction with the surrounding footings are also of special interest for future studies .

APPENDIX.A Abbreviations

(1) Values of V_j and a_j :

The complex-valued velocities , V_j (j=1,2,3) , appearing in equations (2.15) through (2.18) stand for :

$$V_j = V_c/\lambda_j \quad , \quad j = 1,2,3 \qquad , \quad (A1)$$

where the "confined velocity' V_c stands for

$$V_c = (E_c + \alpha^2\alpha')/ \rho \qquad , \quad (A2)$$

and

$$\lambda_{1,2} = [B - (1 + i\omega K E_c \lambda_c/\alpha') \, i\gamma'/(k\rho\omega) \mp \Delta] /(2A) \qquad , \quad (A3)$$

$$\lambda_3 = [C - i\gamma'/(k\rho\omega)] / \{ c_2 K E_c (1+i\omega\lambda_c)[N/f - i\gamma'/(k\rho\omega)]/\alpha' \} \qquad , \quad (A4)$$

In equations (A3) and (A4) , the following contractions are made

$$A = K (1 - \alpha^2 K + i\omega K E_c \lambda_c/\alpha') \qquad , \quad (A5)$$

$$B = K + N (1 + i\omega K E_c \lambda_c/\alpha')/f - 2\alpha K N \qquad , \quad (A6)$$

$$C = N/f - N^2 \quad , \text{(A8)}$$

$$\Delta^2 = B^2 - 4AC - 2i[-2A + B(1+i\omega KE_c\lambda_c/\alpha')]\ \gamma'/(k\rho\omega)$$

$$- (1+i\omega KE_c\lambda_c/\alpha')^2(\gamma'/k\rho\omega)^2 \quad , \text{(A9)}$$

Similarly , the coefficients a_j (j=1,2,3) appearing in equations (2.15) and (2.17) designate the quantities :

$$a_j =[\ 1 -\alpha N - \lambda_j(\ 1 - \alpha^2 K + i\omega KE_c\lambda_c/\alpha')]/[\ \alpha N/f - N - i\alpha\gamma'/(k\rho\omega)]$$

$$, j=1,2 \quad , \text{(A9)}$$

$$a_3 = N [\ i\gamma'/(k\rho\omega) - N/f\ ]^{-1} \quad , \text{(A10)}$$

(2) $\beta_j(s,\omega)$ and $\gamma(s,\omega)$:

Expressions for $\beta_j(s,\omega)$, j=1,2, and $\gamma(s,\omega)$ in equations (3.2) through (3.3) are as follows :

$$\beta_j = \lambda_j (a_j+ \alpha) / [\ \lambda_2(a_2 + \alpha) - \lambda_1 (a_1+ \alpha)\ ] \quad , j=1,2 \quad , \text{(A11)}$$

$$\gamma = \{ \lambda_1 \beta_2 [\alpha\alpha'(\theta_1+\alpha) - E_c(1+i\omega\lambda_c)]$$

$$- \lambda_2 \beta_1 [\alpha\alpha'(\theta_2+\alpha) - E_c(1+i\omega\lambda_c)] \} / [2c_2 E_c(1+i\omega\lambda_c)] \quad , \quad (A12)$$

APPENDIX.B Convergence of certain integrals

To insure rapid convergence at the upper limit in the integrals given in equations (4.18) through (4.19) , the integrands should be replaced such that there is higher order of decay of the integrands when $\bar{s}$ becomes large . For this purpose , the asymtotic behaviors of these integrands for large $\bar{s}$ are examined as follows

Expanding the integrand in equation (4.18a) for large $\bar{s}$ leads to

$$\bar{n}_3(\bar{s})/\bar{F}(\bar{s},\omega) = b_1\bar{s}/(\bar{s}^2 - \omega_3^2/2) + O(\bar{s}^{-3}) \quad , \quad (B1)$$

in which

$$b_1 = 1 / (\beta_2\omega_1^2 - \beta_1\omega_2^2 - 2\gamma\omega_c^2) /2 \quad , \quad (B2)$$

With the aids of relations (B1) and (B2) , the integral (4.18a) with a new integrand having better convergence for $\bar{s}\longrightarrow\infty$ can be rewritten as

$$\alpha_{n\,l} = (-1)^l\, i^{n+l} \{ \int_0^\infty 4\gamma\omega_c^2 \left[\frac{\bar{n}_3(\bar{s})}{F(\bar{s})} - b_1\frac{\bar{s}}{\bar{s}^2 - \omega_3^2}\right] J_n(\bar{s})\, J_l(\bar{s})\, d\bar{s}$$

$$+ \int_0^\infty 4\gamma\omega_c^2\, b_1\frac{\bar{s}}{\bar{s}^2 - \omega_3^2}\, J_n(\bar{s})\, J_l(\bar{s})\, d\bar{s} \} \quad , (B3)$$

The second integral in equation (B3) can easily be evaluated by making use of the identities listed by Erdelyi (1954) . The first integral converges more rapidly than the one given by equation (4.18a) , thus it should pose no difficulties in numerical evaluations . similarly , the integrals like ϖ_{nl} , C_{nl} etc. can be improved in the similar fashion .

APPENDIX C. Reduction to dry case

Discussion is made here of the procedure employed to reduce Biot ' s two-phase equations for saturated media to one-phase equations for dry solid with hysteretic dampings . The resulting equations are used to generate the influence functions for the dry soil .

Setting the parameters $\rho_f = 0$, $\gamma'/k \longrightarrow \infty$, $\alpha = 0$ and pore presure $p = 0$ in equations (2.1) through (2.3) and then substituting these equations into the dynamic equations of motion (2.5) lead to

$$V_c^2 \frac{\partial}{\partial x}(e - \alpha k \varepsilon) + V_s^2 \frac{\partial \Omega}{\partial y} = \ddot{u}_x$$

$$-\frac{E_c}{\rho}\left[\lambda_c \frac{\partial^2 \dot{u}_x}{\partial x^2} + c_2 \lambda_s \frac{\partial^2 \dot{u}_x}{\partial y^2} + (c_1 \lambda_c + c_2 \lambda_s) \frac{\partial^2 \dot{u}_y}{\partial x \partial y}\right] , \quad (C1)$$

$$V_c^2 \frac{\partial}{\partial y}(e - \alpha k \varepsilon) - V_s^2 \frac{\partial \Omega}{\partial x} = \ddot{u}_y$$

$$-\frac{E_c}{\rho}\left[c_2 \lambda_s \frac{\partial^2 \dot{u}_y}{\partial x^2} + \lambda_c \frac{\partial^2 \dot{u}_y}{\partial y^2} + (c_1 \lambda_c + c_2 \lambda_s) \frac{\partial^2 \dot{u}_x}{\partial x \partial y}\right] , \quad (C2)$$

It should be noted that the equations (2.6) or (2.8c) and (2.8d) governing the motion of the fluid portion vanish identically . Equations (C1) and (C2) govern the motion of the solid particles and provide dilitational and distortional waves which are coupled together through the hysteretic dampings ratios . To separate the two waves , similar procedure is used by assuming identical hysteretic damping ratios for both compressional and distortional strains , i.e. $\lambda_c = \lambda_s$. Following the procedure described in Chapter 3 and 4 , and omitting the intermediate steps , it can be readily shown that the solution to th Green ' s functions in the present case :

$$u_x^H(x-\xi) = \frac{1}{2\pi\mu}\int_{-\infty}^{\infty} \frac{n_3\,\omega^2/V_3^2}{F(s,\omega)}\, e^{-is(x-\xi)}\, ds \quad , \qquad (C3)$$

$$u_y^H(x-\xi) = \frac{i}{2\pi\mu}\int_{-\infty}^{\infty} \frac{s\,\bar{F}(s,\omega)}{F(s,\omega)}\, e^{-is(x-\xi)}\, ds \quad , \qquad (C4)$$

$$u_x^P(x-\xi) = -\frac{i}{2\pi\mu}\int_{-\infty}^{\infty} \frac{s\,\bar{F}(s,\omega)}{F(s,\omega)}\, e^{-is(x-\xi)}\, ds \quad , \qquad (C6)$$

$$u_y^P(x-\xi) = \frac{1}{2\pi\mu}\int_{-\infty}^{\infty} \frac{n_1\,\omega^2/V_3^2}{F(s,\omega)}\, e^{-is(x-\xi)}\, ds \quad , \qquad (C5)$$

Here ,

$$F(s,\omega) = (1+i\omega\lambda_c)[(2s^2 - \omega^2/V^2_3)^2 - 4 n_1 n_3] \quad , \quad (C7)$$

$$F(s,\omega) = (2s^2 - \omega^2/V^2_3) - 2 n_1 n_3 \quad , \quad (C8)$$

$$\left.\begin{aligned} n_{1,3} &= \sqrt{s^2 - \omega^2 / V^2_{1,3}} \\ \text{Re } n_{1,3} &\geq 0 \text{ and } \text{Im } n_{1,3} \geq 0 \end{aligned}\right\} \quad , \quad (C9)$$

and $V^2_1 = (1 + i\omega\lambda_c) V^2_c$, $V^2_3 = c_2 V^2_1$, (C10)

In equations (C10) , the velocity V_c now stands for

$$V^2_c = (E_c/\rho)^{1/2} \quad , \quad (C.11)$$

It can readily be seen that upon setting $\lambda_c = 0$, the above equations immediately reduce to those corresponding tothe elastic solid by Dien(1970) . Pursuing the same procedure described in Chapter 4 , the solution to the influence functions may be obtained for the dry media rom equations (4.17) and (4.21) .

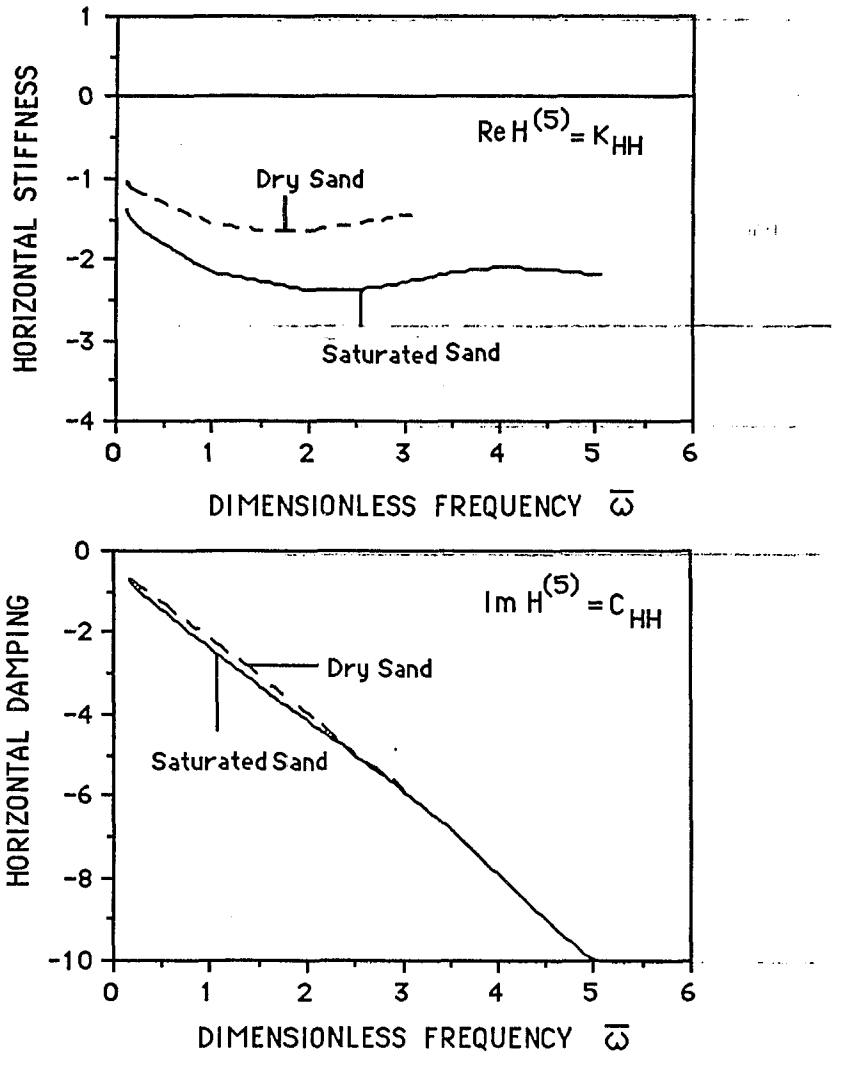

PLOT(1) - INFLUENCE FUNCTIONS $H^{(5)}$ FOR SMOOTH CONTACT; k=0.01cm/sec AND λ_c=0 % (HORIZONTAL MOTION).

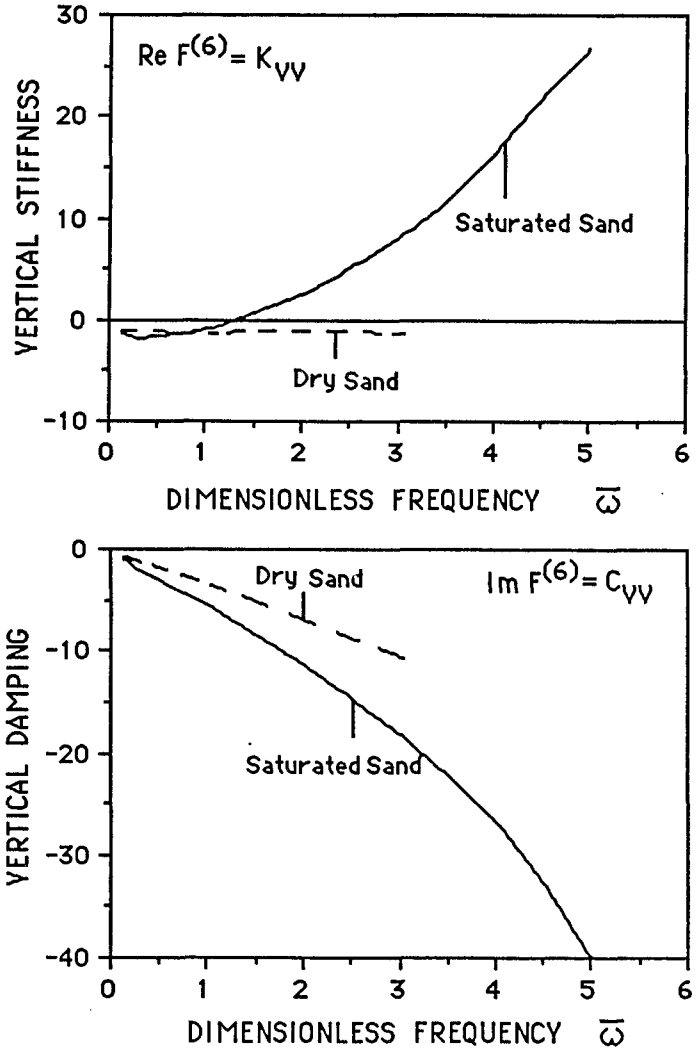

PLOT(2) - INFLUENCE FUNCTIONS $F^{(6)}$ FOR SMOOTH CONTACT, k=0.01 cm/sec AND λ_c =0 % (VERTICAL MOTION).

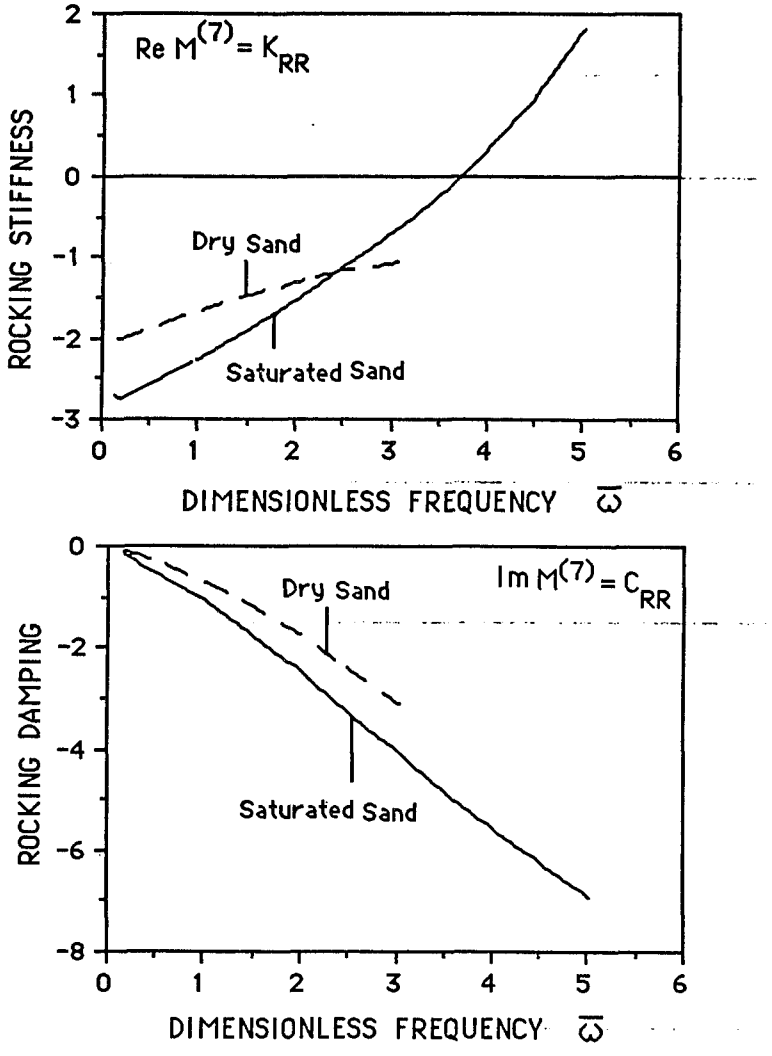

PLOT(3) - INFLUENCE FUNCTIONS $M^{(7)}$ FOR SMOOTH CONTACT, k=0.01 cm/sec AND λ_c =0 % (ROCKING MOTION).

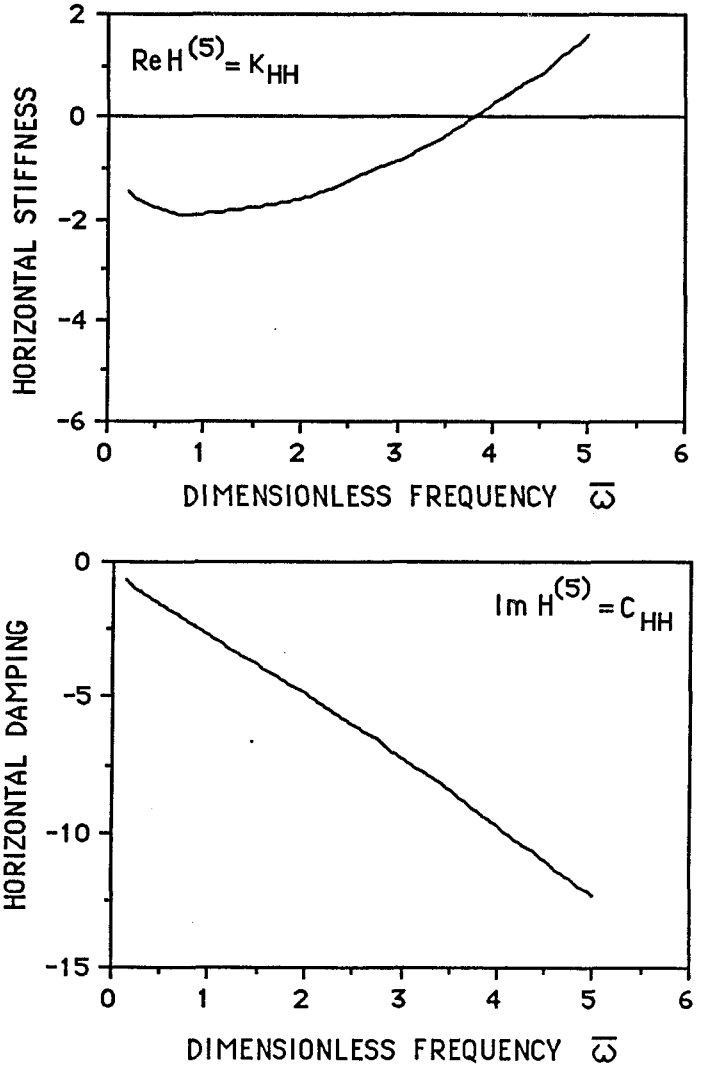

PLOT(4) - INFLUENCE FUNCTIONS $H^{(5)}$ FOR SMOOTH CONTACTS. SATURATED SOIL, k=0.01cm/sec AND $\lambda_c = 1\%$ (HORIZONTAL MOTION).

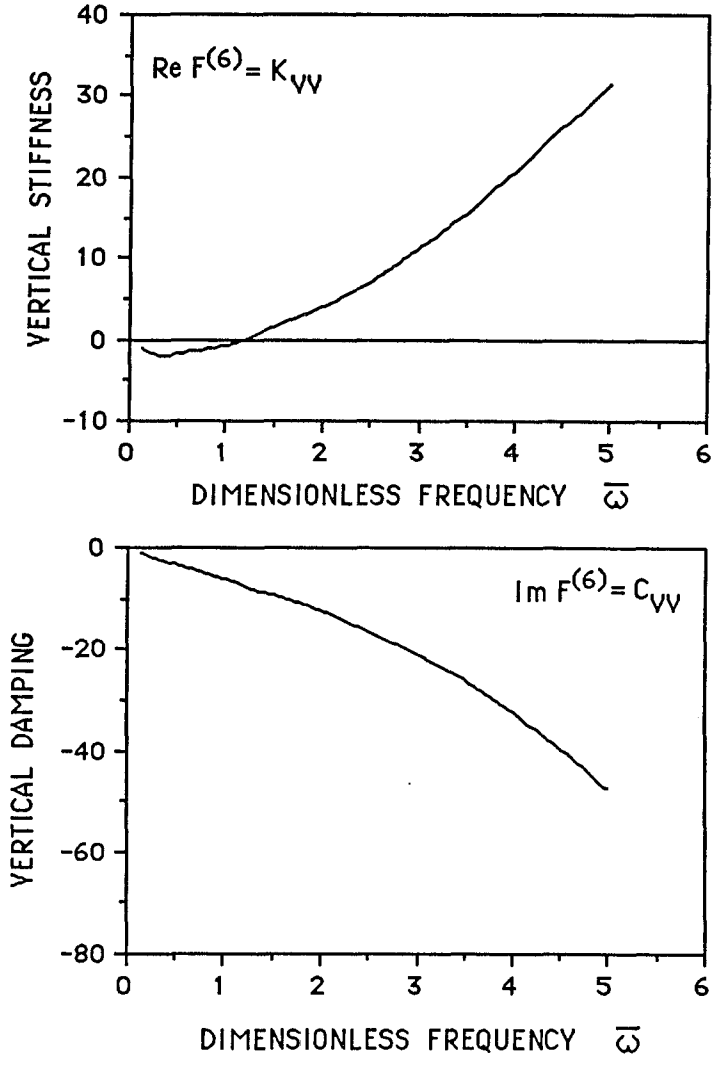

PLOT(5) - INFLUENCE FUNCTIONS $F^{(6)}$ FOR SMOOTH CONTACT. SATURATED SOIL, k=0.01cm/sec AND λ_c = 1 % (VERTICAL MOTION).

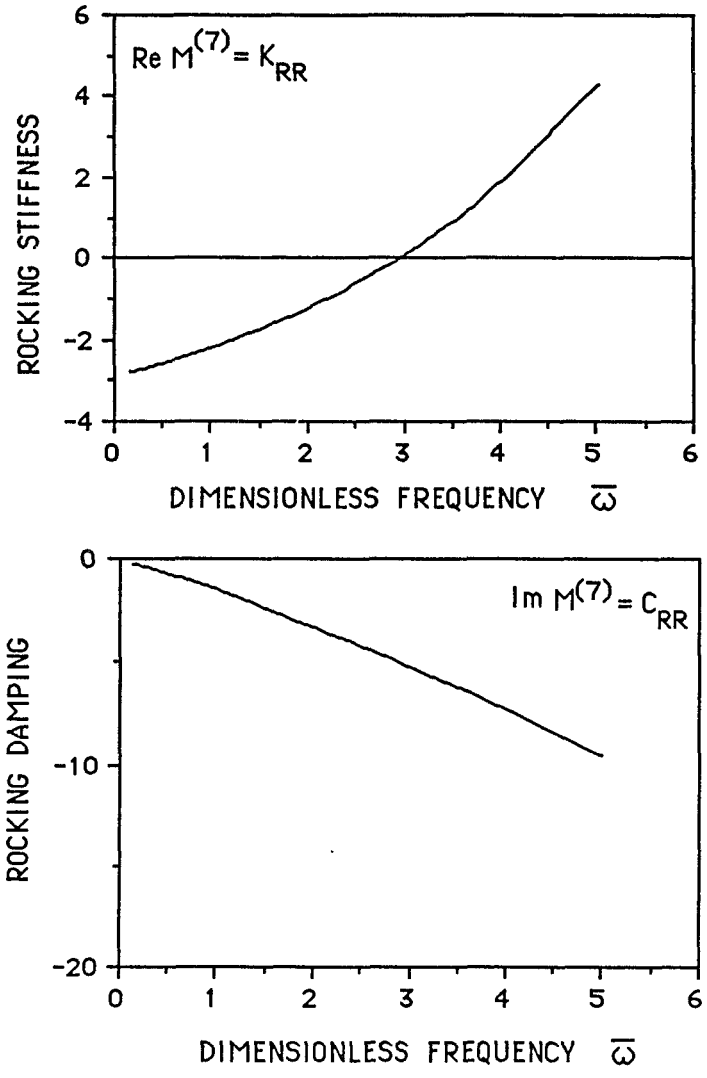

PLOT(6) - INFLUENCE FUNCTIONS $M^{(7)}$ FOR SMOOTH CONTACT. SATURATED SOIL, k=0.01 cm/sec AND λ_c = 1 % (ROCKING MOTION).

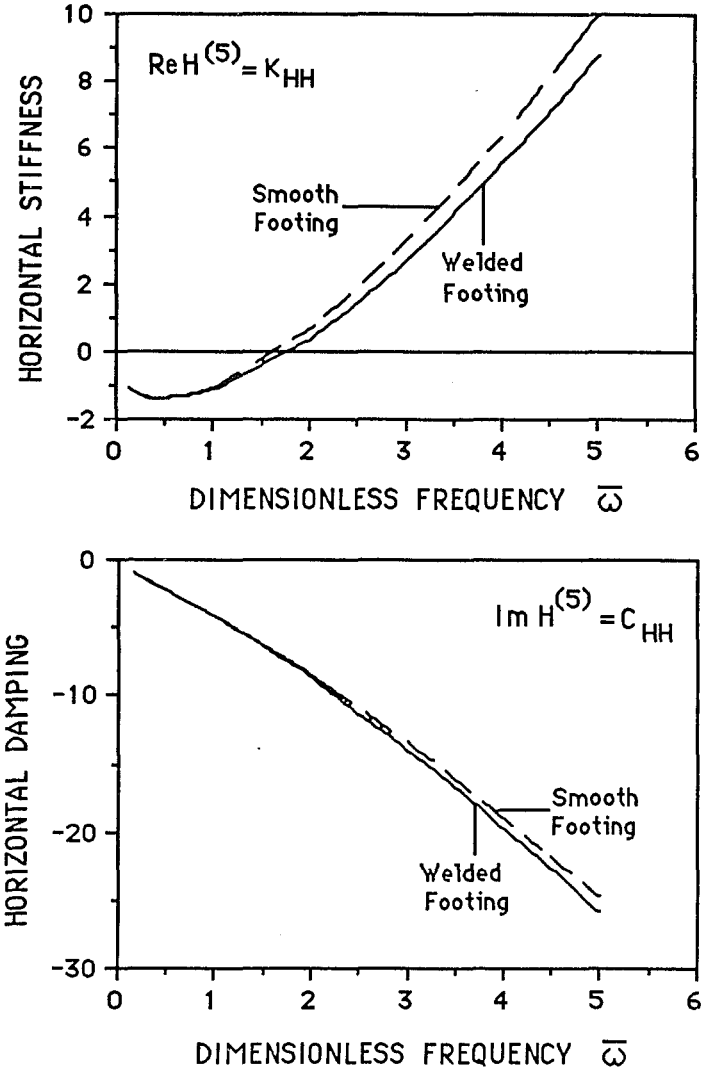

PLOT(7)- INFLUENCE FUNCTIONS $H^{(5)}$ FOR WELDED AND SMOOTH CONTACTS. SATURATED SAND, k=0.01 cm/sec AND λ_c =5 % (HORIZONTAL MOTION).

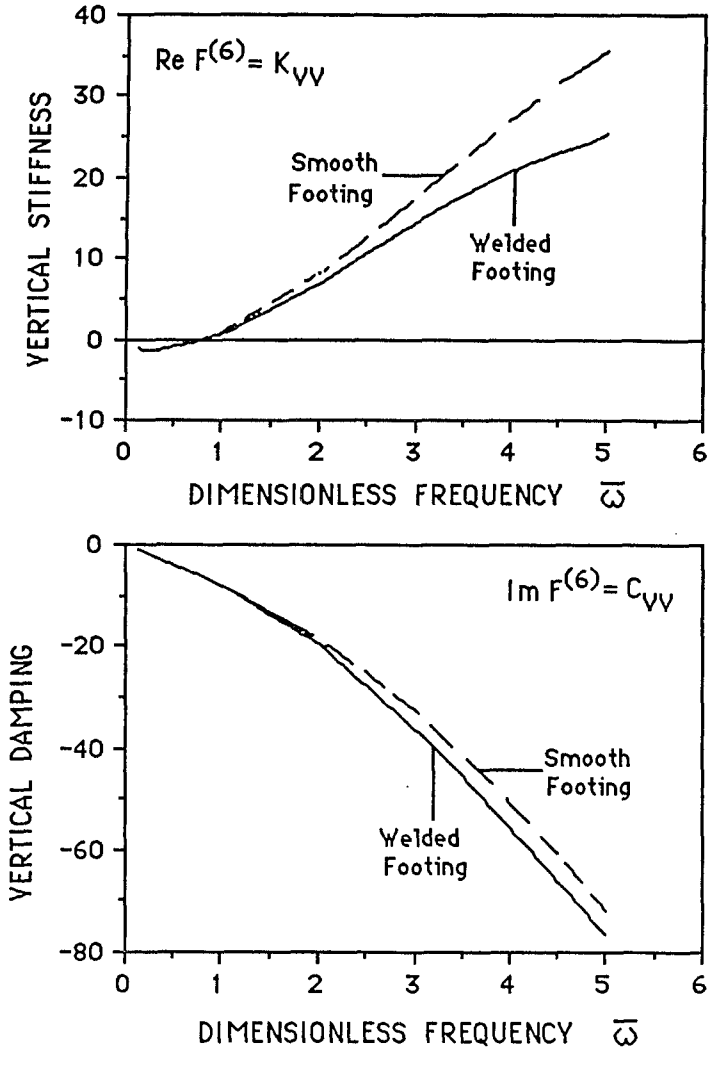

PLOT(8)- INFLUENCE FUNCTIONS $F^{(6)}$ FOR WELDED AND SMOOTH CONTACT. SATURATED SAND, k=0.01cm/sec AND λ_c =5 % (VERTICAL MOTION).

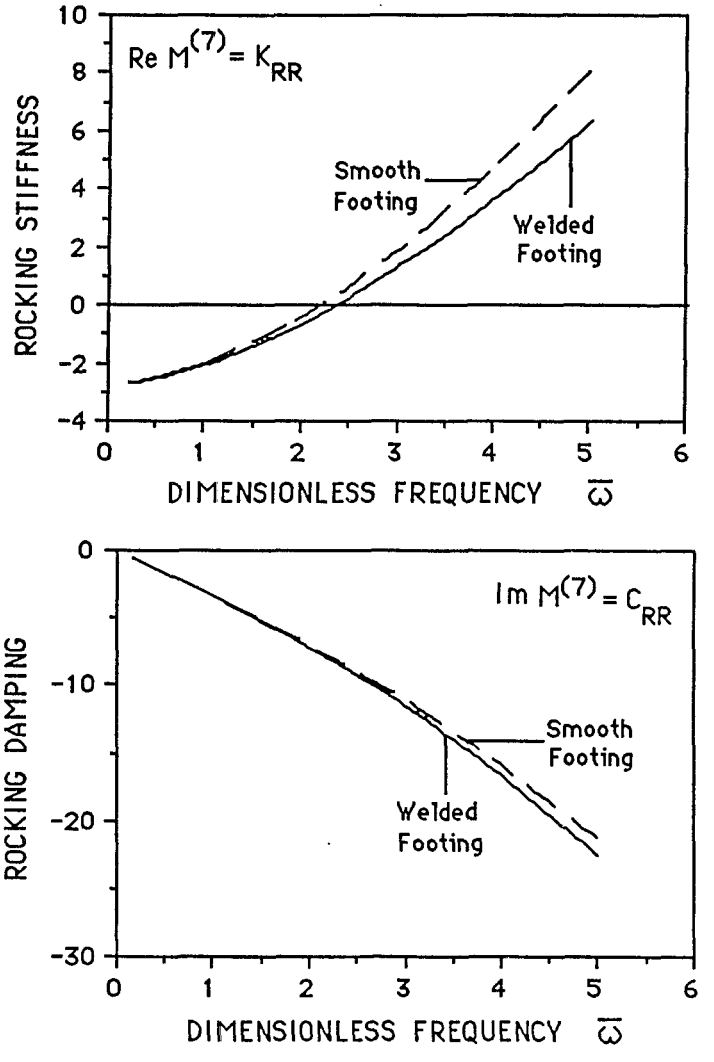

PLOT(9) - INFLUENCE FUNCTIONS $M^{(7)}$ FOR WELDED AND SMOOTH CONTACTS. SATURATED SAND, k=0.01 cm/sec AND λ_c =5 % (ROCKING MOTION).

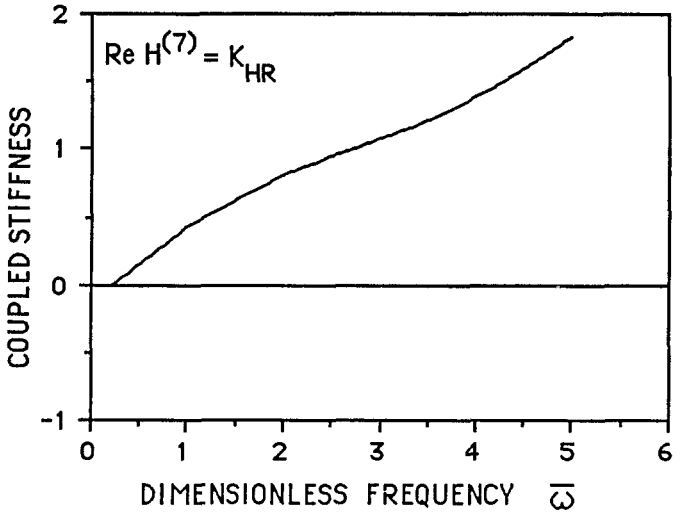

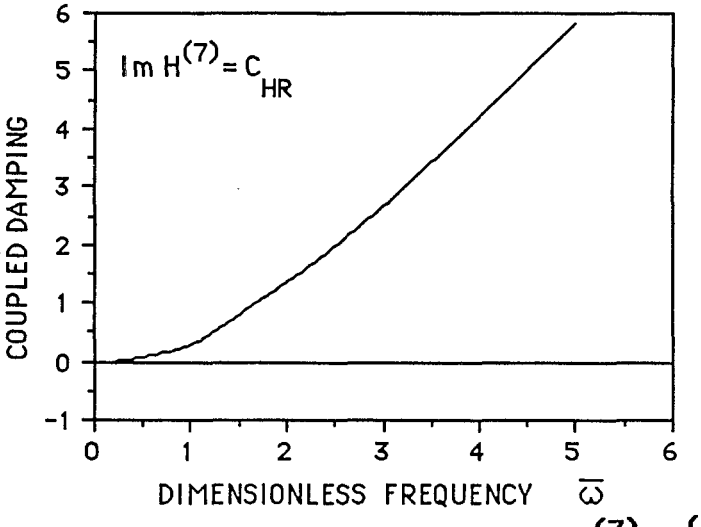

PLOT(10) - INFLUENCE FUNCTIONS $H^{(7)} \equiv M^{(5)}$ FOR WELDED CONTACT. SATURATED SAND, k=0.01cm/sec AND λ_c=5 %.

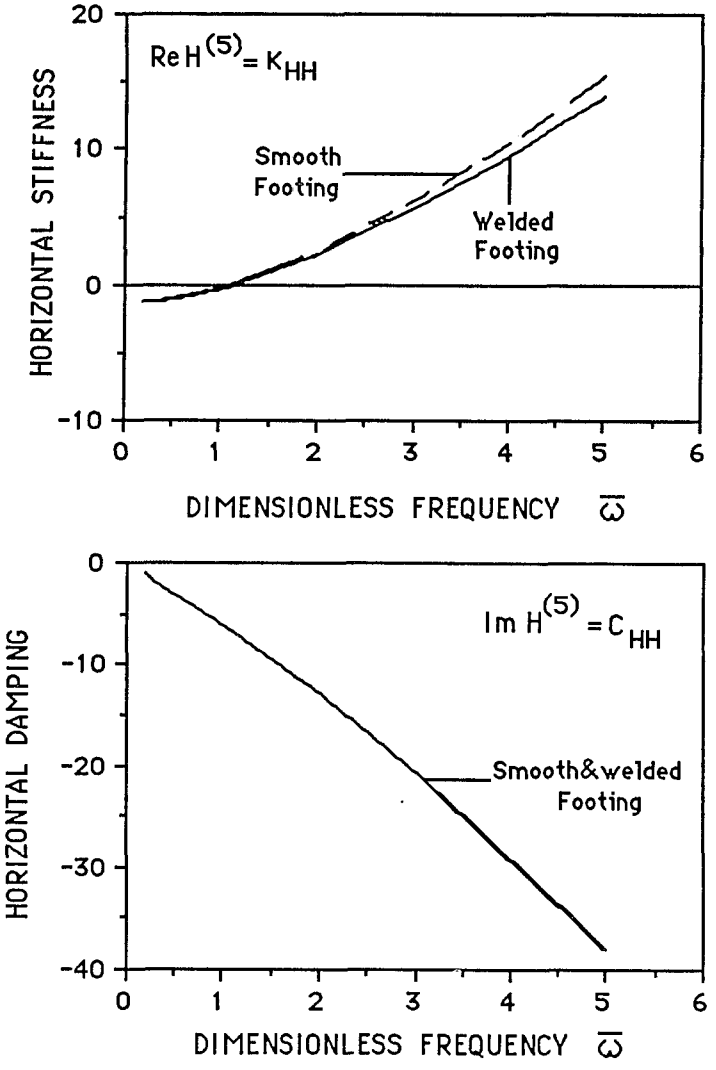

PLOT(11)- INFLUENCE FUNCTIONS $H^{(5)}$ FOR WELDED AND SMOOTH CONTACTS FOR SATURATED SAND, k=0.01 cm/sec AND λ_c = 10% (HORIZONTAL MOTION).

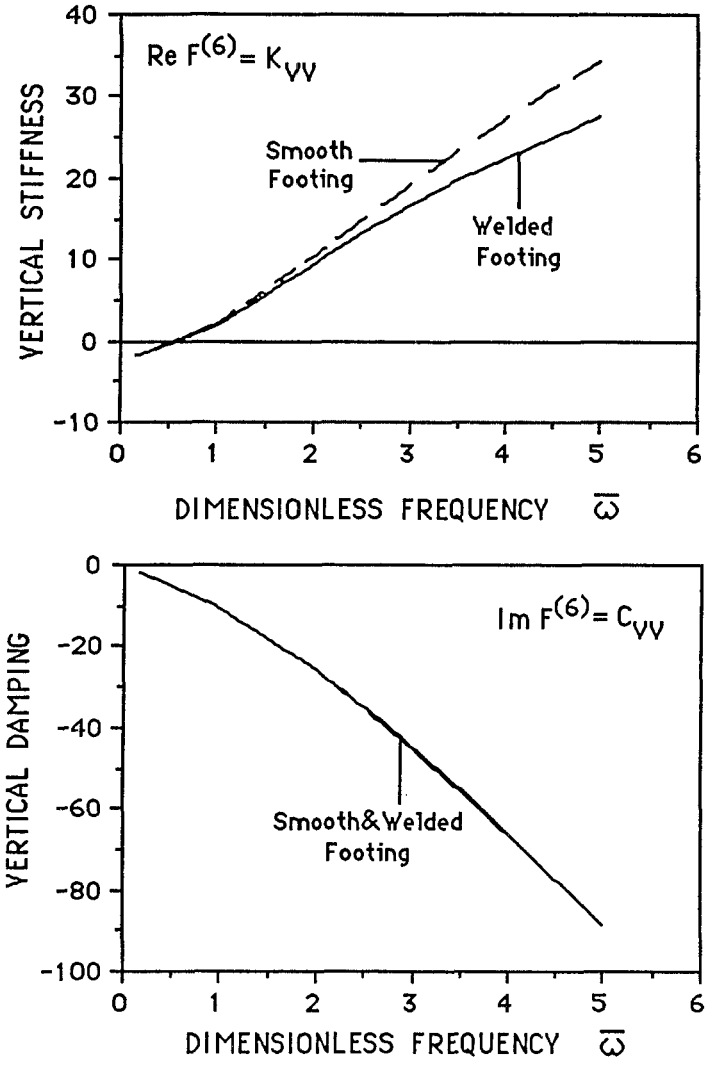

PLOT(12) - INFLUENCE FUNCTIONS $F^{(6)}$ FOR WELDED AND SMOOTH CONTACT, FOR SATURATEDSAND,k=0.01cm/sec AND λ_c = 10 % (VERTICAL MOTION).

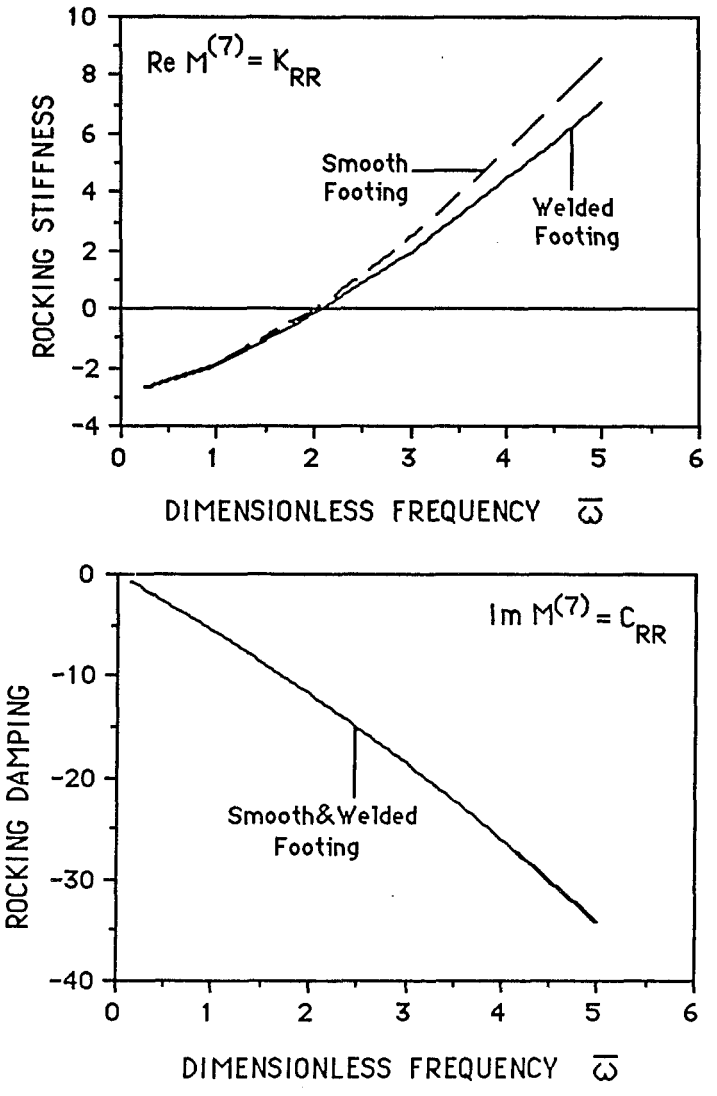

PLOT(13)- INFLUENCE FUNCTIONS $M^{(7)}$ FOR WELDED AND SMOOTH CONTACTS FOR SATURATED SAND, k=0.01 cm/sec AND λ_c = 10 % (ROCKING MOTION).

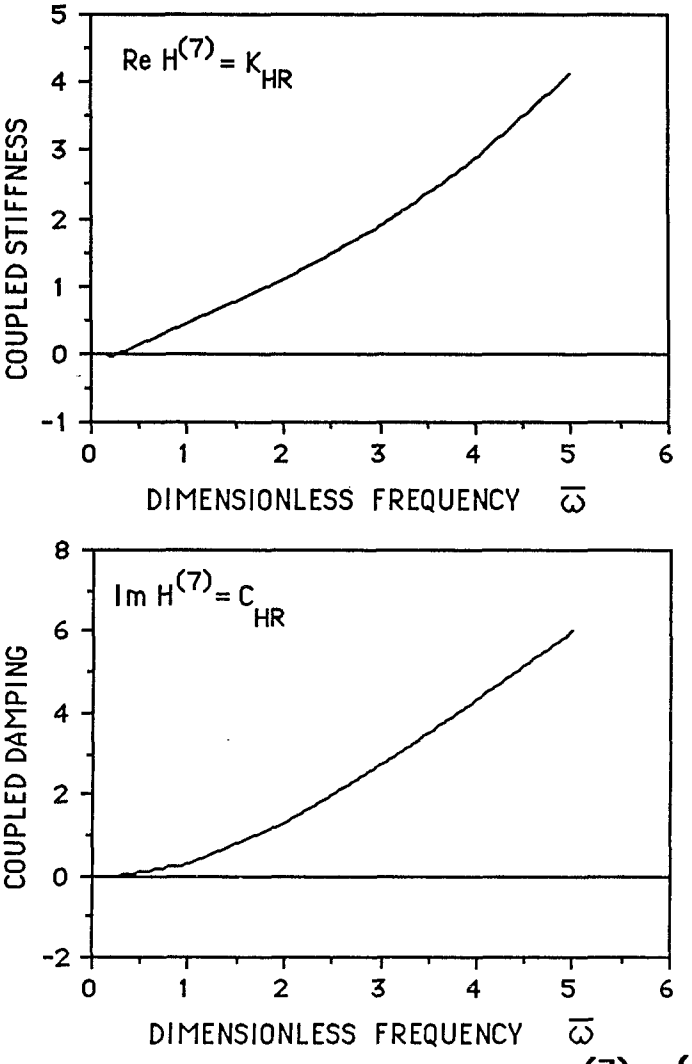

PLOT(14) - INFLUENCE FUNCTIONS $H^{(7)} \equiv M^{(5)}$ FOR WELDED CONTACT. SATURATED SAND, k=0.01cm/sec AND λ_c=10%.

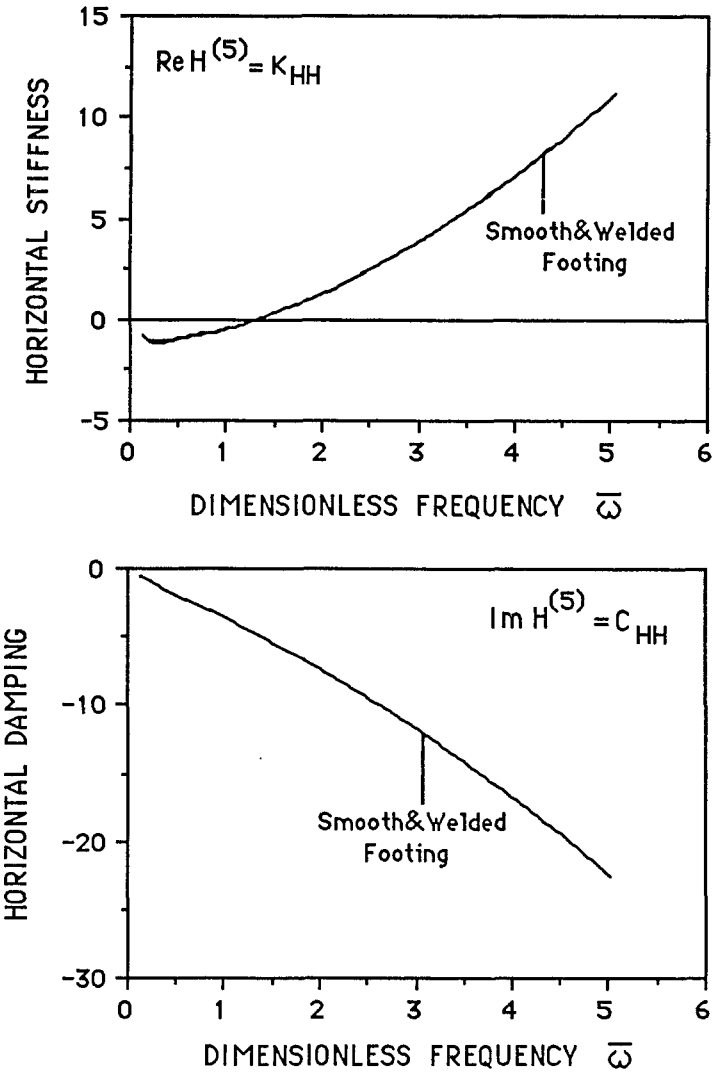

PLOT(15) - INFLUENCE FUNCTIONS $H^{(5)}$ FOR WELDED AND SMOOTH CONTACTS. DRY SAND , $\lambda_c = 5\%$ (HORIZONTAL MOTION).

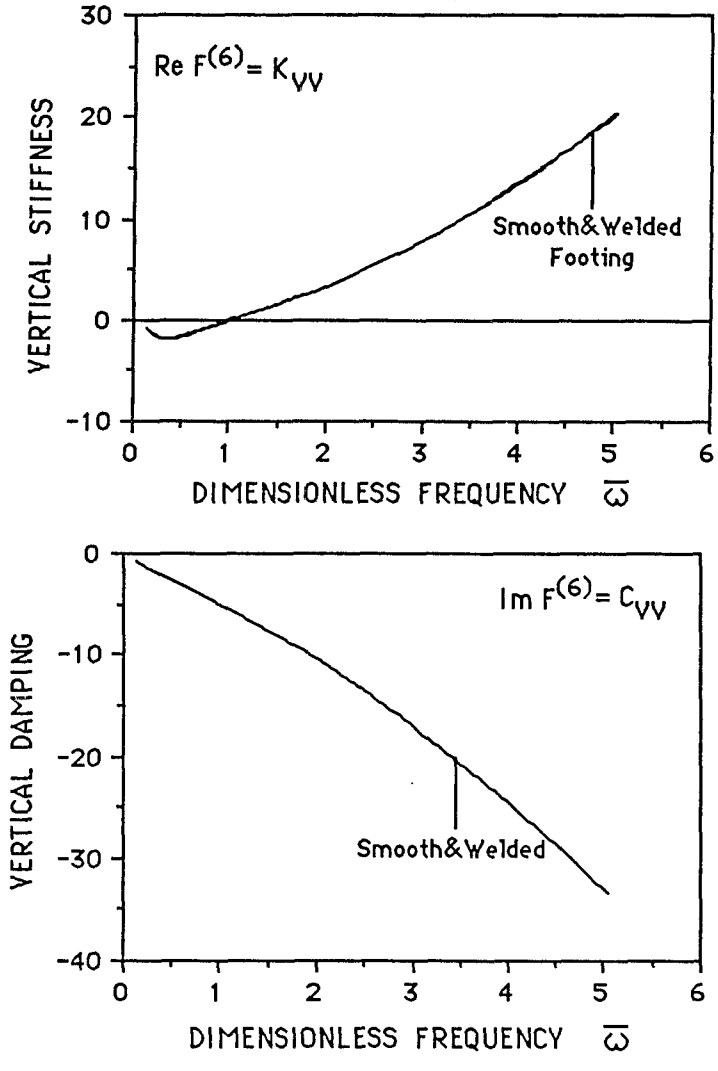

PLOT(16) – INFLUENCE FUNCTIONS $F^{(6)}$ FOR WELDED AND SMOOTH CONTACT. DRY SAND , $\lambda_c = 5\%$ (VERTICAL MOTION).

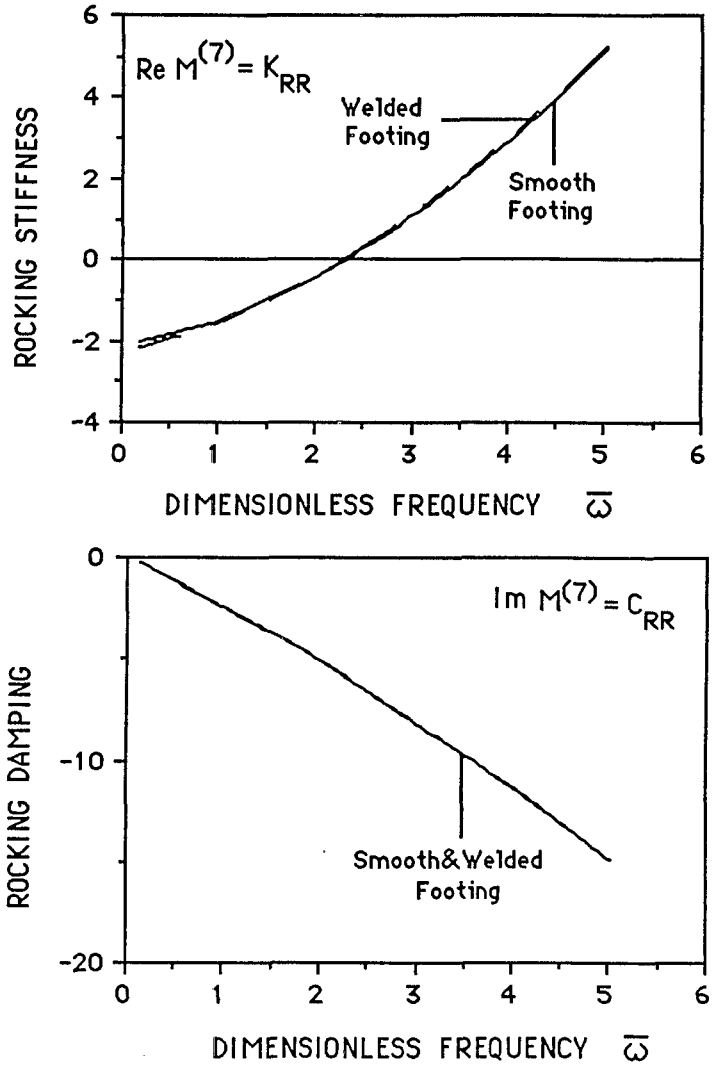

PLOT(17)- INFLUENCE FUNCTIONS $M^{(7)}$ FOR WELDED AND SMOOTH CONTACTS. DRY SAND , λ_c =5 % (ROCKING MOTION).

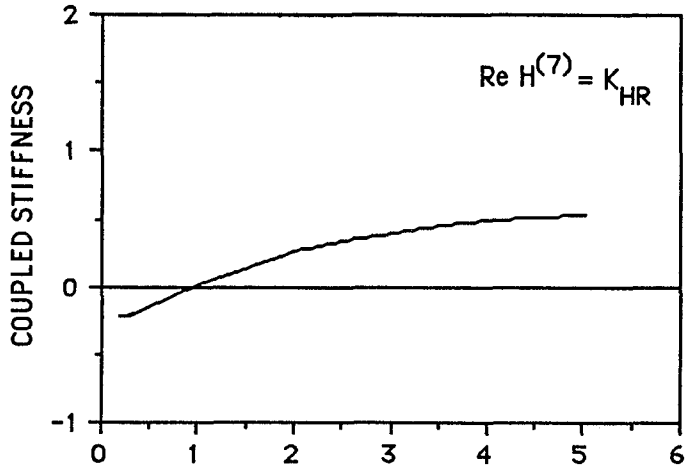

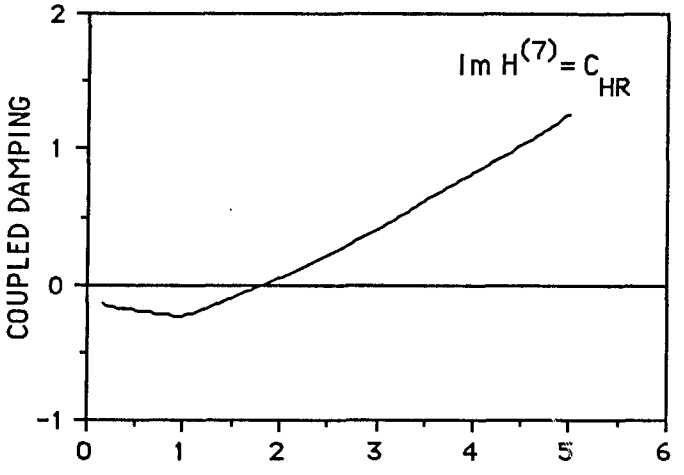

PLOT(18) - INFLUENCE FUNCTIONS $H^{(7)} \equiv M^{(5)}$ FOR WELDED CONTACT. DRY SAND , λ_c=5 %.

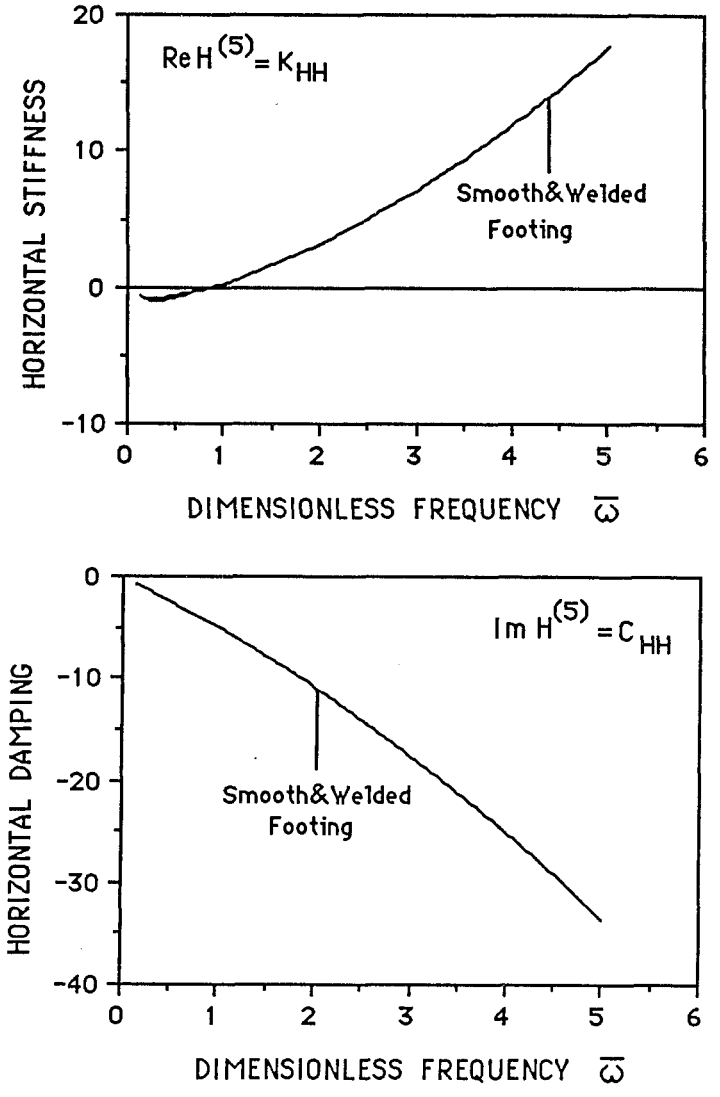

PLOT(19) - INFLUENCE FUNCTIONS $H^{(5)}$ FOR WELDED AND SMOOTH CONTACTS FOR DRY SAND , $\lambda_c = 10\%$ (HORIZONTAL MOTION).

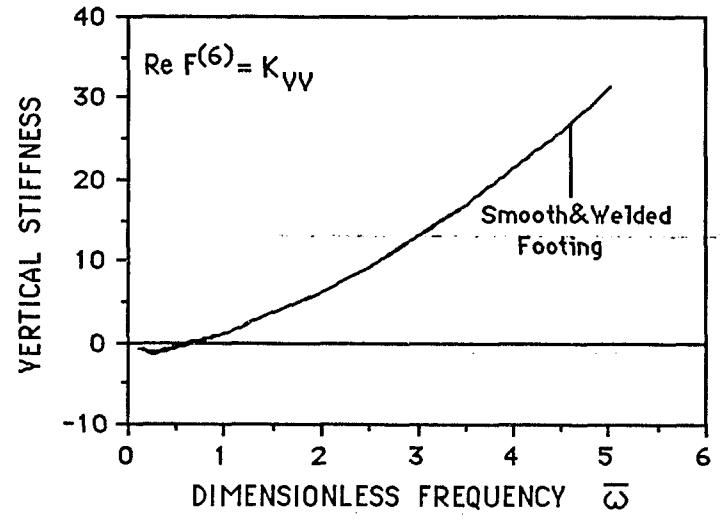

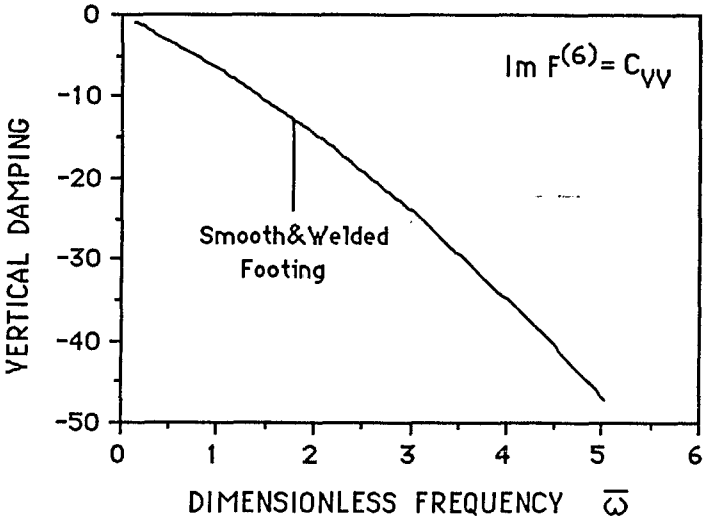

PLOT(20) – INFLUENCE FUNCTIONS $F^{(6)}$ FOR WELDED AND SMOOTH CONTACT, FOR DRY SAND , $\lambda_c = 10\%$ (VERTICAL MOTION).

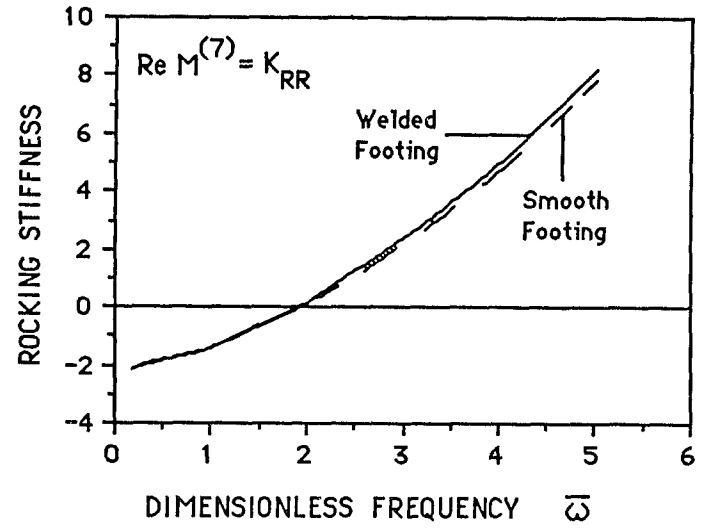

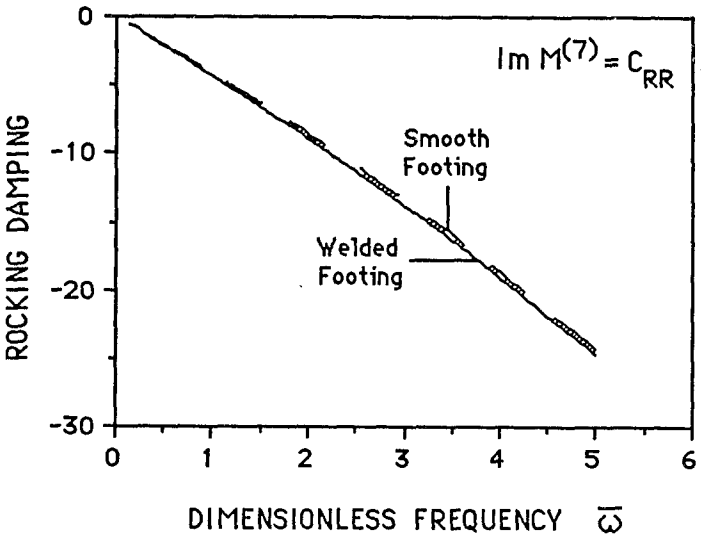

PLOT(21) - INFLUENCE FUNCTIONS $M^{(7)}$ FOR WELDED AND SMOOTH CONTACTS FOR DRY SAND , $\lambda_c = 10\%$ (ROCKING MOTION).

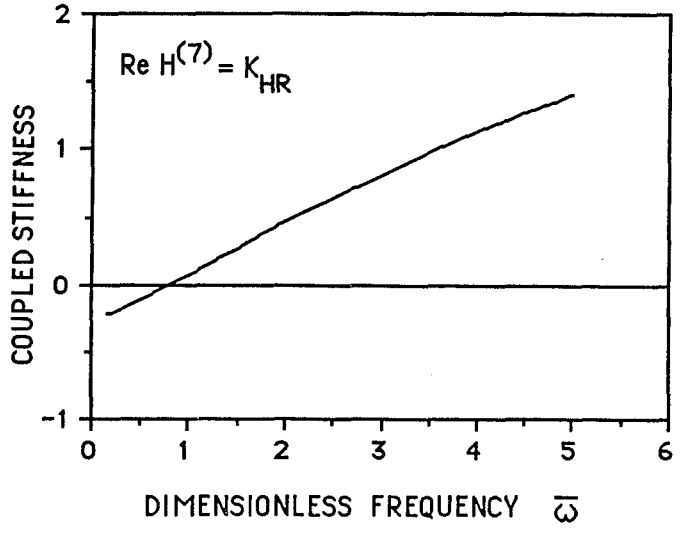

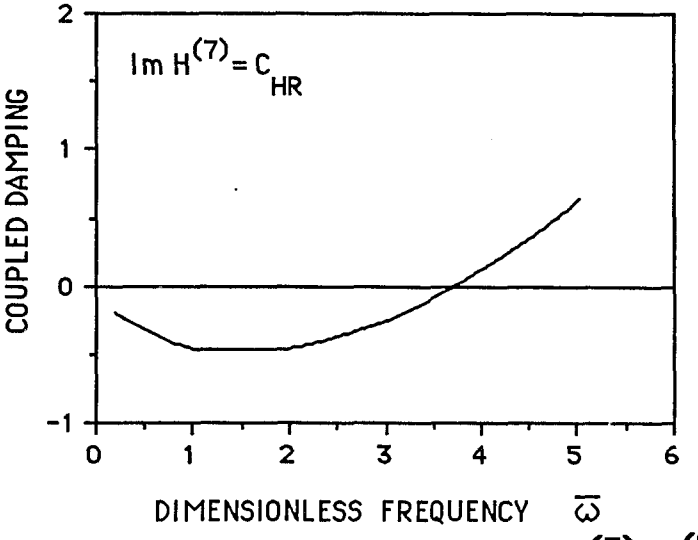

PLOT(22) - INFLUENCE FUNCTIONS $H^{(7)} \equiv M^{(5)}$ FOR WELDED CONTACT FOR DRY SAND , $\lambda_c = 10\%$

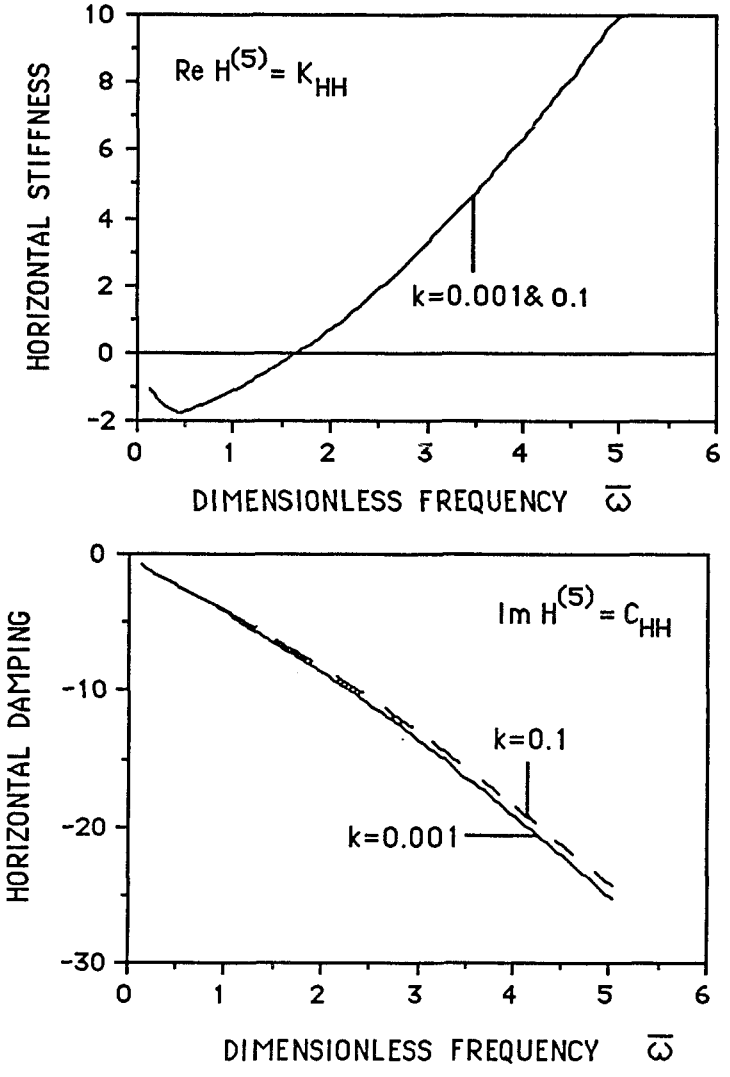

PLOT(23)- INFLUENCE OF PERMEABILITY ON INTERACTION COEFFICIENTS $H^{(5)}$ FOR SMOOTH CONTACT($\lambda_c = 5\ \%$). (SAND).

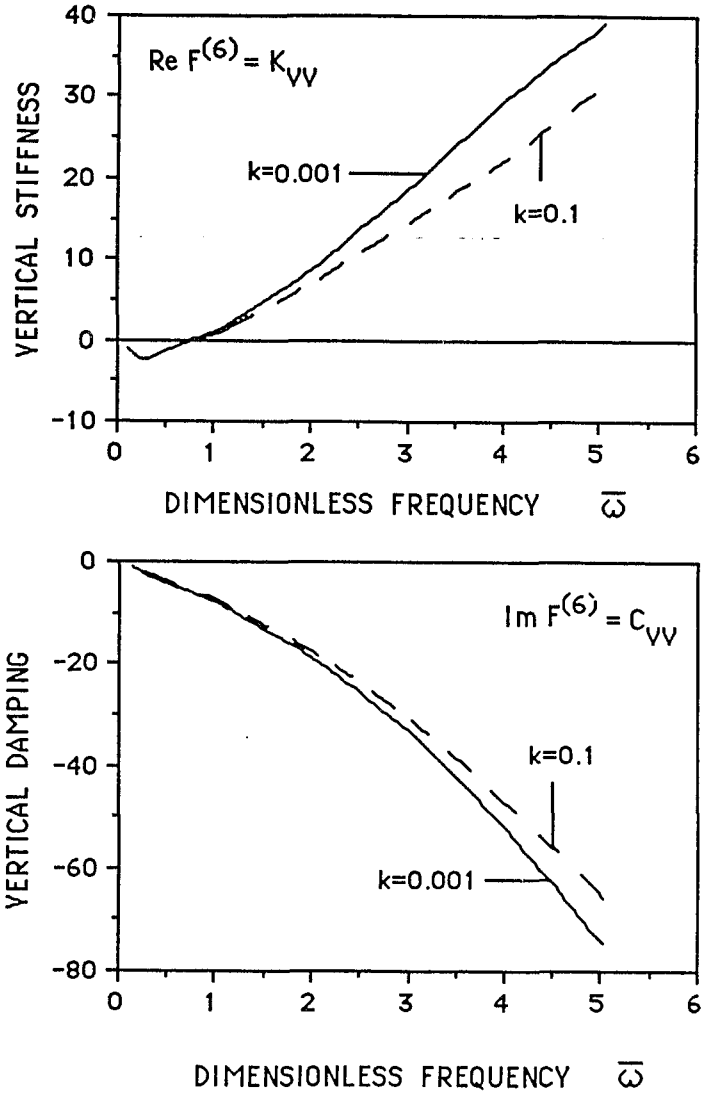

PLOT(24)- INFLUENCE OF PERMEABILITY ON INTERACTION COEFFICIENTS $F^{(6)}$ FOR SMOOTH CONTACT($\lambda_c = 5$). (SAND).

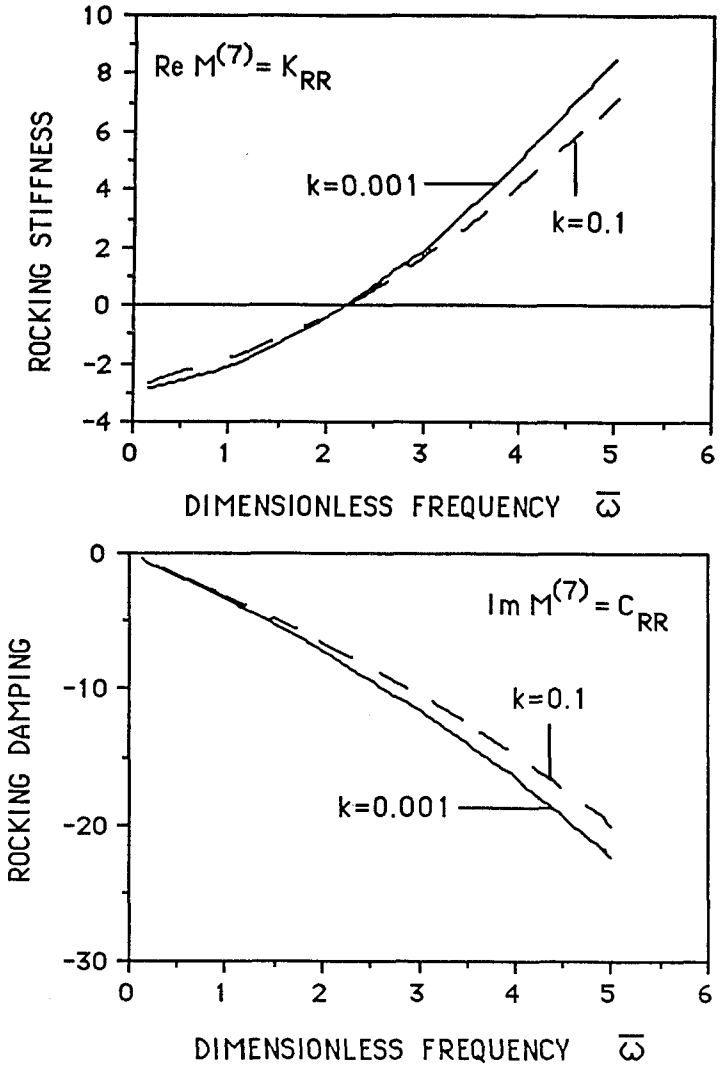

PLOT(25) - INFLUENCE OF PERMEABILITY ON INTERACTION COEFFICIENTS $M^{(7)}$ FOR SMOOTH CONTACT($\lambda_c = 5\ \%$). (SAND)

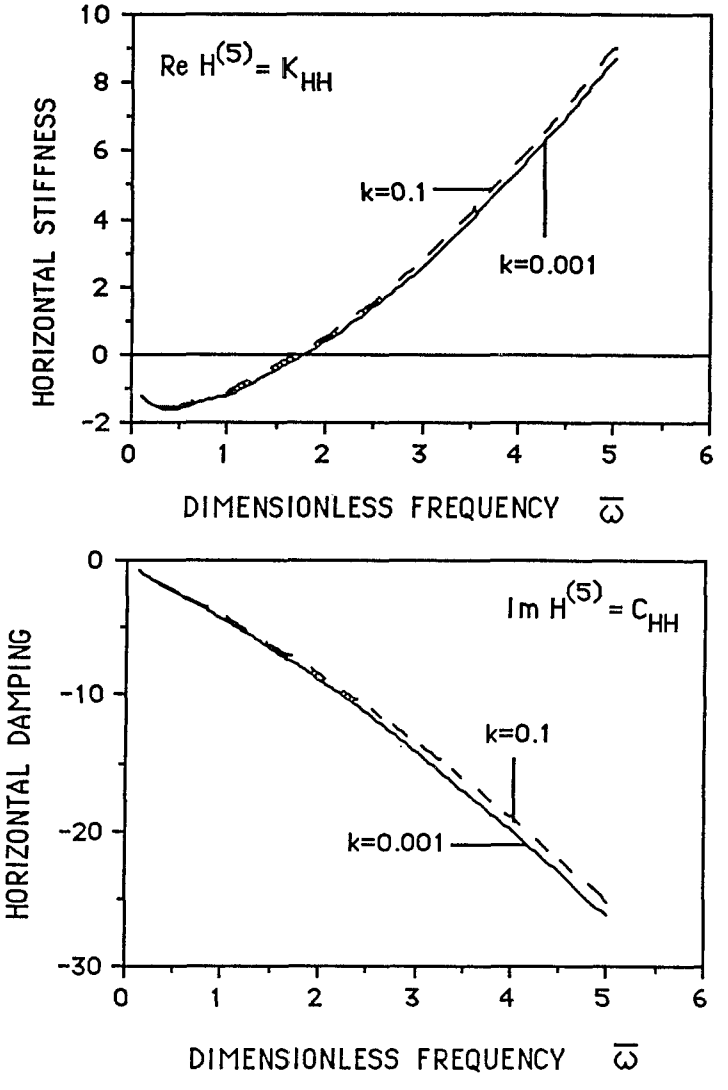

PLOT(26)- INFLUENCE OF PERMEABILITY ON INTERACTION COEFFICIENTS $H^{(5)}$ FOR WELDED CONTACT($\lambda_c = 5$ %). (SAND)

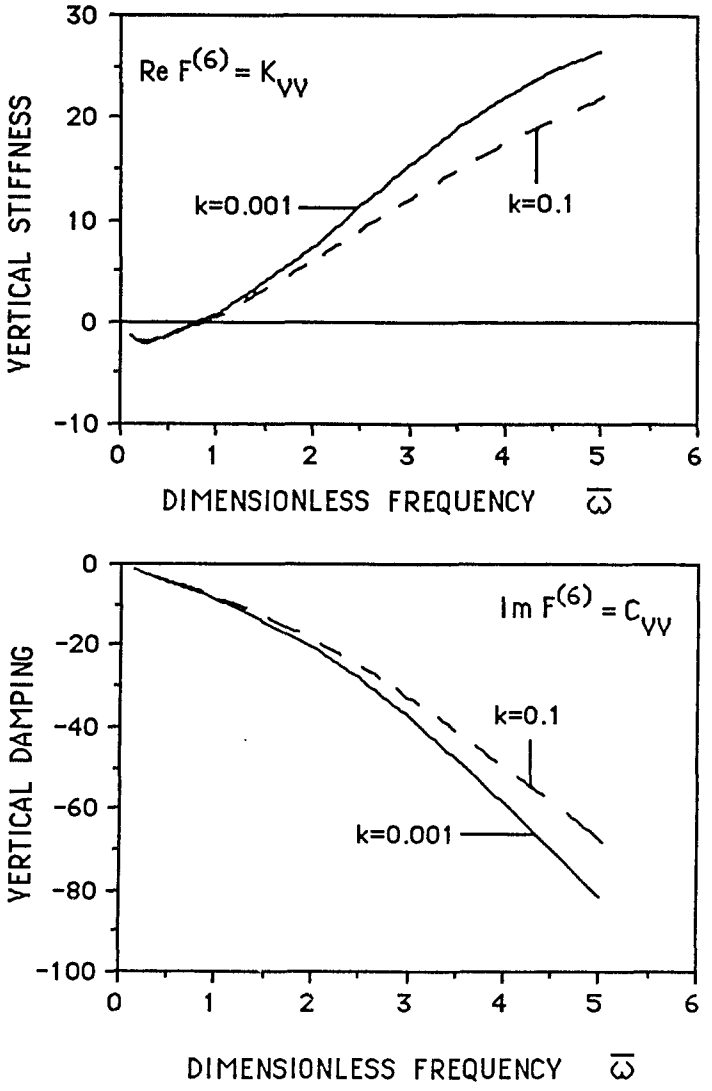

PLOT(27)- INFLUENCE OF PERMEABILITY ON INTERACTION COEFFICIENTS $F^{(6)}$ FOR WELDED CONTACT($\lambda_c = 5\ \%$). (SAND)

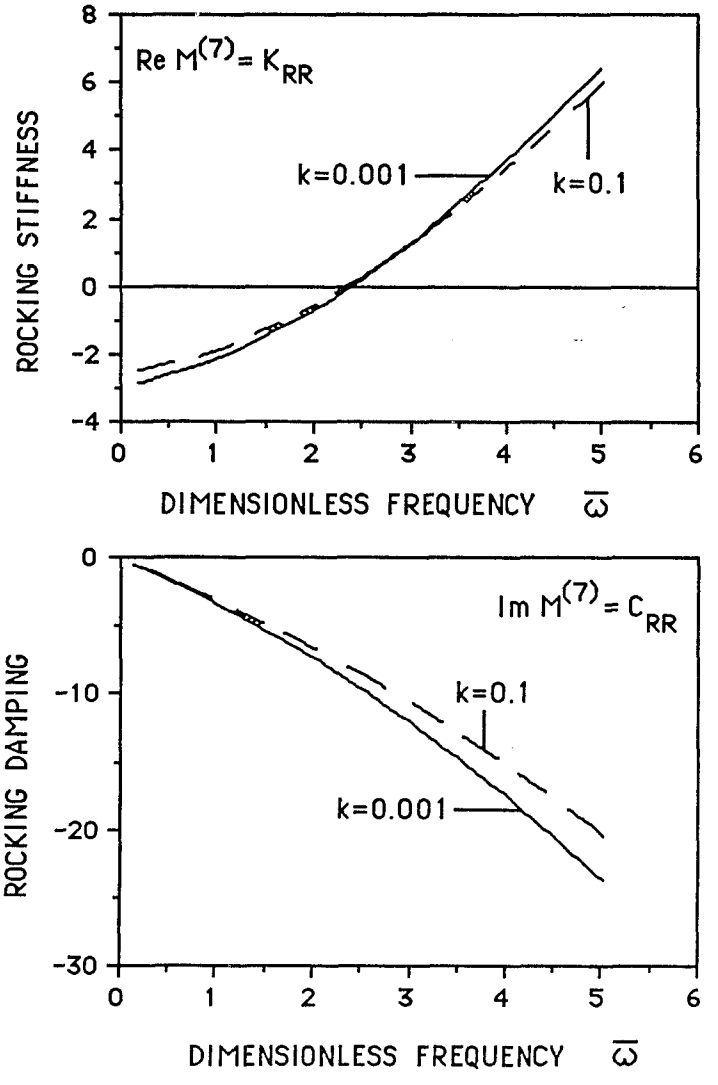

PLOT(28)- INFLUENCE OF PERMEABILITY ON INTERACTION COFFFICIENTS $M^{(7)}$ FOR WELDED CONTACT($\lambda_c = 5\ \%$). (SAND)

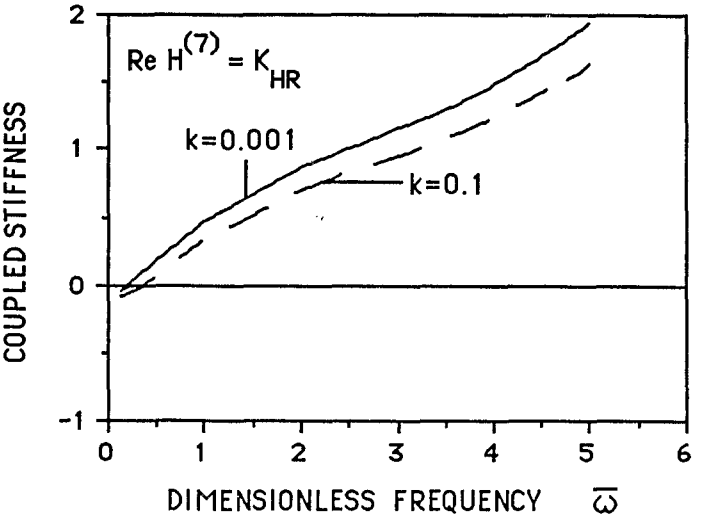

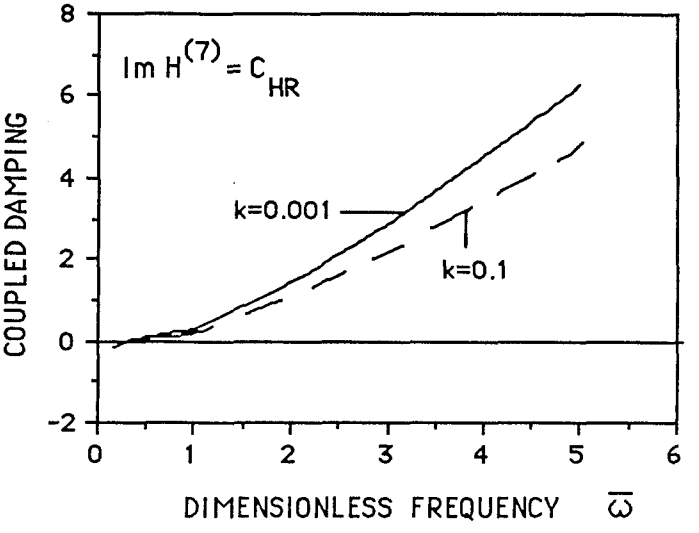

PLOT(29)- INFLUENCE OF PERMEABILITY ON COUPLING FUNCTION $H^{(7)}$ FOR WELDED CONTACT($\lambda_c = 5\ \%$). (SAND).

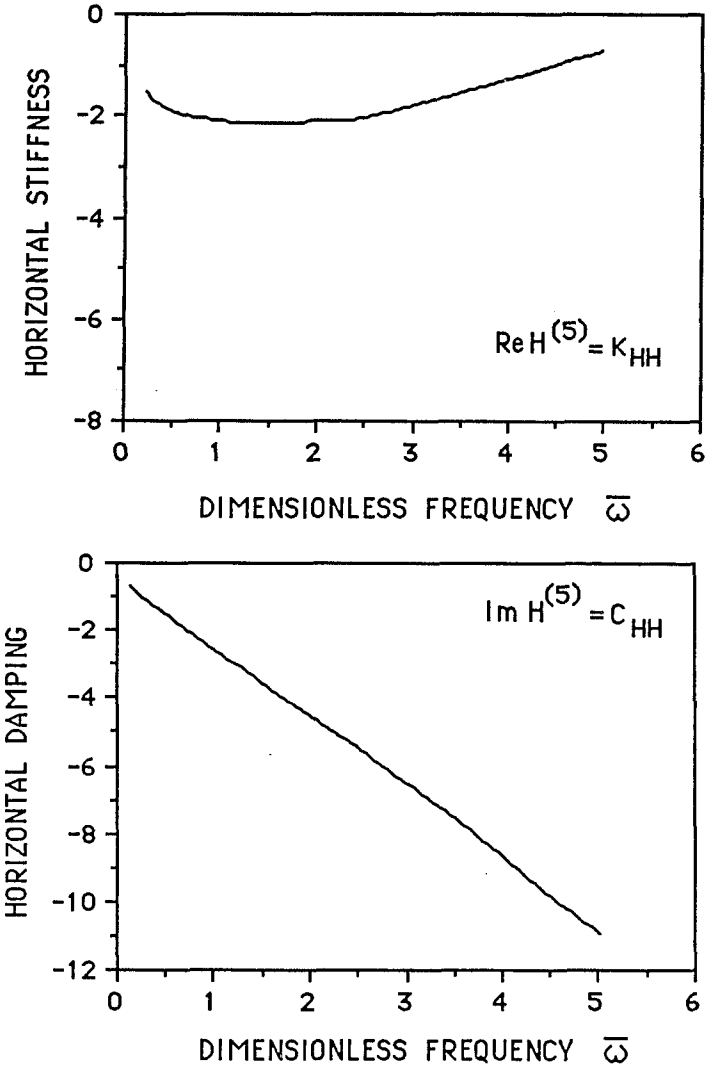

PLOT(30)- INFLUENCE FUNCTIONS $H^{(5)}$ FOR SMOOTH CONTACT SATURATED CLAY, $k = 10^{-5}$ cm/sec AND $\lambda_c = 1$ % (HORIZONTAL MOTION).

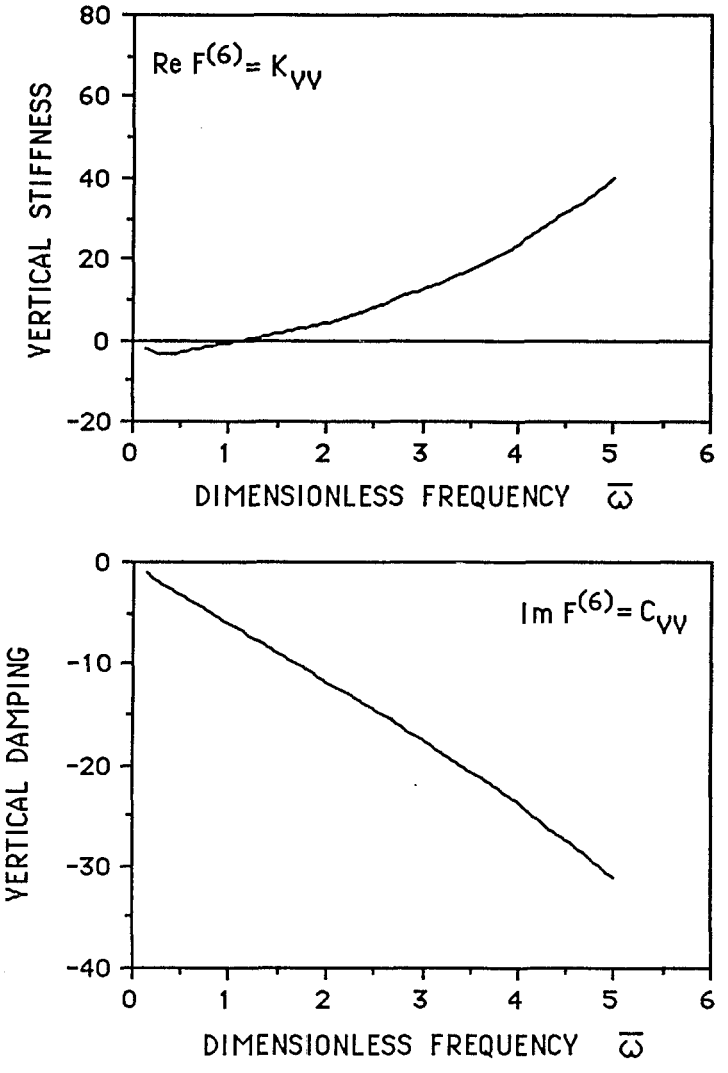

PLOT(31)- INFLUENCE FUNCTIONS $F^{(6)}$ FOR SMOOTH CONTACT, SATURATED CLAY, $k = 10^{-5}$ cm/sec AND $\lambda_c = 1$ % (VERTICAL MOTION).

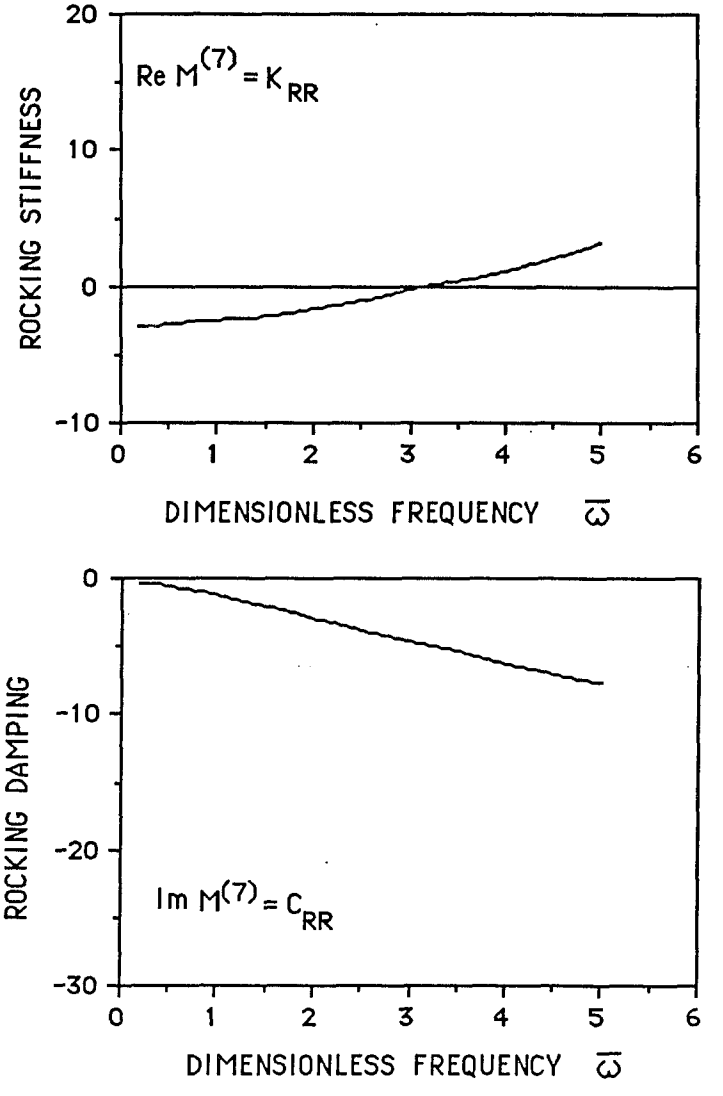

PLOT(32)- INFLUENCE FUNCTIONS $M^{(7)}$ FOR SMOOTH CONTACT , SATURATED CLAY, $k = 10^{-5}$ cm/sec AND $\lambda_c = 1\ \%$ (ROCKING MOTION).

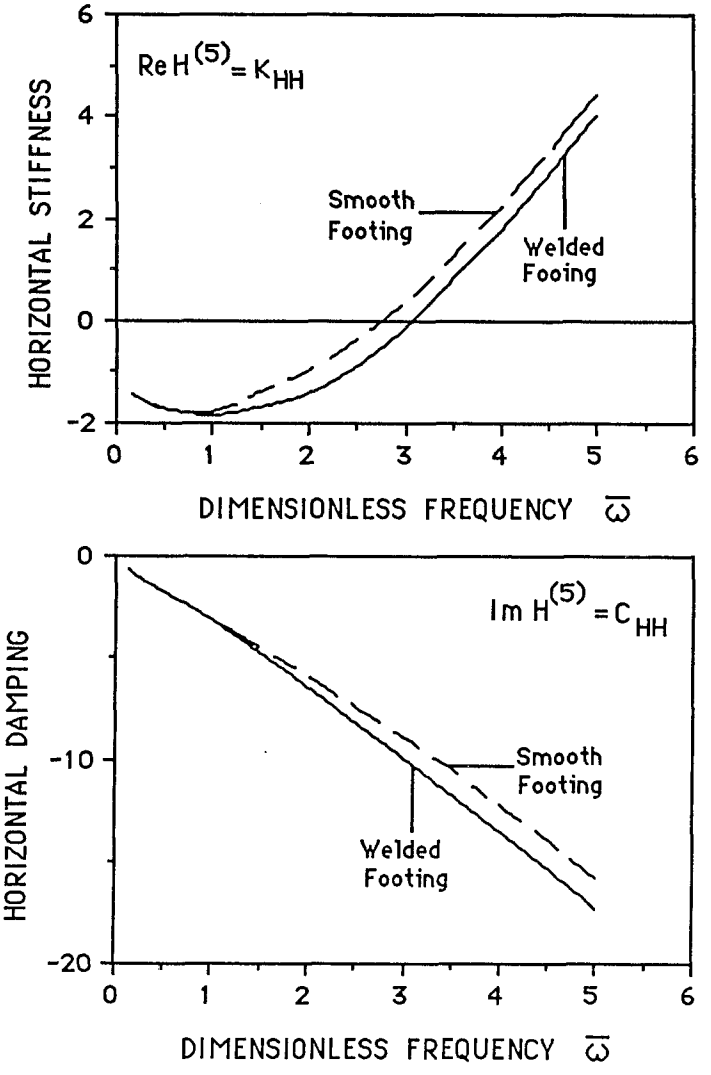

PLOT(33)- INFLUENCE FUNCTIONS $H^{(5)}$ FOR WELDED AND SMOOTH CONTACTS FOR SATURATED CLAY, $k = 10^{-5}$ cm/sec AND $\lambda_c = 5\%$ (HORIZONTAL MOTION).

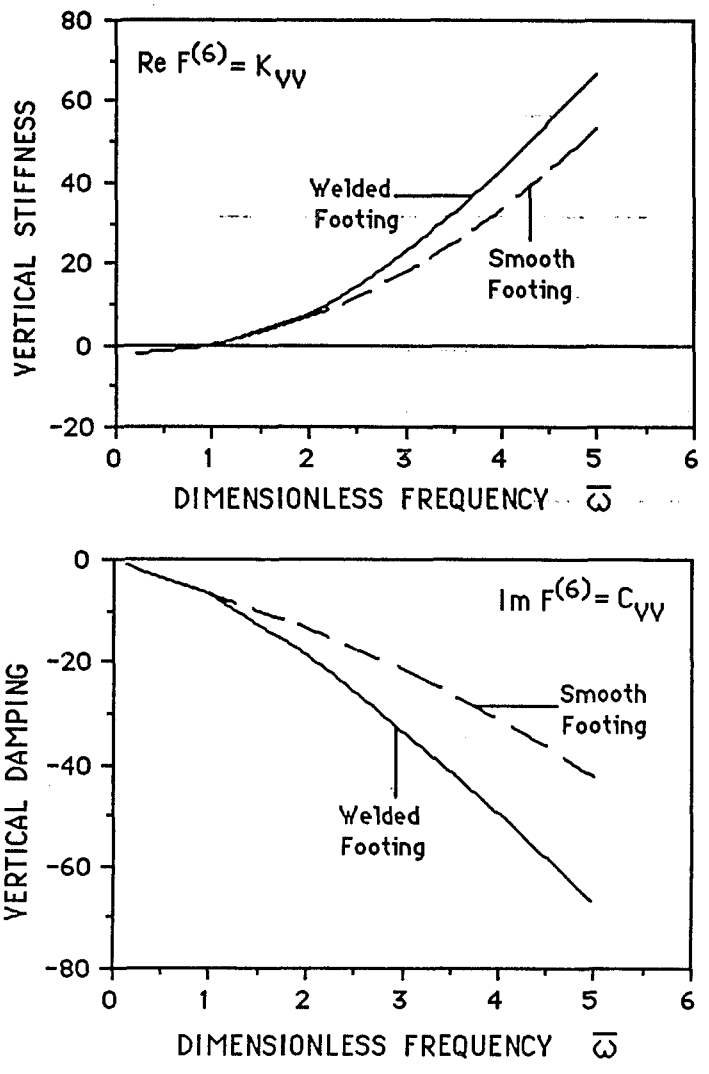

PLOT(34)- INFLUENCE FUNCTIONS $F^{(6)}$ FOR WELDED AND SMOOTH CONTACT, FOR SATURATED CLAY, $k = 10^{-5}$ cm/sec AND $\lambda_c = 5$ % (VERTICAL MOTION).

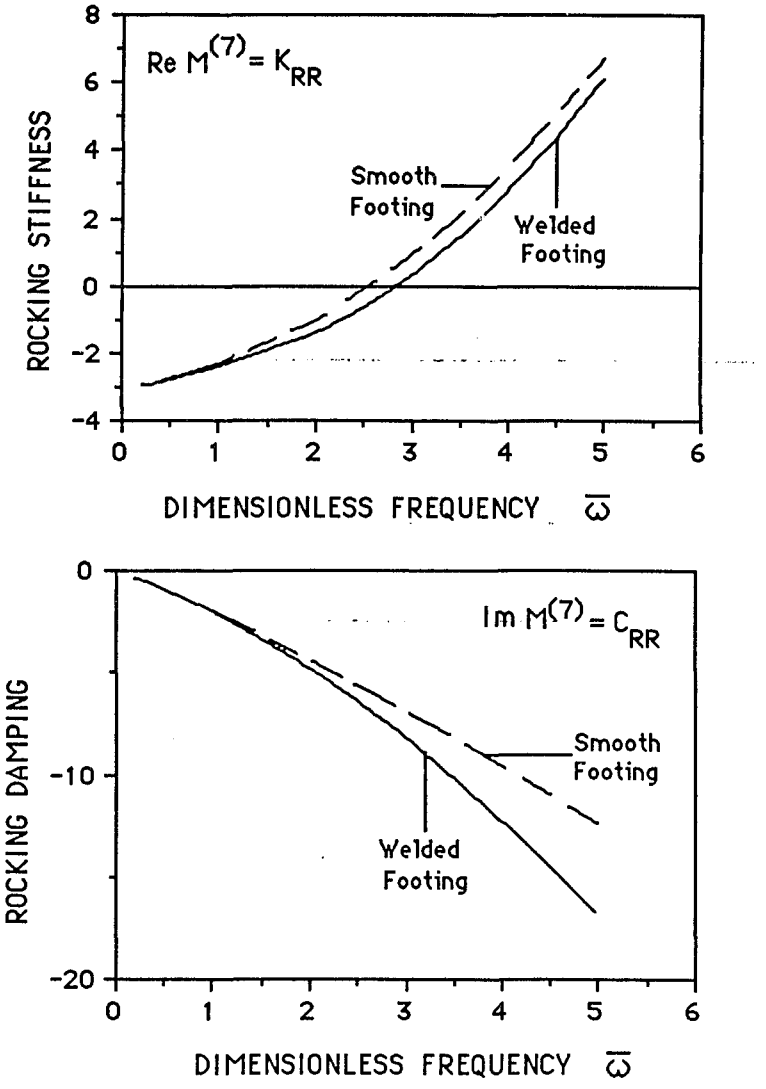

PLOT(35)- INFLUENCE FUNCTIONS $M^{(7)}$ FOR WELDED AND SMOOTH CONTACTS FOR SATURATED CLAY, $k = 10^{-5}$ cm/sec AND $\lambda_c = 5\%$ (ROCKING MOTION).

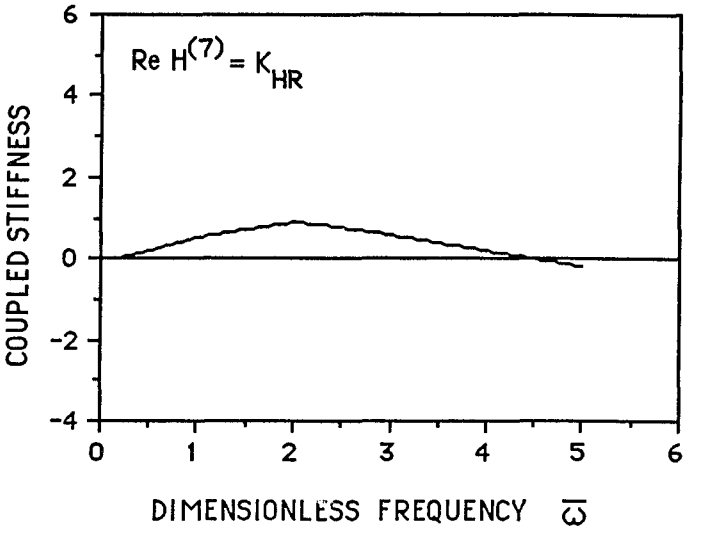

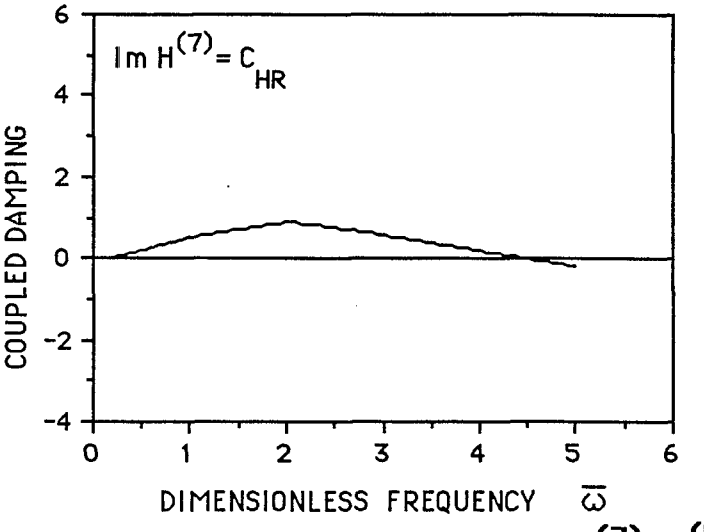

PLOT(36) - INFLUENCE FUNCTIONS $H^{(7)} \equiv M^{(5)}$ FOR WELDED CONTACT FOR SATURATED CLAY, $k = 10^{-5}$ cm/sec AND $\lambda_c = 5$ %.

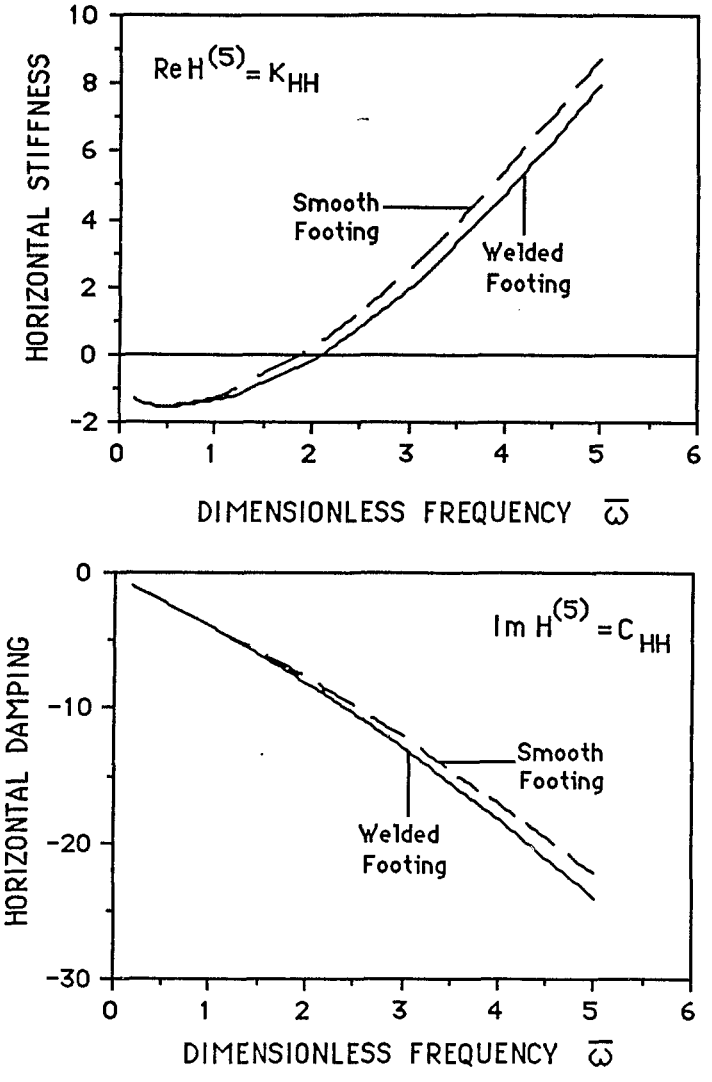

PLOT(37) - INFLUENCE FUNCTIONS $H^{(5)}$ FOR WELDED AND SMOOTH CONTACTS FOR SATURATED CLAY, $k = 10^{-5}$ cm/sec AND $\lambda_c = 10\%$ (HORIZONTAL MOTION).

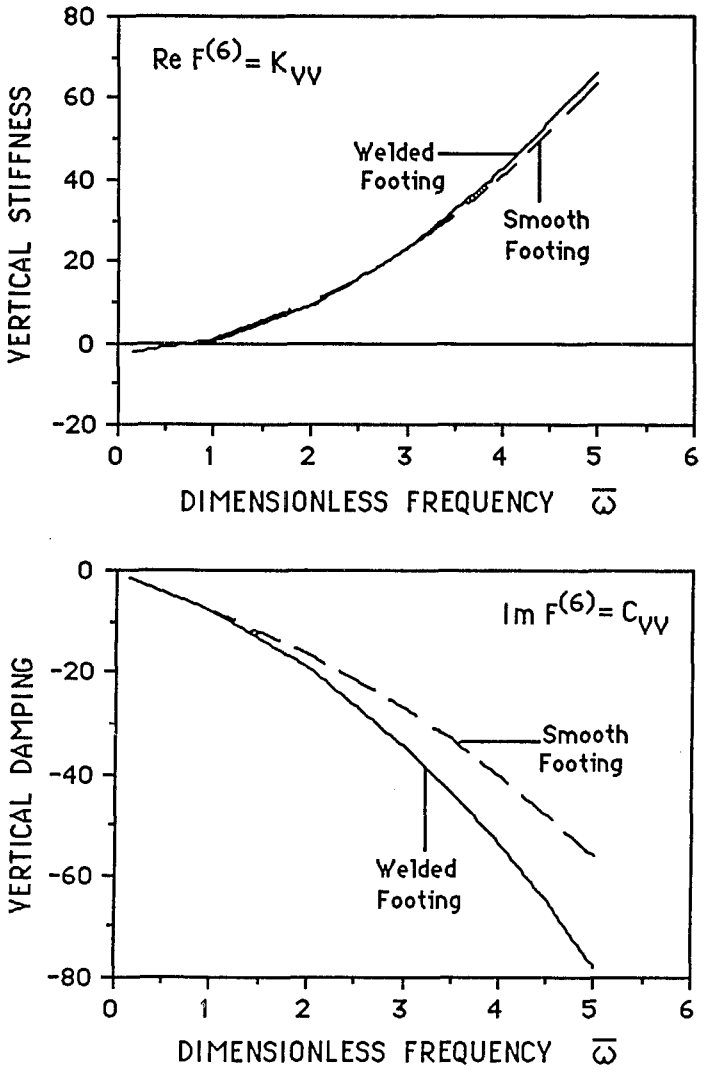

PLOT(38)- INFLUENCE FUNCTIONS $F^{(6)}$ FOR WELDED AND SMOOTH CONTACT. FOR SATURATED CLAY, $k = 10^{-5}$ cm/sec AND $\lambda_c = 10\%$ (VERTICAL MOTION).

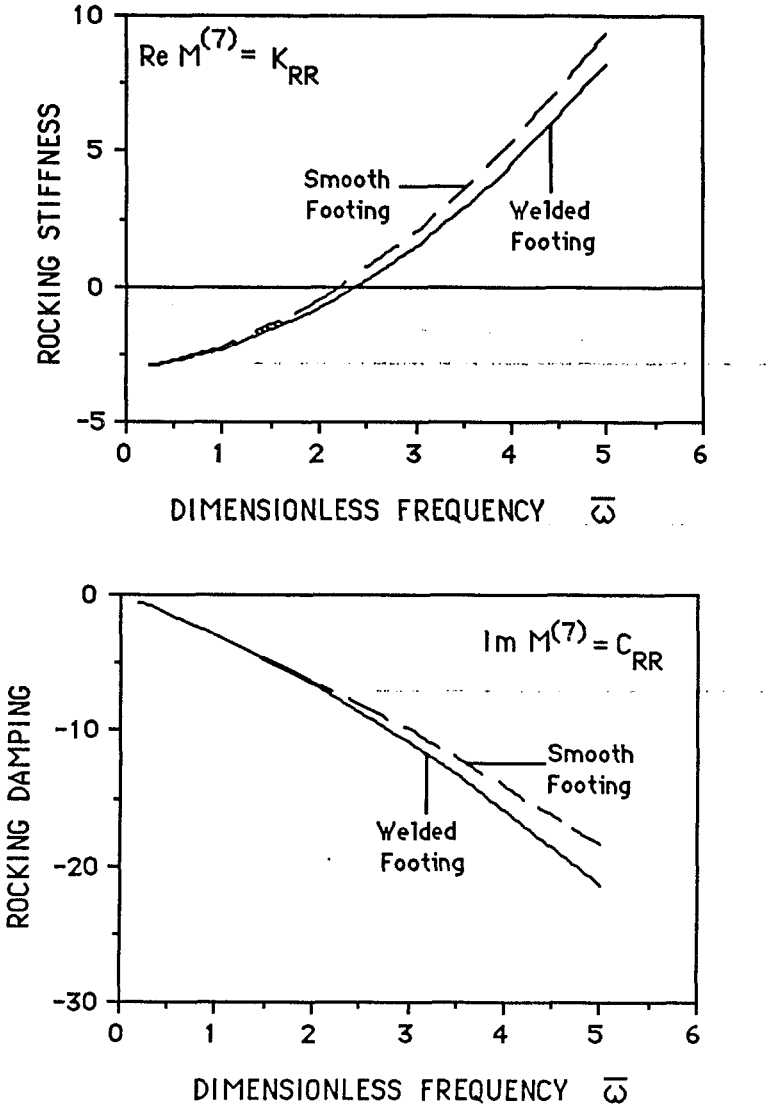

PLOT(39)- INFLUENCE FUNCTIONS $M^{(7)}$ FOR WELDED AND SMOOTH CONTACTS FOR SATURATED CLAY, $k = 10^{-5}$ cm/sec AND $\lambda_c = 10\%$ (ROCKING MOTION).

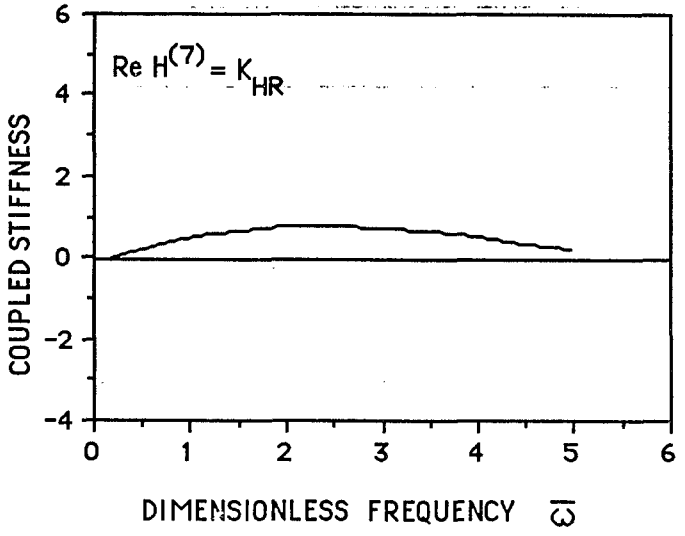

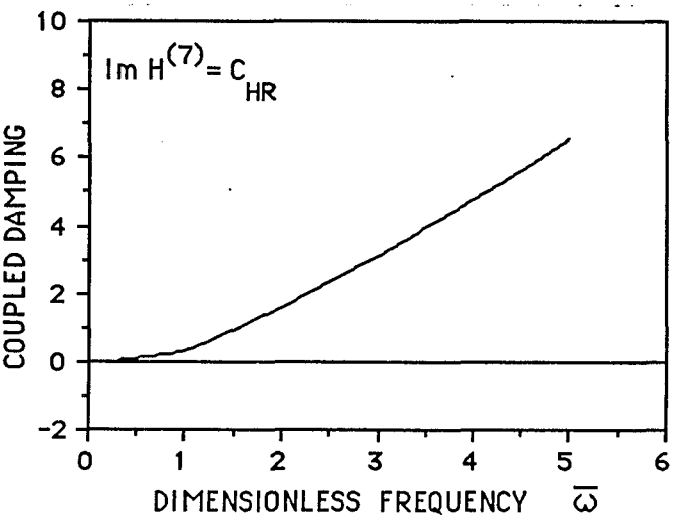

PLOT(40)- INFLUENCE FUNCTIONS $H^{(7)} \equiv M^{(5)}$ FOR WELDED CONTACT FOR SATURATED CLAY, $k = 10^{-5}$ cm/sec AND $\lambda_c = 10\%$.

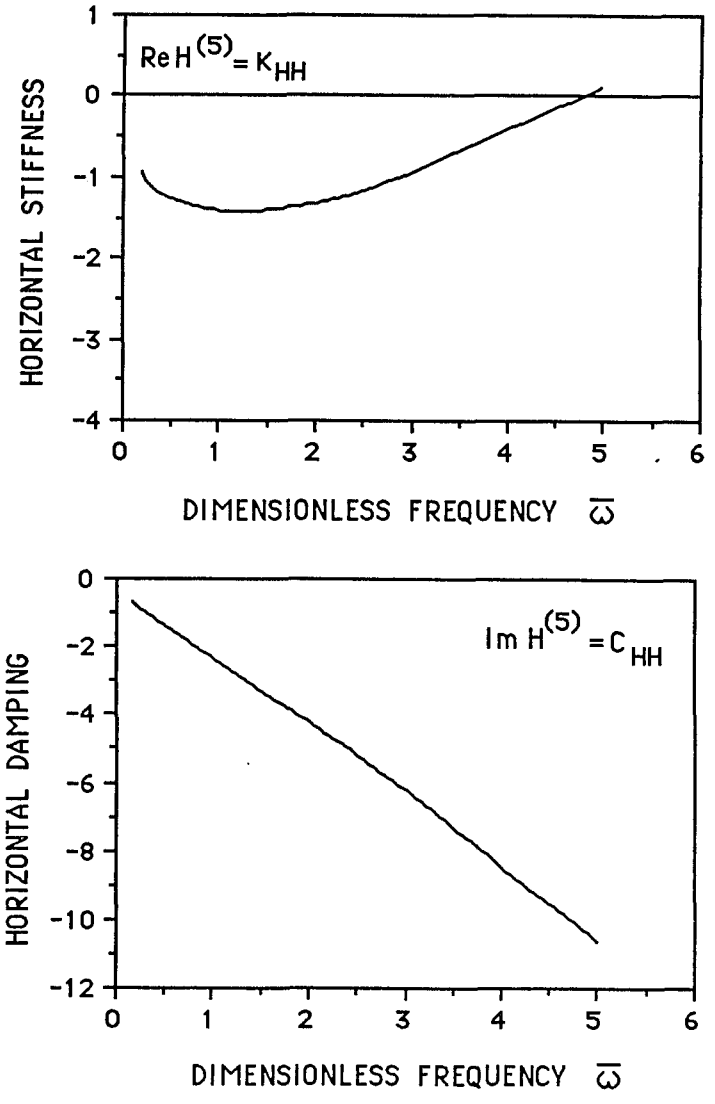

PLOT(41)- INFLUENCE FUNCTIONS $H^{(5)}$ FOR SMOOTH CONTACT, DRY CLAY, $\lambda_c = 1$ % (HORIZONTAL MOTION).

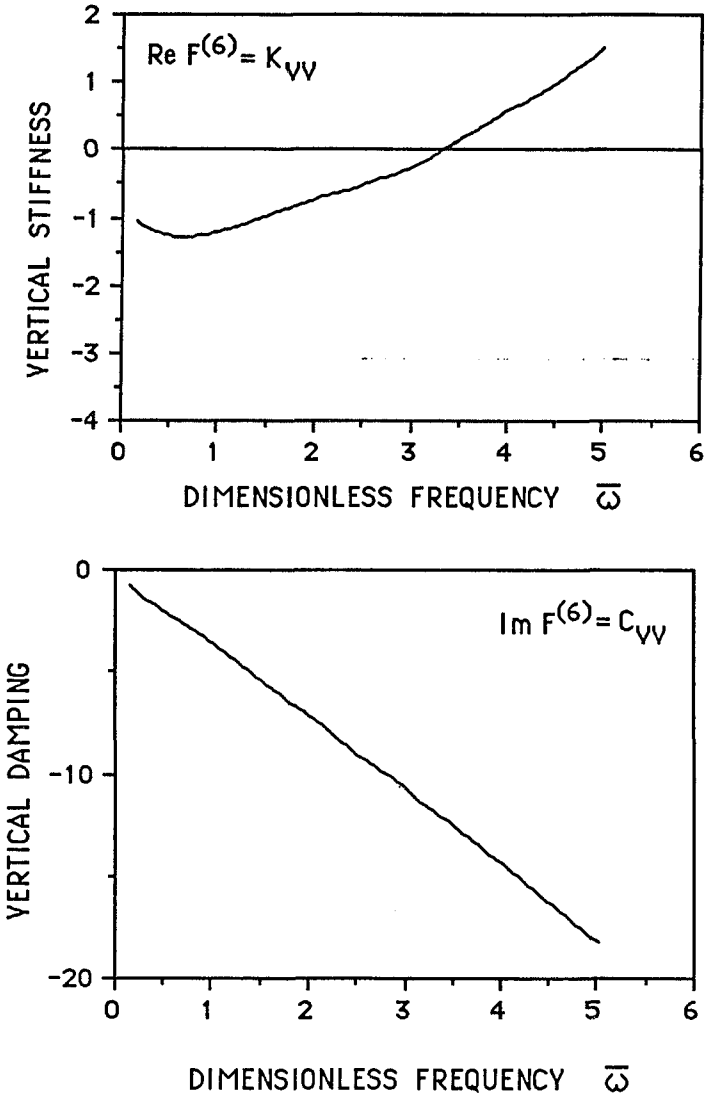

PLOT(42)- INFLUENCE FUNCTIONS $F^{(6)}$ FOR SMOOTH CONTACT. DRY CLAY , $\lambda_c = 1$ % (VERTICAL MOTION).

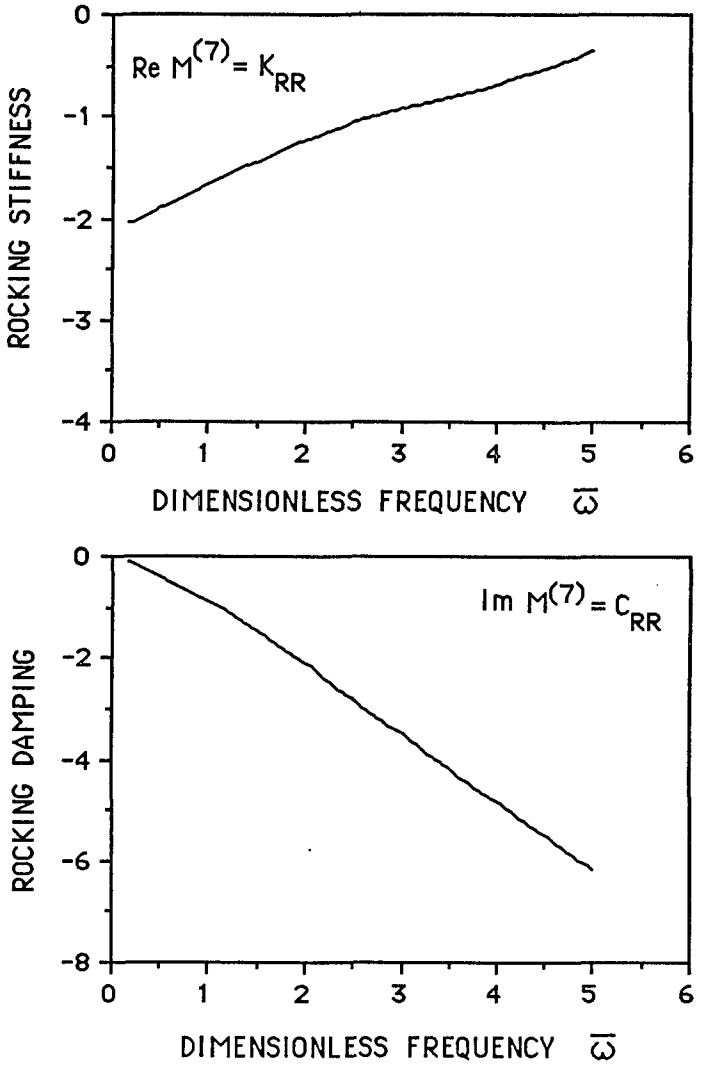

PLOT(43) - INFLUENCE FUNCTIONS $M^{(7)}$ FOR SMOOTH CONTACT, DRY CLAY, $\lambda_c = 1\,\%$ (ROCKING MOTION).

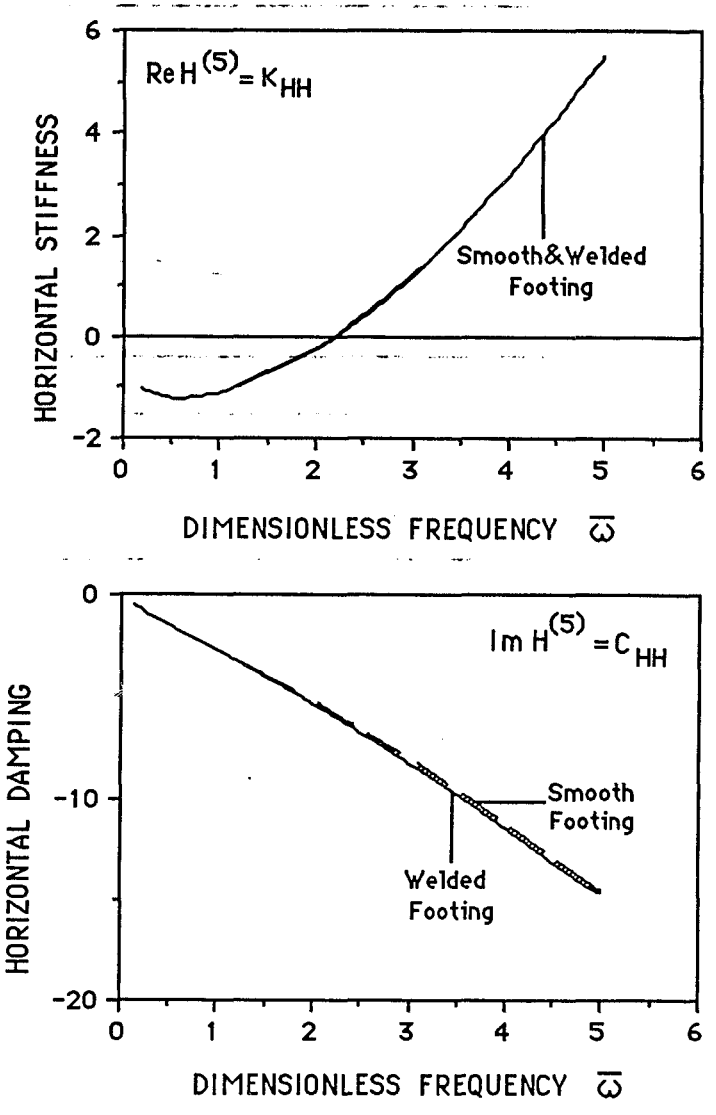

PLOT(44)- INFLUENCE FUNCTIONS $H^{(5)}$ FOR WELDED AND SMOOTH CONTACTS. DRY CLAY , $\lambda_c = 5\,\%$ (HORIZONTAL MOTION).

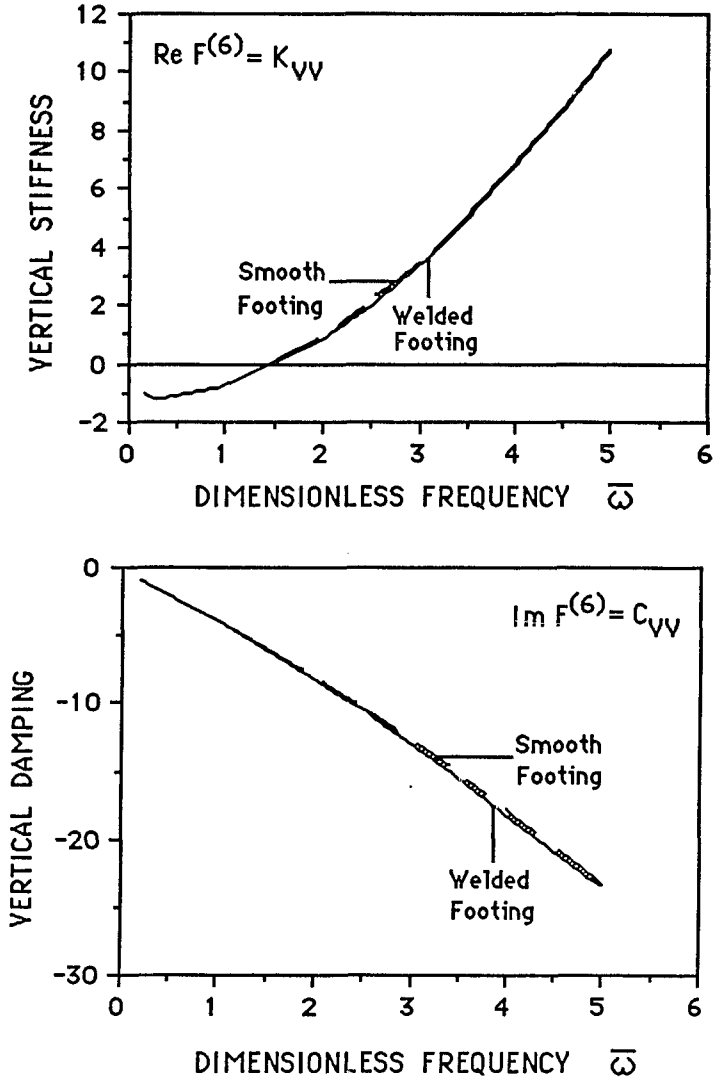

PLOT(45)- INFLUENCE FUNCTIONS $F^{(6)}$ FOR WELDED AND SMOOTH CONTACT. DRY CLAY , $\lambda_c = 5\ \%$ (VERTICAL MOTION).

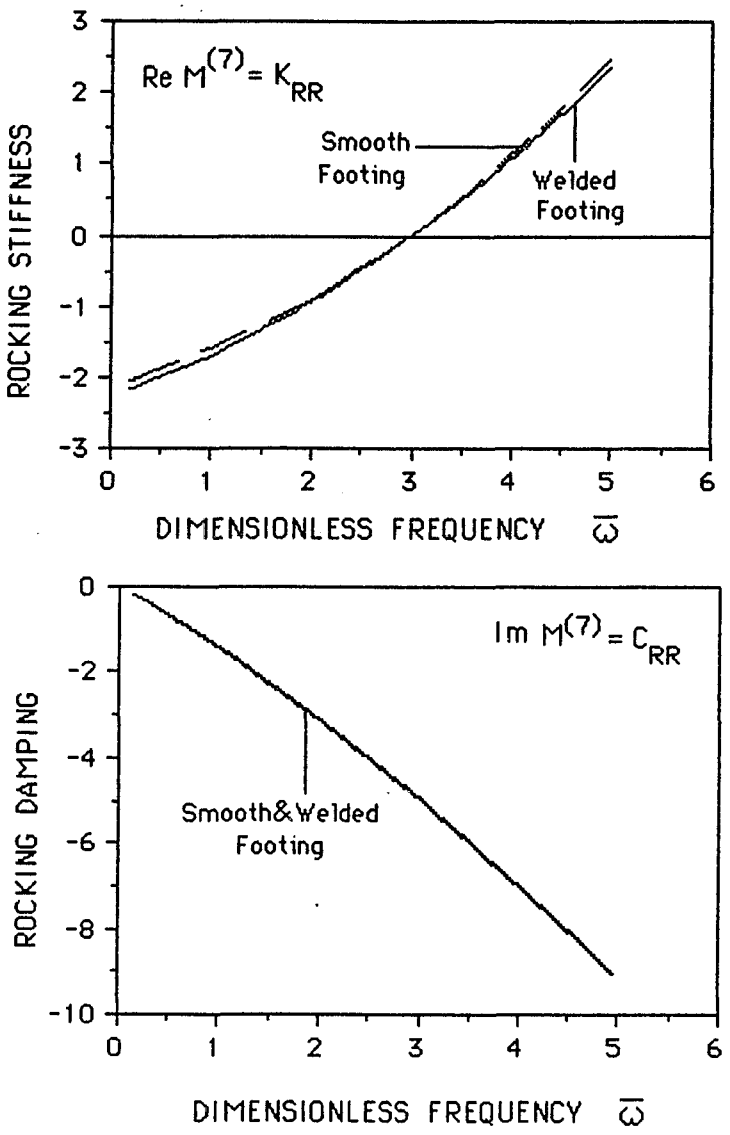

PLOT(46)- INFLUENCE FUNCTIONS $M^{(7)}$ FOR WELDED AND SMOOTH CONTACTS. DRY CLAY , λ_c =5 % (ROCKING MOTION).

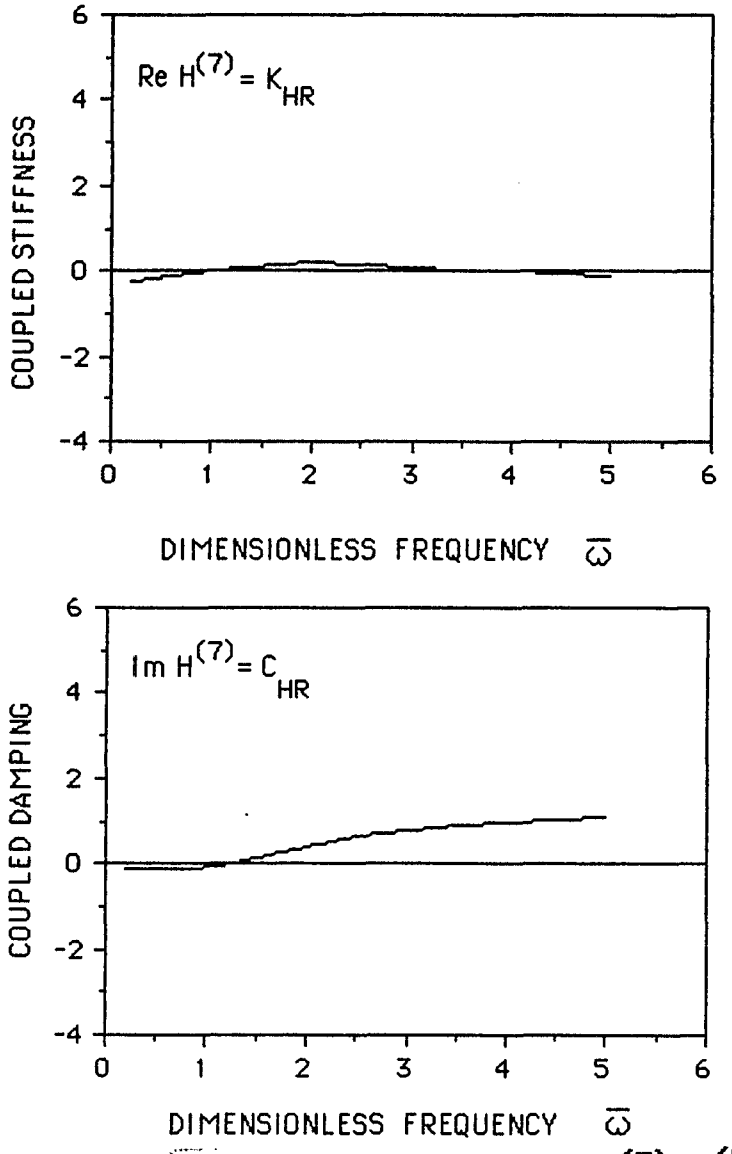

PLOT(47) - INFLUENCE FUNCTIONS $H^{(7)} \equiv M^{(5)}$ FOR WELDED CONTACT. DRY CLAY , λ_c=5 %.

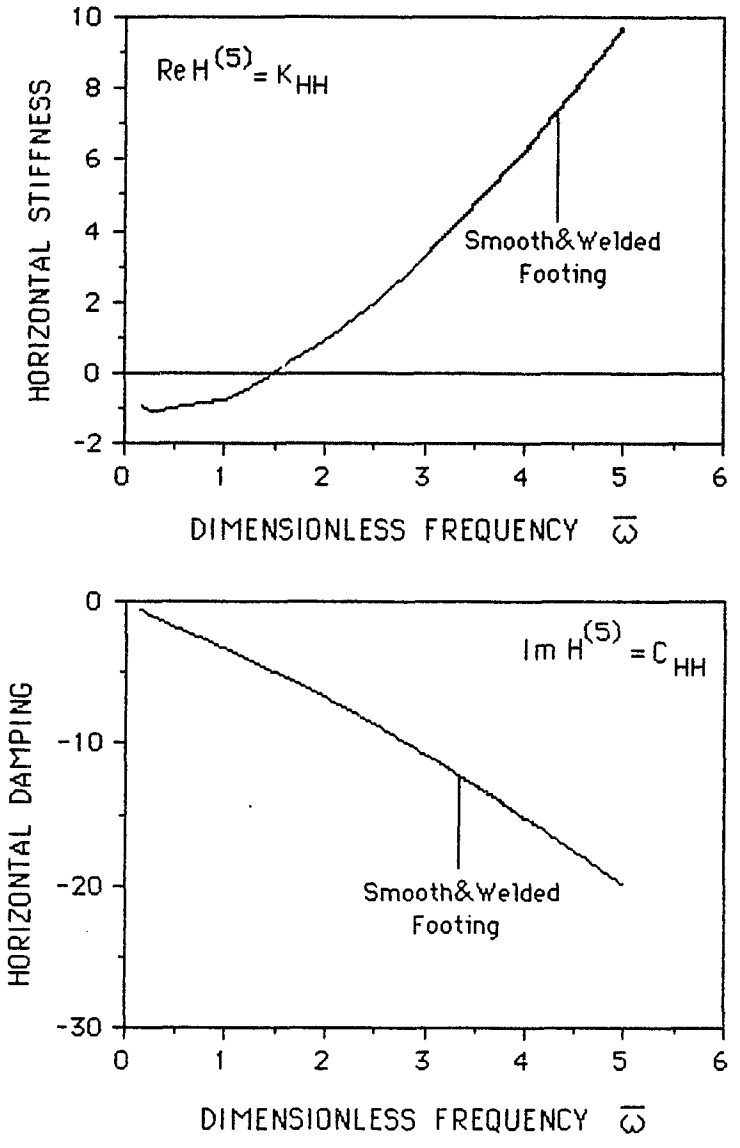

PLOT(48) - INFLUENCE FUNCTIONS $H^{(5)}$ FOR WELDED AND SMOOTH CONTACTS FOR DRY CLAY , $\lambda_c = 10\%$ (HORIZONTAL MOTION).

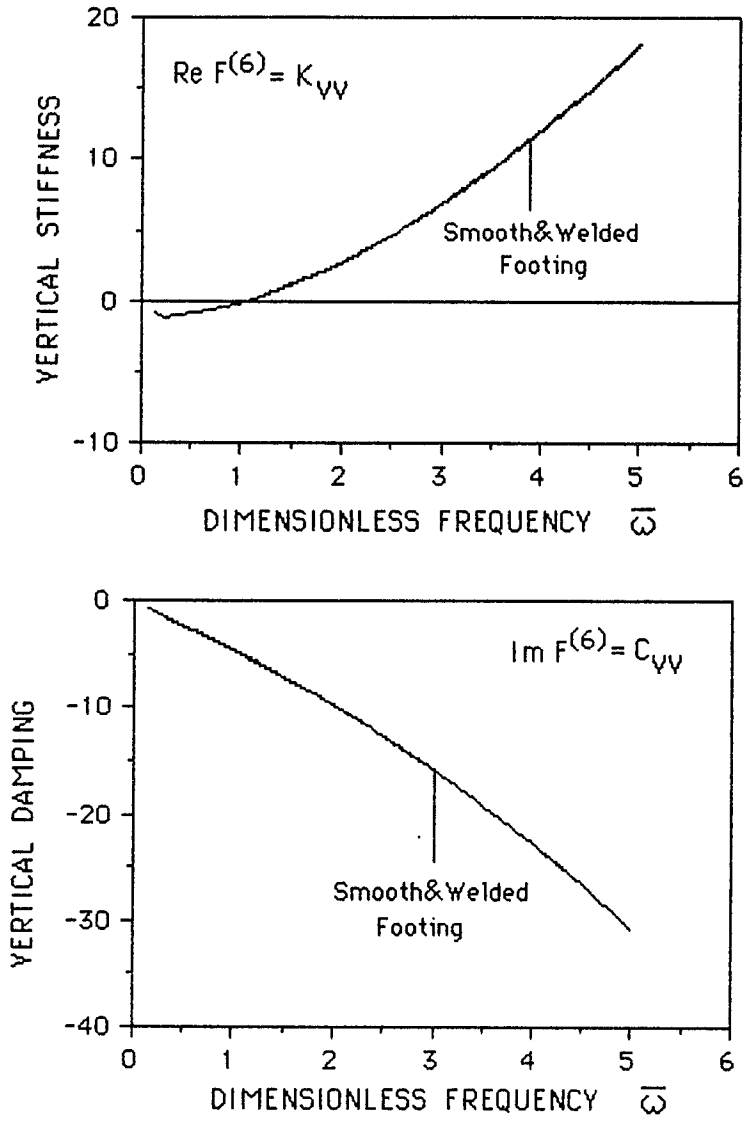

PLOT(49) – INFLUENCE FUNCTIONS $F^{(6)}$ FOR WELDED AND SMOOTH CONTACT, FOR DRY CLAY , $\lambda_c = 10\%$ (VERTICAL MOTION).

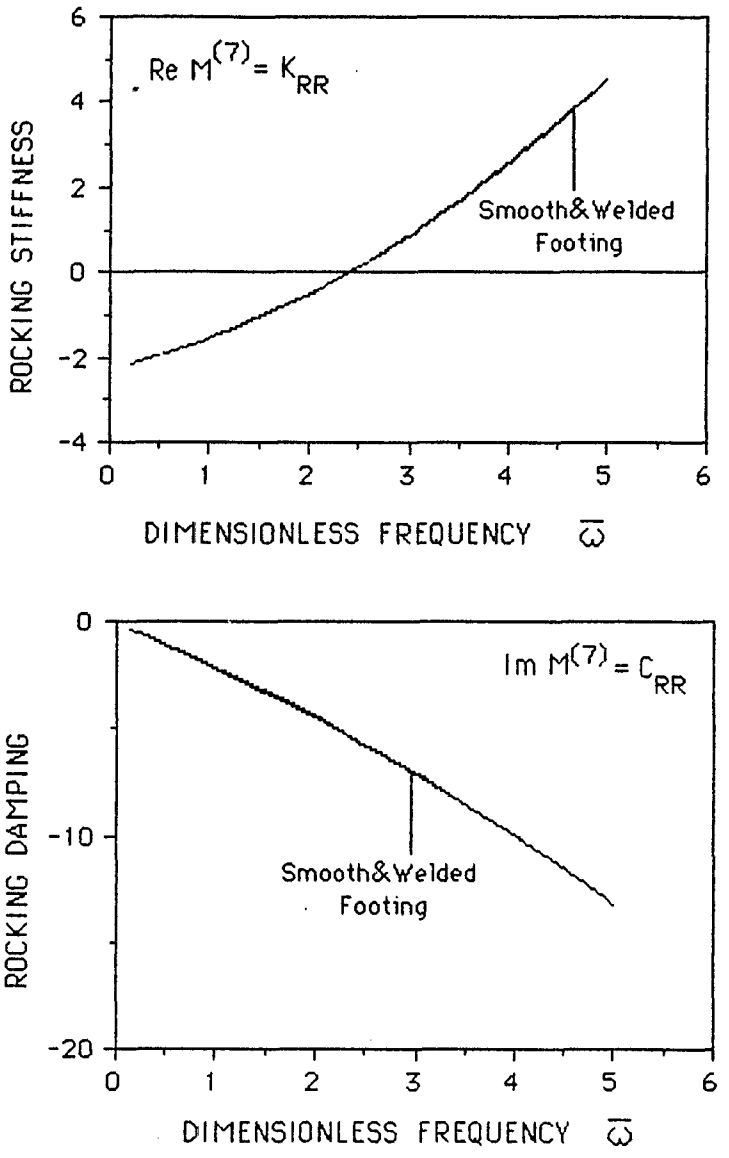

PLOT(50)- INFLUENCE FUNCTIONS $M^{(7)}$ FOR WELDED AND SMOOTH CONTACTS FOR DRY CLAY , $\lambda_c = 10\%$ (ROCKING MOTION).

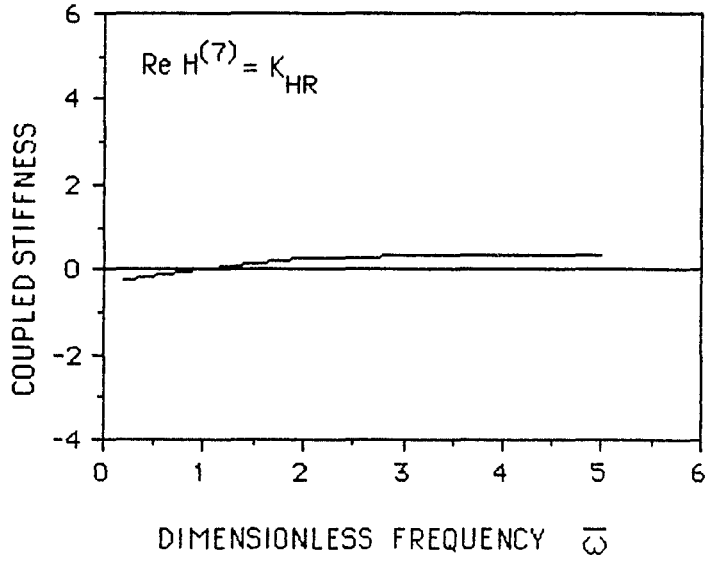

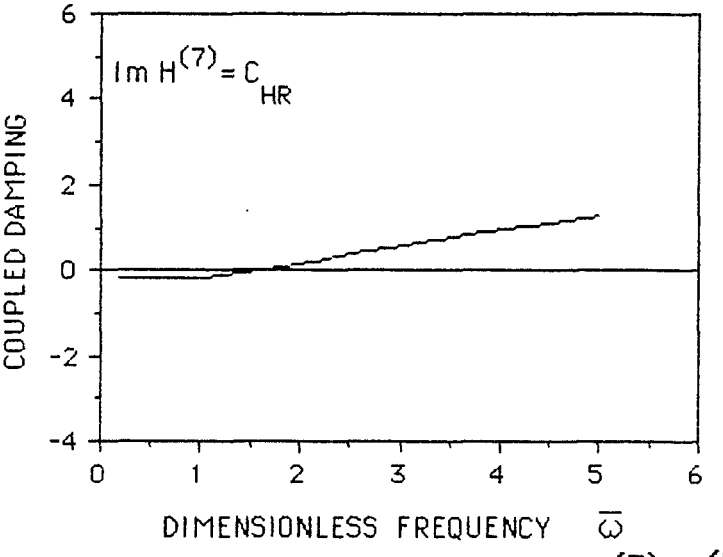

PLOT(5 1)- INFLUENCE FUNCTIONS $H^{(7)} \equiv M^{(5)}$ FOR WELDED CONTACT FOR DRY CLAY , $\lambda_c = 10\%$

REFERENCES/BIBLIOGRAPHY

1. Auriault,J. , Borne, L. and Chambon, R.(1985), "Dynamics of Porous Saturated Media ; Checking of the Generalized Law of Darcy ". Journal of Accoustical Society of America , vol.77(5).

2. Awjobi, A . O . and Grootenhuis P . (1965), "Vibrations of Rigid Bodis on Semi Infinite Elastic Media ", Proceedings of the Royal Society , Lodon, vol.287, Series A, pp.27-63.

3. Bazant, Z.P.(1967) , Theory of Vibration of Saturated Granular Medium. Proceedings , Inter. Symposium on Wave Propagation and Dynamic Properties of Earth Materials , Univ. of New Mexico Press , Albuquerque , NM .

4. Bazant, Z.P. and Krizek , R.J.(1975) , "Saturated Sand as an Inelastic Two-Phase Medium ". Journal of Engineering Mechanics Division , ASCE , vol.101(EM4) .

5. Biot , M . A . (1941) , "General Theory of Three Dimensional Consolidation" . Journal of Applied Physics , vol. 12 . pp155-164.

6. Biot , M . A . (1941) ," Consolidation Settlement Under a Rectangular Load Distribution" . Journal of Applied Physics , vol.12 . pp.426-430.

7. Biot , M . A . (1941) , "Consolidation Settlement of a Soil With an Impervious Top Surface" . Journal of Applied Physics , vol.12 . pp.578-581.

8. Biot , M . A . (1955) , "Theory of Elasticity and Consolidation for a Porous Anisotropic Solid ". Journal of Applied Physics , vol.26(2) . pp.182-185.

9. Biot , M . A . (1956) , "Theory of Propagation of Elastic Waves in a Fluid-Saturated Porous Solid : 1- Low Frequency Range" . Journal of the accoustical Society of America , vol.28 , pp.168-178 .

10. Biot , M . A . and Willis , D.G.(1957) , "The Elastic Coefficients of the Theory of Consolidation" . Journal of Applied Mechanics , vol.24 . pp.594-601.

11. Biot , M . A . (1962) , "Mechanics of deformation and Accoustic Propagation in Porous Media" . Journal of Applied Physics , vol.33 , pp.1482-1498 .

12. Cedergren ,H.R. (1968) , Seepage , Drainage and Flow Nets . John Wiley&Son , NY .

13. Collins , W . D . (1962), "The Forced Torsional Oscillations of an Elastic Half-Space and an Elastic Stratum ". Proceedings of the London Mathematical Society , vol.12 , pp.226-244 .

14. Costantino , C . J .(1969) , "Two-Dimensional Wave Propagation Through Nonlinear Media" . Journal of Computational Physics , vol.4(2)

15. Costantino , C. J. and Miller, C.A. and Lufrano, L.A.(1969) , "Soil-Structure Interaction Parameters from Finite Element Analyses". Proceedings , Conference on Extreme Load Conditions , Berlin .

16. Costantino , C . J . (1986),"Influence of Ground Water on Soil-Structure Interaction" . Report NUREG/CR-4588 , BNL-NUREG_51983 , vol.3 .

17. Dasgopta , G . (1980) , "Foundation Inpedance Matrices by Substructure Deletion" . Journal of the Engineering Mechanics Division , ASCE , vol.106 , 517-526 .

18. Deresiewicz, H . (1962), "The Effect of Boundaries of Wave Propagation in a Liquid-Fluid Porous Solid : IV-Surface Waves in a Half-Space" . Bulletin of the Seismological Society of America , vol. 52 , pp.627-638 .

19. Erdelyi , A . , et al (1954) , Tables of Integral Transforms ,vol. 2 , pp.49 , Mcgraw-hill , New York .

20. Freedman , J.M. and Keer , L.M.(1971) ," Vibratory Motion of a Body on an Orthotropic Halp Plane" . Journal of Applied Mechanics , ASME.

21. Gladwell , G . M . L . (1968), "Forced Tangential and Rotatory Vibration of a Rigid Circular Disk on a Semi - Infinite Solid" . International Journal of Engineering Sciences , vol.6 , pp.591-607 .

22. Ishihara , K, (1967) , Propagation of Compressional Waves in a Saturated Soil . Proceedings , Inter. Symposium on Wave Propagation and Dynamic Properties of Earth Materials, Univ. of New Mexico Press , Albuquerque , NM.

23. Jones , J . P . (1961) , " Rayleigh Waves in a Porous , Elastic , Saturated Solid ". Journal of the Accoustical Society of America , vol.33 , pp.959-962 .

24. Junger , M . C . (1953) , "Concept of Radiation Scattering and its Application to Reinforced Cylindrical Shells" . Journal of the Accoustical Society of America , vol.25 , pp.899-896 .

25. Karasudhi , P . , keer , L . M . and Lee , S . L . (1968), "Vibratory Motion of a Body on an Elastic Half-Space ", Journal of Applied mechanics , ASME , vol. 35 , pp.697-705 .

26. Lamb , H . (1904)," On the Propagation of Tremors over the Surface of an Elastic Solid ". Philosophical Transactions of the Royal Society , London , vol. 203 , Series A , pp.1 - 42 .

27. Luco , J . E . and Westmann , R . A . (1971) , "Dynamic Response of Circular Footings" . Journal of Engineering Mechanics Div. , ASCE (EM5).

28. Luco , J . E . and Westmann , R . A . (1972) , "Dynamic Response of a Rigid Footing Bonded to an Elastic Half-Space" , Journal of Applied Mechanics , ASME , vol. 39 , pp.527 - 534 .

29. Luco , J . E . and Mita , A. (1987) , "Response of a Circular Foundation on a Uniform Half-Space to Elastic Waves ". Earthquake Engr. and Structure Dynamics , vol.15,pp.105-118.

30. Lung , R . H . (1980) , "Seismic Analysis of Structures Embeded in Saturated Soils ". ph.D. Dissertation , Department of Civil Engineering , City University of New York .

31. Mei , C. C. and Foda , M.A. (1981) , "Wave Induced Responses in a Fluid Filled Poroelastic Solid with a Free Surface - a Boundary Layer Theory ". Geophysics Journal of the Royal Astronomical Society , vol.66(3) .

32. Mei ,C. C. and Mynett , A. E. (1983) , "Earthquake Induced Stresses in a Poroelastic Foundation Supporting a Rigid Structure" . Geotechnique ,vol.33(3) .

33. Miller ,G.F. and Pursey , H. (1954) , "The Field and Radiation Impedance of Mechanical Radiators on the Surface of a Semi-Infinite Isotropic Solid" , Proceedings of the Royal Society , London , England , vol.233, Series A , pp.521-541 .

34. Muskhelishvili , N . I . (1953) , Some Basic Problems of the Mathematical Theory of Elasticity . P . Nourdhoff , Groningen , The Netherlands.

35. Oien , M . A . (1970) , "Steady motion of a Rigid Strip Bonded to an Elastic Half-Space ", Journal of Applied Mechanics , ASME , vol. 38 , pp.328-334.

36. Paul , S . (1976a) , "On the Displacements Produced in a Porous Elastic Half-Space by an Impulsive Line Load (non-dissipative case) ". Pure and Applied Geophysics , vol. 114 , pp.605-614 .

37. Paul , S . (1976b) , "On the Disturbance Produced in a Semi-Infinite Poroelastic Medium by a Surface Load" . Pure and Applied Geophysics , vol.114 , pp.615-627 .

38. Philippacopouplos ,A.J. (1987), "Waves in A Partially Saturated Layered Half-Space: Analytic Formulation", Bulletin of the Seismological Society of America , Vol.77, No.5 , pp.1838-1853.

39. Quilan , P. M. (1953), "The Elastic Thoery of Soil Mechanics", ASTM Special Technical Publication No. 156, Symposium on Soil Dynamics, pp.3-34 .

40. Reissner , E. (1936) ,"Stationare axialsymmetrishe , durch eine Schuttelnde Masse erregte Schwingungen eines homogenen elastischen Halbraumes", Ingenieur-Archiv, vol.7 , pp.381-396.

41. Reissner , E. and Sagoci , H.F. (1944) , "Forced Torsional Oscillations of an Elastic Half-Space", Journal of Applied Physics , vol.15 , No.9 .

42. Robertson , I . A . (1966), "Forced Vertical Vibration of a Rigid Circular Disk on a Semi- Infinite Elastic Solid" , Proceedings of the Cambridge Philosophical Society , vol. 62 , Series A , pp.547-553 .

43. Smith, P . W . Jr.(1962) , "Response and Radiation of Structural Modes Excited by Sound ". Journal of the accoustical Society of America , vol. 34 , pp.640-645 .

44. Sung , T.Y. (1953) , "Vibrations in Semi-Infinite Solids Due to Periodic Surface Loading" , ASTM, Special Technical Publication No. 156, Symposium on Soil Dynamics ,pp.35-63 .

45. Thau , S . A . (1967) , "Radiation and Scattering from a Rigid Inclusion in an Elastic Medium ", Journal of Applied Mechanics , ASME , vol.34 , pp.509- 511 .

46. Ufliand , Ia.S (1961) "On Torsional Vibrations of Half-Space", Prikladnaya Mathematika i Mechanika,vol.25, No.1 .

47. Williams , M . L . (1959) , " The Stresses around a Fault or Crack in Dissimilar Media ". Bulletin of the Seismological Society of America , vol.49 .

48. Znkorko, V . N . and Rostovtsev , N . A . (1965) , "Dynamic Contact Problem of Steadt Vibrations of an Elastic Half Space ", Journal of Applied Mathematics and Mechanics , vol. 29 , pp.644-653 .